ACETONE-INDUCED PHOTODEGRADATION OF ORGANIC DYES IN THE PRESENCE OF HYDROGEN SOURCE

By

Sui-Mei Shadow, TSUI

A Thesis of the Degree of Doctor of Philosophy

Department of Civil and Structural Engineering

THE HONG KONG POLYTECHNIC UNIVERSITY

2001

DECLARATION

I hereby declare that this thesis entitled "Acetone-Induced Photodegradation of Organic Dyes in the Presence of Hydrogen Source" has not been, either in whole or in part, previously submitted to any other institution for a degree or other qualification, and contains no material previously published or written by another person, except where due reference is made in the text.

Sui-Mei Shadow, TSUI

ACKNOWLEDGEMENT

I would like to express my sincere gratitude to my chief supervisor, Dr. W. CHU for his constant guidance, critical discussion and invaluable comments in the course of research and writing up the thesis. His consecutive encouragement and supervision make this research possible.

I am greatly indebted to my co-supervisors, Mr. P. C. FUNG and Dr. K. M. SIN for their valuable suggestions and commenting on the research compilation.

Thanks also go to the technicians in the Waste and Wastewater Laboratory, Mr. W. S. Lam, Mr. C. W. Ng and Mr. K. H. Lau for their kind assistance in the analytical works, instrumental and technical support throughout my study.

Finally, I would like to acknowledge the financial support provided by the University Research Grant from the Hong Kong Polytechnic University.

Abstract of thesis entitled

"Acetone-Induced Photodegradation of

Organic Dyes in the Presence of Hydrogen Source"

Submitted by Sui-Mei Shadow, TSUI

for the degree of Doctor of Philosophy

at the Hong Kong Polytechnic University in January, 2001.

ABSTRACT

Many organic dyes that are usually used by the textile dyeing industry are resistant to UV degradation. The photodegradation of textile dyes with different chromophores in the presence of acetone (ACE), which performs as a solvent and/or a photo-sensitizer, was investigated in this study. All photolytic experiments were carried out in the Rayonet^{TM} RPR-200 merry-go-round photoreactor, at 253.7 nm monochromatic ultraviolet (UV) lamps.

Hydrophobic disperse dyes are known to have very low photodegradation rates in the natural environment because of their low solubility. In this study, ACE acts not only as a solvent to increase the dye's solubility but also as a photosensitizer to enhance the photodegradation rate. The results demonstrated that photochemical reaction in the presence of ACE could rapidly and effectively enhance color removal. The photosensitization follows pseudo first-order decay and is dominated by photoreduction process. The rate constants of dye degradation by UV depended on the solution pH and solvent system, (*i.e.*, ACE/H_2O ratio). The decay quantum yields of dyes were normally observed with the increase of the ACE/H_2O ratio and the photosensitization of disperse dye found to be optimized at alkaline conditions. In general, more than ten times of quantum yield increment is observed in the presence of ACE photo-sensitizer than in water alone. Further increase in ACE/H_2O ratio reduces the quantum yields, possibly due to the light attenuation by excess ACE.

In addition, the BOD_5/COD ratio of the treated solution was increased, indicating that the dye structure was shattered and more biodegradable in the ensuing biological treatment. ACE in the wastewater could be recycled by a simple gas stripping process, which not only recovered the ACE for reuse but also increased the dissolved oxygen in the wastewater stream and facilitated the biological treatment.

Photochemical reaction of disperse dye in a cocktail solution containing ACE and triethylamine (TEA) has been also examined. Adding a low concentration of TEA to the aqueous ACE can further enhance the reaction, because TEA can be used as additional hydrogen source. However, an overdose of TEA will quench the reaction. The possible photoreduction mechanisms of disperse dye in aqueous ACE and TEA were proposed, two models based on the Stern-Volmer plot were derived and successfully described the reaction at both low and high concentration of TEA, which made the process performance predictable.

Besides the study of photodegradation of disperse dyes, a typical highly soluble and non-biodegradable dye contaminant, azo reactive dye – C. I. Reactive Red 2 (RR2), was used to explore the reaction mechanisms and kinetics of photodegradation in the cocktail solutions. The photodegradation of RR2 in aqueous ACE or TEA solution was found to be kinetically controlled by the pseudo first-order and zero-order kinetics respectively. In the presence of TEA, the rate enhancement is mostly due to the electron transfer from TEA to RR2 and results in the reduction of dye chromophore. Photosensitization is likely the dominant mechanism in the presence of ACE. The photodegradation of RR2 through photoreduction was shown to be the

main decay pathway. In addition, some minor pathways were observed including photodechlorination and photodesulphonation.

The modeling of cocktail photodecolorization of RR2, in the mixture aqueous of ACE and TEA solution was investigated. It was interested to find that three distinct stages were obviously observed in the cocktail photosensitization profiles. A lag phase was observed at the commencement of the degradation, but its duration was gradually reduced with the increment of the TEA concentration as well as the incident light intensity. Subsequently, a fast decay of RR2 was observed in which over 80% of the dyes were reduced in this stage and it was interesting to find a tailing stage after 90-95% of color was removal. Since the dye photodegradation processes were found to be kinetically controlled, a quantitative estimation of RR2 in the cocktail photosensitization system was also studied. The system of differential equations has been solved by numerical integration to calculate the concentration of RR2 as a function of time. A mathematical Cocktail model was proposed and the predicted data was compared with the experiments, generally very good agreement was achieved. Furthermore, the sensitivity analysis of the Cocktail model confirmed that photosensitization process was the dominant mechanism in the cocktail system and it was mainly contributed to the presence of ACE.

TABLE OF CONTENT

CHAPTER 5 RESULTS AND DISCUSSION II:

PHOTODEGRADATION OF HYDROPHILIC DYE

CHAPTER 6 CONCLUSIONS AND RECOMMENDATIONS

LIST OF TABLE

LIST OF FIGURE

CHAPTER 1 INTRODUCTION

1.1 Dye Effluents Of The Textile Industry

Environmental regulations have become more stringent over the past two decades. The authority of environmental protection will continue passing legislation that affects to the textile dyeing and finishing industry (O'Neill *et al.*, 1999; Cooper, 1992). One specific issue of anticipated change is the presence of color in discharged effluent. Compared with other pollutants in dye wastewater, color is especially noticeable and needs to be removed from wastewater before it is discharged into the water stream. Because of the diversity of dyes used for printing and dyeing processes, the composition of dye wastewater may be very complex and difficult to decolorize in one simple step by conventional treatment. This is the obvious reason for unceasing researches on the advanced treatment technologies of color removal from the dye wastewater.

Dye houses produce significant quantities of wastewater every day, over 4.4×10^6 m^3/day in the Mainland China (Wu *et al.*, 1999), and the effluent containing various types of soluble and/or insoluble dyes might interference with the transmission of light that posses a serious hazard to aquatic living beings. The removal of dyes from industrial effluent is a major environmental concern of textile industry because government legislation is becoming increasingly stringent, conventional wastewater

treatment processes do not readily remove dyes in textile wastewater, and some dyes might have carcinogenic and/or teratogenic effects (Habner *et al.*, 1997).

A range of conventional treatment technologies for dye removal has been investigated (Philippe *et al.*, 1998; Walker & Weatherley, 1997; Ganesh *et al.*, 1994; Lin & Lin, 1993) such as the trickling filter, activated sludge, chemical coagulation and carbon adsorption processes might remove certain categories of dyes to about 90%.

Philippe and co-workers (1998) reported that textile plants often utilize coagulation and flocculation compounds (e.g., lime, alum, ferric salts, or polyelectrolytes) followed by sedimentation or dissolved air flotation to remove organic dyes and pigments from wastewater. However, these physio-chemical processes merely transfer dyes from water phase to solid waste, resulting in generation of large amount of sludge that requires disposal. Nevertheless, activated carbon does not adsorb some vat dyes, disperse dyes, and pigment dyes (Walker & Weatherley, 1997). Sarasa *et al.* (1998) and Liakou *et al.* (1997) reported that ozone was effective in removing soluble dye (direct, reactive and basic dyes) from wastewater but ineffective in decolorizing wastewater that contains hydrophobic disperse dye.

Dyestuffs represent a class of organic pollutants that absorb light. Since commercial dyes are usually designed to resist photodegradation, the direct photolysis of dyeing wastewater can be difficult in the natural environment because it strongly depended on the dye solubility, reactivity and photosensitivity (Chu & Ma, 1997).

A subject of current interest has been the photochemical degradation of dyeing wastewater by using UV light with the aid of photocatalysts or sensitizers that can effectively remove color from the wastewater without generating chemical sludge or toxic residues in the treated effluent (Galindo *et al.*, 2000; Herrera *et al.*, 1999). These studies generally focused on the photodegradation of hydrophilic dyes, for example, direct, acid, sulphur and metal complex dyes. Investigations of the photochemical reaction of hydrophobic dyes, such as disperse dye, are very limited. In addition, these processes are based on the generation of active oxygen species or hydroxyl radicals and resulted in oxidation of the dye chromophore. Apart from this, photoreduction process of dyes is also recognized as an important fading pathway. Many dyes are noted for their ease of photodecolorization in the absence of oxygen when a suitable electron donor or hydrogen source is presenting (Allen, 1980).

1.2 Degradation Of Organic Dyes In Cocktail Photosensitization System

1.2.1 Photodegradation of Hydrophobic Disperse Dye

Disperse dyes are scarcely soluble in water, but are soluble in organic solvents and widely applied in the dyeing of polyester and acetate fibre. Chu and Ma (1997) indicated that the solubility of the dyestuff is one of the dominant parameter for photodegradation, and Yang *et al.* (1998) showed that the low solubility of hydrophobic dyes has impeded the rate of photodecolorization processes. Acetone (ACE) has high energy in the triplet state (79 - 82 kal/mol), which makes the photosensitization process possible (Chu & Javert, 1994). Therefore, in this study, ACE has been used not only as a photosensitizer, but also as a solvent to increase the solubility of the disperse dye. Since the photoreduction reaction is found to be the dominant mechanism for dye photodegradation, it is possible that photosensitization can be further enhanced if an addition hydrogen source (*i.e.* electron donors) is co-existent in the solution.

The tasks of this part were: (a) to explore the photodegradation of hydrophobic disperse dyes with different chromophores in aqueous ACE solution; (b) to investigate the reaction rates and quantum yields under various ACE/H_2O ratio (v/v); (c) to find out the effect of the solution pH; (d) to explore the possible rate improvement of dye photodegradation by using additional hydrogen source (TEA) in the aqueous ACE solution (*i.e.* cocktail photosensitization system); and (e) to elaborate the reaction mechanisms of the cocktail system.

1.2.2 Photodegradation of Hydrophilic Reactive Dye

Reactive dye represents an important fraction of the commercialised synthetic pigments used (currently about 20 - 30% of the worldwide production), however, it is generally regarded as the most difficult to remove from textile dyeing effluents, because of its distinctive chemical nature and stability of modern dye. Chu and Jafvert (1994) reported that photoreduction reaction for aromatic compounds in the presence of sensitizers or hydrogen source in which high reaction quantum yields were observed, indicating that the indirect photodegradation (photosensitization, in this case) is a useful approach to overcome the low performance of direct photolysis.

The primary interest of this part of study was to investigate and quantify the degradation of chlorinated reactive dye in cocktail photosensitization system. This study includes (a) exploring the photodegradation of chlorinated reactive dye by using sensitizing agent or hydrogen source; (b) examining the reaction kinetics and reaction rates of the reactions; (c) analyzing the impact of the initial pH and (d) investigating the photodecay pathways.

CHAPTER 2 THEORY AND LITERATURE REVIEW

2.1 Dye Chemistry

Dyes derive their color from electron transitions between various orbitals. All organic dye compounds containing an unsaturated group or groups absorb light energy that the electrons are more mobile and resonance will cause absorption of the lower energy light in the visible range. Certain groups conferred the potentiality of color are termed chromophores, for example, azo, carbonyl, nitro and nitoso. However, colored molecules (i.e. chromogens) are not dyes unless they contain auxochromes such as amino, substituted amino, hydroxyl, sulphonic groups. Auxochrome substituents did not give rise to strong colors, but had a significant effect on the shade and the solubility character of the chromophoric molecules.

Textile dyes may be classified by their chromogenic systems, and this has been achieved in the Colour Index (C.I.) (1987, 1974) published jointly by the Society of Dyers and Colorists, and the American Association of Textile Chemists and Colorists. According to the classification of dyes by the chemical structure, there are about 12 classes of chromogenic groups, the most important being the azo type which makes up to 60 – 70% of all textile dyestuffs, followed by the anthraquinone type.

2.1.1 Dye Chromophore

Azo Dye

Azo dyes contain at least one azo group (—N=N—) which are linked to sp^2-hybridized carbon atoms. In accordance with the number of such groups the dyes are described as mono-, di-, tri- and poly- azo dyes. Particularly, all azo dyes are synthesized by diazotization and azo coupling. The azo groups are mainly bound to benzene or naphthalene rings and exist in the trans form with the bond angle is ca. 120°. Azo dyes can be further classified in various ways depending on the structure, for example, metallized, carbocyclic and heterocyclic azo dyes (Zollinger, 1991).

Anthraquinone Dye

Anthraquinone dyes are the second most important class after azo dyes, also one of the oldest types of dyes. The chromophore of these dyes are based on 9, 10-anthraquinone, as shown in Figure 2.1 (Aspland, 1993) which absorbs light principally in the near ultraviolet that has a faintly yellow color in dichloromethane (λ_{max} = 327 nm). To produce commercially useful dyes, substituents such as amino or hydroxy groups are introduced to the parent compound and intense colors ranging through orange to red and blue can be obtained. To achieve desired region of the visible spectrum, it is highly depended on the positions and strength of the substituents.

Anthraquinone dyes are generally characterized by high fastness to light in comparison with those of many other dye classes. In contrast to the azo dyes, which have no natural counterparts, most of the important natural red dyes were anthraquinones.

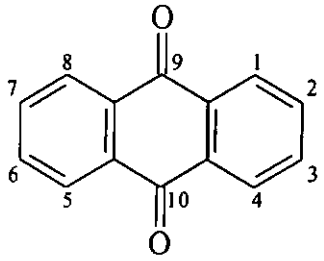

Figure 2.1: Basic structure of anthraquinone dye

2.1.1. Disperse Dye and Reactive Dye

An alternative approach of classification of dyes is based on their mode of application to textile fibers and distinguishes acid, basic, direct, disperse, mordant, metal-complex, reactive, sulfur, and vat dyes (Carr, 1995). In this study, we are mainly focused on those disperse and reactive dye pollutants which often pose problems in the conventional treatment technologies.

Disperse Dye

Hydrophobic dyes like disperse dye are slightly soluble to water in nature and are either azo compounds or anthraquinone derivatives. The importance of the hydrophobic disperse dyes has increased to a very great extent with the appearance

of synthetic fibers, such as polyesters and Tricel. The low treatment performance of dye removal from wastewater results in the remaining dyes escaping from treatment system that may be discharged to rivers or harbors and eventually readily sorbed onto soil or deposited in the sediment. Therefore, contamination of soils and sediments by hydrophobic dyes is an environmental concern.

Reactive Dye

Reactive dyes are capable of forming a covalent bond between the dye molecule and the fiber. The dye structures thus produced are essentially into three parts, the chromogen, the reactive system and the solubilizing group. The main function of chromogen is to demonstrate color for the dyes and the azo chromophore are the most important class (80%) for reactive dyes to give wide ranges of color. Besides, reactive systems contained in the dyes also govern their stability. The reactive systems are with regard to the number and inherent chemical reactivity of reactive groups in dye molecules. The most common types of reactive groups are n-chlorotriazine. Research on textile effluent decolorization has often focused on reactive dyes for three reasons:

i) Reactive dyes represent an increasing market share, currently about 20 – 30% of the total market for dyes, because they are used to dye cotton which makes up about half of the world's fiber consumption.

ii) A large fraction, typically around 30% of the reactive dyes is wasted because of their low degree of fixation to fibers, compared with other dye classes and

fibers. As a consequence, substantial amounts of unfixed reactive dyes are released in the wastewater.

iii) The distinctive chemical nature of reactive dye is generally regarded as the most difficult to remove or degrade from textile wastewater. Owing to the stability of modern dye and the high composition of aromatic present in dye molecules, conventional wastewater treatment plants, which rely on sorption and aerobic biodegradation, have low removal efficiency for reactive dyes that leads to colored waterways, and public complaints (Philippe *et al.*, 1998).

2.2 Research On Color Removal Technologies

Industrial developments is pervasively connected with the disposal of a large number of various toxic pollutants that are harmful to the environment, hazardous to human health, and difficult to degrade by natural means. The decolorization of textile wastewater is a worldwide problem to which many diverse technologies have been applied. Methods available for color removal from textile effluents are mainly divided into five categories including physical, electrochemical, photochemical, chemical and biological treatment (Patricio *et al.*, 1999; Philippe *et al.*, 1998; Tünay *et al.*, 1996; Cooper, 1993) and are described in Figure 2.2.

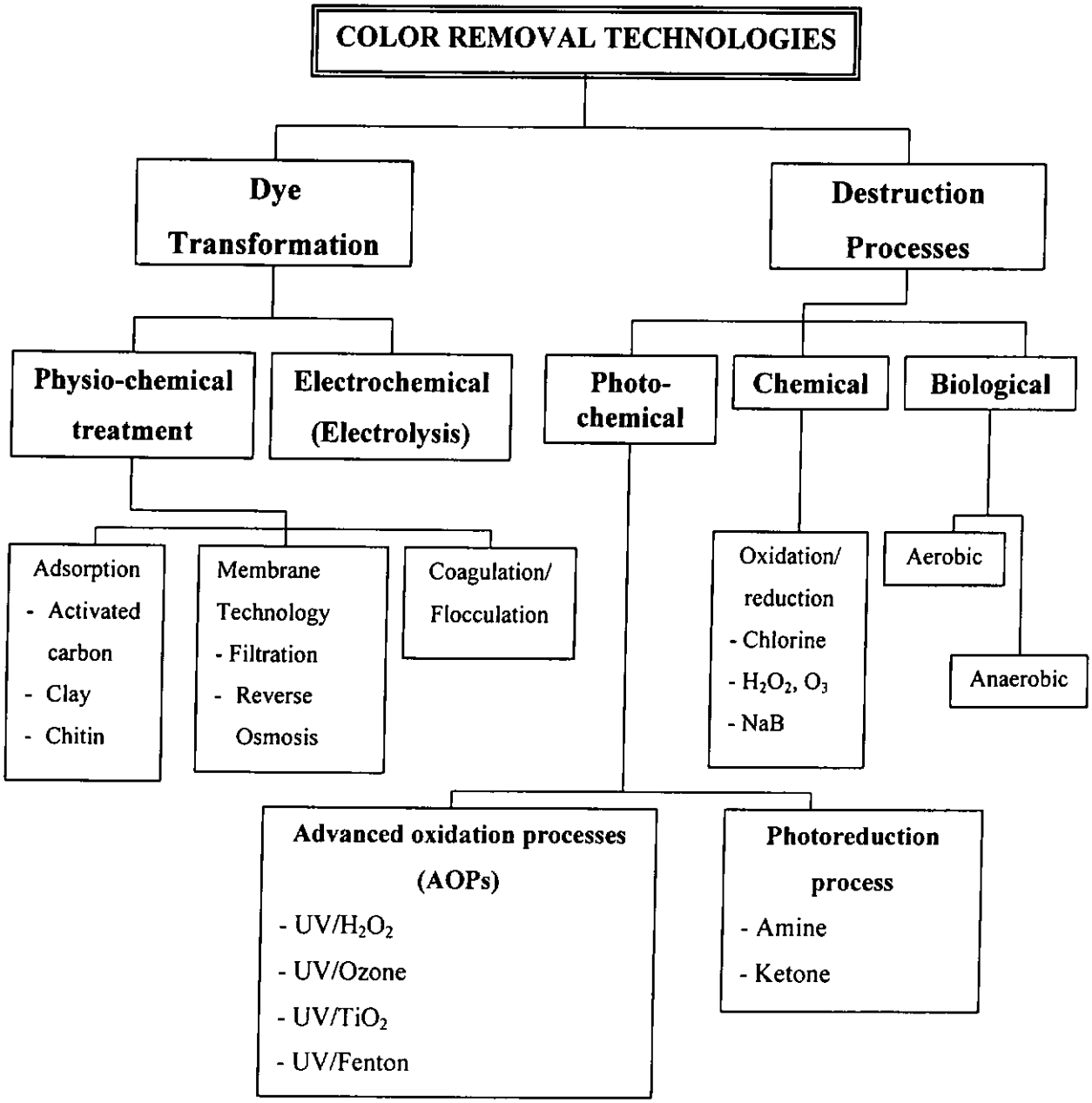

Figure. 2.2: Wastewater treatment technologies on dye wastewater

2.2.1 Physio-Chemical Transformation of Dye Waste

Conventional wastewater treatment technologies (Philippe *et al.*, 1998; Ganesh *et al.*, 1994; Lin & Lin, 1993) such as adsorption, filtration and chemical coagulation/flocculation (Kang & Chang, 1997), are available for treating of dye effluents but with limited success because they are less or even ineffective against to the very stable modern dyestuffs. However, these processes merely transfer dyes from one phase (water) to another (solid waste) and ultimately there is still a sludge disposal problem.

Dye removal by adsorption to biomass, such as waste agricultural byproducts, chitin, etc., has been the subject of a considerable amount of researches (Morais *et al.*, 1999; Juang *et al.*, 1997; Yoshida & Takemori, 1997). Meyer *et al.* (1992) evaluated the abilities of natural adsorbent materials such as vermiculite, sawdust, barbecue charcoal, maize stalks, sand, rice husks and peat moss on textile plant effluents and obtained around 50% color removal. Although this approach has the potential to provide a low-cost solution to the problem, unmodified biomass has poor dye-binding properties. Chemically modified biomass products can have very high dye-binding capacities but incur a concomitant increase in cost.

Walker and Weatherley (1997) conducted experiments on dyeing wastewater using activated carbon and obtained complete removal of color, however, a large carbon dosage was required. Membrane filtration (Dhale & Mahajani, 1999) is capable of

remove color in the effluent but it is expensive in terms of both capital and operation cost.

Electrolysis (Dávila-Jiménez *et al.*, 2000) allows the effluent passing through an electrochemical cell containing cold rolled steel electrodes. Vlyssides and co-workers (1999) suggested that the use of Pt/Ti as anode and stainless steel as cathode to treated reactive azo dye by means of electrochemical oxidation. Charged ions are attracted to the electrodes to give a precipitate of metallic hydroxide with a very active surface. Since the dye treatment performance is highly sensitive to the characteristics of wastewater, which may easily interfere by those present impurities. Furthermore, subsequent treatments such as coagulation and sedimentation are necessary.

2.2.2 Destructive Decolorization of Dye Wastewater

Biological Treatment

Under aerobic/anaerobic biodegradation, the chromophore of dyes are readily cleaved and the by-products of aromatic amines are not further metabolized under anaerobic conditions but are readily biodegraded in an aerobic environment (Chang & Lin, 2000; O'Neill *et al.*, 1999). It is important to note that most of dyes are partially degraded under aerobic/anaerobic conditions, though less readily than azo dyes (Baughman & Weber, 1994). Pilot scale investigation on the anaerobic treatability of the reactive dyebath effluents in three different colors by using a pilot scale two-phase system was studied by Sopa *et al.* (2000) and they found that

the rate of degradation is proportional to the structural complexity of the dye molecule.

Beydilli *et al.* (1998) generated a technical background for the development of a fixed-film anaerobic reactor to renovate reactive textile dyebaths and reuse the high salt-containing mixture in the dyeing process. Schliephake *et al.* (2000) stated that the pure laccase present in a strain of Pycnoporus cinnabarinus initiate destruction of the dye chromophore and the rate at which the dye was transformed by purified laccase was shown to increase with increasing concentration of the enzyme.

Previous investigations found that there is a trend of more color removal with increased organic loading which is probably due to the high cellular growth rate and associated color adsorption at higher organic loading rates (Young & Yu, 1997; Grau, 1991). They also indicated that color desorption may occur during sludge treatment.

Chemical Destructive by Oxidation or Reduction

Oxidative degradation process of organic materials in wastewater is an area of significant current interest. McCallum *et al.* (2000) studied on the oxidation of commercial anthraquinone textile dye Uniblue A in the presence of peroxdisulfate (PDS) and four reaction products were identified. A variety of oxidizing agents such as chlorine, hydrogen peroxide, ozone and fenton's reagent were used for

decolorization. They have been used to destroy various hazardous aromatic pollutants in solution and chromophoric system of dye molecules by means of oxidation process.

- The use of chlorinated oxidants, such as chlorine (Cl_2), sodium hypochlorite or chloramine, are effective for color removal and a low-cost technique (Hamada *et al.*, 1998). They are not suggested as toxic or less biodegradable chlorinated by-products may be formed. Public concerns about the release of adsorbable organic halogens (AOXs) including most of the chlorinated monophenolics over the course from excess chlorine. Nevertheless, the total AOX emissions of a mill may become an important regulatory criterion in Europe and North America (Frederick & Line, 1995).

- Ozone (O_3) is a highly powerful oxidizing agent and the oxidation potential of ozone (2.07 volts) is 1.52 times higher than that of chlorine. The high oxidation potential allows it to degrade most organic dyes (Hsu *et al.*, 1998; Sarasa *et al.*, 1998; Liakou *et al.*, 1997). Chu and Ma (2000) investigated the direct and indirect ozonation of six textile dyestuffs, including reactive, direct and disperse dyes, in which ozone and hydroxyl radicals generated in the aqueous solution are able to oxidized the dye chromophores. Nevertheless, the low degradation rate for hydrophobic dyes were considered to be the main drawback.

- Tünay *et al.* (1996) stated that there is no decolorization of the textile wastewater with hydrogen peroxide (H_2O_2) at neutral pH values. If the pH level was raised to 12, a significant color removal is obtained with hydrogen peroxide after 24 hours. Hydrogen peroxide itself is not a powerful oxidizing agent comparatively, therefore, slower decolorization rate was observed at ambient conditions. However, the presence of catalysts such as Fe powder (Tang & Chen, 1996) or fly ash (Chaudhuri & Sur, 2000) may result in faster oxidation rate.

The use of bisulfite-mediated borohydride reduction for the decolorization of wastewaters containing azo dyes has shown some commercial success. Cook (1996) described this process by consisting the reduction of bisulfite to dithionite by borohydride, spontaneously dissociation to $SO_2^{\cdot-}$ anion radicals which in turn reduce the dye azo bond (Eq. 2.1)

$$4SO_2^{\cdot-} + Ar_1N=NAr_2 + 4H_2O + 2H^+ \rightarrow 4HSO_3^- + 2Ar_1NH_3^+ + 2Ar_2NH_3^+ \quad (2.1)$$

However, the actual products generated from dyes treated with the borohydride/bisulfite redox couple have not been reported, nor have the reduction stiochiometry and reaction kinetics been detailed. A potential drawback of using borohydride and bisulfite is that the treatment of dilute dye solutions results in the generation of large volumes of decolorized wastewater contaminated by boron and potentially toxic aromatic amines (Laszlo, 1997).

2.2.3 Photodegradation of Dye Waste

An affordable and easy-operated control technology without the formation of sludge is needed to comply with today's demanding legislation. UV irradiation for dye removal (Patricio *et al.*, 1999; Shu & Huang, 1995) might be a promising process due to the following reasons:

i) No chemical sludge nor toxic residue is left in the treated effluent.

ii) UV degradation has the potential to accomplish both color removal and toxicity reduction in one step (Ho & Bolton, 1998).

iii) Not only was the residual color completely removed, almost 90% of residual total organic carbon was removed from the effluents (Wang, 2000).

iv) Less space is required, and it is easily installed on site that require the minimum amount of civil engineering work.

2.3 Photodegradation Of Organic Dyes

A photochemical reaction occurs when the electron in a molecule is raised from its ground state to a higher state. In this excited state the molecule can follow a variety of reaction paths. Thus photochemistry is concerned with the interaction of a photon or light quantum of electromagnetic energy with an atom or molecule, and of the resulting chemical and related physical changes that occur. Such excited species can be produced in a variety of ways, but by far the most commonly used method for their generation is through absorption by a molecule of a photon of ultraviolet or visible light. Absorption is a prerequisite to any photochemistry since only light which is absorbed can bring about a photochemical change.

Photodegradation processes have been scrutinized for several organic substrates and lead to their degradation, e.g., halogenated aliphatics and aromatics (Miao *et al.*, 1999; Lin *et al.*, 1996), phenols and substituted phenols (Marcì *et al.*, 1995), and surfactants (Chu & Choy, 2000). A recent development in treating dyes is the photochemical degradation of dyes in aqueous solution by using UV light, which was proven effective to remove color from the wastewater without generating chemical sludge or toxic residues in the treated effluent (Wu *et al.*, 1999; Chu & Ma, 1997).

The photodegradation of dyes in solution involves a complex series of chemical reactions. The absorption of light by organic dyes is followed by various chemical and physical interactions, which result from the dye molecules being promoted to an excited state that is more reactive than the ground state (Peters & Freeman, 1996).

Dye in such excited states are extremely unstable and short lived and will either decay back to their ground states releasing the excitation energy in some physical ways or undergo chemical reactions and form new species.

Photofading is one of the important reactions for UV radiation upon dye molecules. The UV light may cause various types of reactions, bringing about structural changes or transformation in dye molecules that might greatly contribute to their degradation in the environment and the photodegradation in solution can be classified into three principal areas:

a. Direct photodegradation – processes where degradation proceeds following direct excitation of the pollutant by UV light.
b. Photooxidation – light-driven oxidation processes principally initiated by active oxidizing species such as singlet oxygen or hydroxyl radicals.
c. Photoreduction – light-driven reduction processes principally initiated by hydrogen source.

2.3.1 Direct Photodegradation

Some organic pollutants are able to dissociate in the presence of UV light only (Zepp & Cline, 1977). In direct photolysis, the contaminant must absorb the incident light and have a reasonable quantum yield of photodissociation. This can only be possible when the contaminant efficiently absorbs the light and is highly photo-active, a situation which is difficult to achieve under typical practical conditions, i.e., when the

contaminant absorbs light only mildly and is present only at very low concentrations. Organic pollutants absorb light over a wide range of wavelengths, but generally more absorption is observed at lower wavelengths especially below 250 nm. In addition, the quantum yield of photodissociation tends to increase at lower wavelengths, since the photon energy is increasing; this increases the chance of photofragments escaping the solvent cage.

Bolter and Cater (1994) reported that N-nitrosodimethylamine (NDMA) can be successfully photodegraded, which has a strong absorption band at 227 nm (ε_λ = 7000 M^{-1} cm^{-1}) and a photodissociation quantum yield of 0.13 at pH 7 and 0.25 at pH 2. Other group of pollutants, halogenated compounds, normally react slowly with •OH. The net chemical result of photodissociation is usually oxidation, since the free radicals generated from the dissociation can react with dissolved oxygen in the water. In practice, the range of pollutants that can be successfully treated by UV alone is very limited. It will almost always be advantageous to add an oxidizing or reducing agent for the treatment.

Direct photolysis of organic dye pollutants has been found to be difficult in the natural environment because it strongly depends on the dye reactivity and photosensitivity (Chu & Ma, 1997). Usually commercial dyes are designed to resist light irradiation. Therefore, recent efforts have been directed at investigating the photodegradation of organic dyes by sensitizers or catalysts in aqueous/dispersions under UV-light irradiation (Herrera *et al.*, 2000; Plelgrini *et al.*, 1999).

2.3.2 Photooxidation

Indeed, the photodecolorization reaction can either undergo photooxdiation or photoreduction depending on the surrounding environments. Photooxidation reactions are the additions of O atoms or O_2 molecules to some reactant R. Here the photophysical properties of the oxygen molecule O_2 are the most important, since many of these reactions involve the generation of highly reactive species and then attack of 'excited singlet' oxygen $^1O_2^*$ on the ground state reactant molecule:

$$R + {}^1O_2^* \longrightarrow RO_2 \qquad (2.2)$$

where the products are usually peroxides or hydroperoxides. The photodegradation of organic dyes are generally associated with oxidative cleavage of the dye chromophore.

Numerous investigations have reported on the oxidative photofading behavior and products of azo dyes, which mostly occur via the hydrazone form in solution, to yield the unstable peroxide, which then decomposes to produce the diazonium ion and quinone, as shown in Scheme 2.1 (Poulios & Tsachpinis, 1999; Peters & Freeman, 1996; Neevel *et al.*, 1990). Upon the optimal conditions, nearly a complete oxidation (or mineralization) of the dye may bring to the yield of HCO_3^-, H_2O, and a small amount of acid.

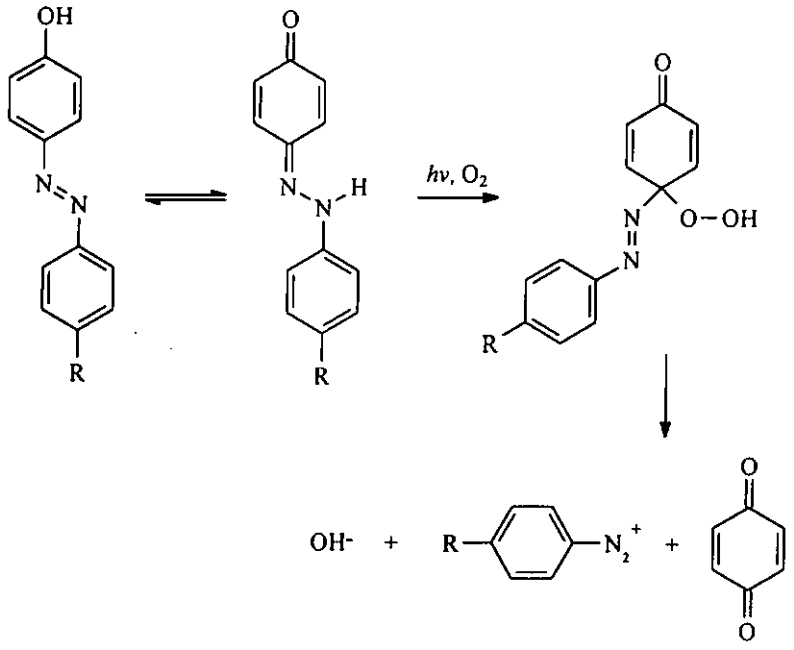

Scheme 2.1: The photooxidation of azo dye

In the recent years, a number of new technologies, called Advanced Oxidation Processes (AOPs), have emerged that are capable of converting the organic pollutants into harmless chemicals (Arslan & Akmehmet, 1999; Wu *et al.*, 1999; Kim & Vogelpohl, 1998; Beltrán *et al.*, 1997; Namboodri & Walsh, 1996; Davis & Huang, 1989). Examples of AOPs include UV/H_2O_2, UV/O_3 or UV/TiO_2. AOPs technologies almost all rely on the generation of highly reactive free radicals species, such as the hydroxyl radical ($^{\bullet}OH$), which initiate rapid reactions with organic compounds, either by addition to a double bond or through abstraction of a hydrogen atom from aliphatic compounds or side groups. The resulting organic radicals then react with oxygen to initiate a series of degradative oxidation reactions ultimately resulting in complete mineralization to CO_2 and H_2O (Mack & Bolton, 1999).

Galindo and co-worker (2000) reported that hydroxyl radicals were substituted to the aromatic rings in the photodegradation of aminoazobenzene dye by comparing three different types of AOPs. Currently, many commercial AOPs installation utilize the UV photolysis of H_2O_2 to produce •OH radicals:

$$H_2O_2 \xrightarrow{hv} 2\ \cdot OH \tag{2.3}$$

however, the use of hydrogen peroxide as a source of •OH is limited by the relatively low molar extinction coefficient, which means that in waters with high inherent UV absorption the fraction of light absorbed by the hydrogen peroxide can be low unless exceeded doses are used. This increases the costs for the treatment of the water (Bolton & Cater, 1994).

Photocatalytic processes involving semiconductor oxides under UV light illumination have been shown to be potentially advantageous and useful in several cases (Bandara *et al.*, 1999; Zhao *et al.*, 1998; Reutergårdh & Iangphasuk, 1997; Wang *et al.*, 1997), although practical process efficiencies remain somewhat contentious. As a photocatalysts, TiO_2 is a semiconductor with a band gap of 3.2 eV (anatase); it is only activated by ultraviolet light at wavelengths less than 385 nm to produce electrons and holes in the conduction and valence bands, respectively. After their migration to the particle surface in short time and in competition with other photophysical phenomena, they react with chemisorbed O_2 and/or OH^-/H_2O molecules to generate reactive oxygen species (e.g., $O_2^{\cdot-}$, HOO•, and/or OH• radicals) that can attack organic substrates and lead to degradation and ultimately to total mineralization to carbon dioxide.

Earlier studies (Qu *et al.*, 1998; Zhao *et al.*, 1997; Vinodgopal & Kamat, 1995) reported that dyes can photodegrade to CO_2 under visible light irradiation in aqueous TiO_2 suspensions. In such cases, dyes are excited by the irradiating source to appropriate singlet or triplet states, a process then followed by electron injected into the conduction band (or surface state) of the semiconductor, whereas the dyes are converted to cationic dye radicals, $dye^{\bullet+}$. The injected electron, TiO_2 (e^-), can reduce such chemisorbed oxidant, typically O_2, to also yield the oxidizing species $O_2^{\bullet-}$, HOO•, and/or OH• that can bring about photooxidations. Thus, TiO_2 can play an important role in electron-transfer mediation, even though it is not excited itself.

2.3.3 Photoreduction

Photoreduction occurs by hydrogen atom abstraction or by electron transfer. The process is a common photochemical reaction of carbonyl derivatives and other unsaturated molecules in the presence of suitable hydrogen atom donors.

Photoreduction of organic dyes is also recognized as an important fading process. Many dyes are noted for their ease of photodecolorization in the absence of oxygen when a suitable electron donor or hydrogen source is presenting (Allen, 1980). Bolton and Cater (1994) depicted that an UV photoreduction treatment of chloroform (and other chloroalkanes) proceeds at rates up to four times faster than is possible with a UV-H_2O_2 treatment.

Dyes in anaerobic solution can be reduced to the corresponding amines by hydrogen donors produced on photo-excitation of suitable simple molecules. The reductive path shown in Scheme 2.2 will vary from one dye types to another, but, essentially, reduction gives a hydrazo compound.

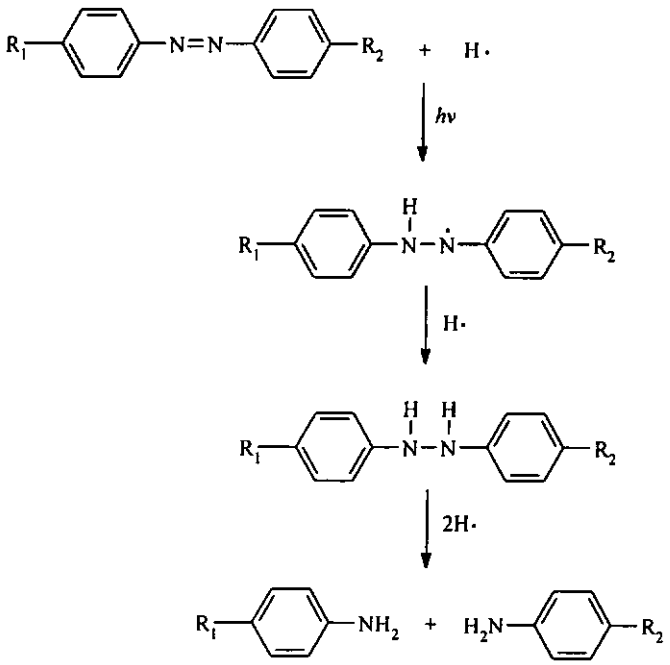

Scheme 2.2: The photoreduction pathways of azo dye

Furthermore, anthraquinone dyes are normally expected to undergo photoreduction at the 9- and 10- positions to give the corresponding hydroquinone. Previous researches (Peters & Freeman, 1996) showed that the photodegradation of some acid anthraquinone dyes is dominated by reductive process, involving hydrogen abstraction from the solvent to form 'leuco' anthraquinone derivatives occurred in the absence of oxygen. The photodegradation behavior of anthraquinone disperse dye in

solution was investigated by Katsuda (1997) at different wavelengths from 201 to 701 nm and also the mechanism of the dye photofading was also elucidate. A simplified mechanism of anthraquinone dye photodegradation is illustrated in Scheme 2.3.

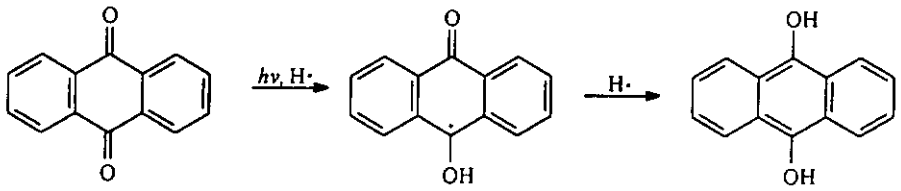

Colorless leuco structure

Scheme 2.3: Photodegradation mechanism of anthraquinone dye

Chu and Jafvert (1994) showed a photoreduction reaction for aromatic compounds in the presence of hydrogen sources in which high reaction quantum yields were observed. In addition, some previous workers suggested that the photodegradation of organic dyes could involve several reaction pathways including decolorization, dechlorination and desulphonation processes (Tanaka *et al.*, 2000; Wang, 2000).

Hydrogen Source/Electron Donor

In the presence of hydrogen sources or electron donors such as aliphatic amines the photoreduction reaction can take place by direct electron transfer rather than by hydrogen abstraction (Sato *et al.*, 1998). Bunce (1982) showed that the aliphatic and aromatic amine assisted photodechlorination of chlorides of the benzene, naphthalene and biphenyl series take place mainly from the triplet excited state. Three pathways were inferred: hydrogen abstraction from the solvent and

protonation both within the exciplex (or radical ion pair) and by external proton donors (Bunce & Challacher, 1982).

Neumann *et al.* (1996) studies on the photophysical and photochemical properties of the dye resazurin in the presence of tripropylamine which the dye is photoreduced to resorufin or dihydroresorufin. They also pointed out that the photoreduction process proceeded through the triplet state and is inhibited by the presence of oxygen.

Jockusch and co-workers (1996) stated that nucleophilic radicals, such as α-amino and ketyl radials, produced by reaction of benzophenone triplets with amines and alcohols respectively, reacted efficiently by electron transfer with cationic organic dyes. The rate constants of hydrogen source with amines are much higher than those of hydrogen atom transfer, e.g. by over three orders of magnitude between triethanol amine and 2-propanol. However, hydrogen atom transfer leads in most cases to irreversible reactions, but electron transfer is often reversible through the recombination of the ions either within the solvation cage prior separation or through diffusional encounter after separation in polar solvents.

2.3.4. Cage effects in solution

When a molecule decomposes photolytically in the gas phase, the fragments fly apart with no restrictions. However, in a condensed medium, such as an aqueous solution, "cage" effects have an enormous impact on chemical reactivity (Lindfors *et al.*, 1996; Isaacs, 1995), and in fact the reduction of photolysis quantum yield was observed. For example, if a molecule AB photodissociates in solution,

$$A{-}B \rightleftharpoons (A\cdot.....B\cdot) \longrightarrow A\cdot + B\cdot \qquad (2.4)$$

there is a significant probability for the recombination of the primary radicals within the solvent cage. The reason for this is that the rate of diffusion of the primary radicals out of the cage is often much lower than the rate of recombination. This is why quantum yields are reduced in the liquid phase. For example, the quantum yield for the photolysis of H_2O_2 in aqueous solution is only about half of its value in the vapor phase.

2.4 Photosensitization And Quenching Reactions

2.4.1 Photosensitization Process

A molecule in the ground state is raised to its excited state by energy transfer from another excited state molecule, is known as sensitization process. This process is particularly important when direct excitation or intersystem crossing in the desired species is inefficient. Through sensitization, photochemically inert substances can be made to undergo photochemical reactions.

The direct photolysis of hazardous organic compounds often proceeds with very low quantum efficiency. Sensitizers such as amines, borohydrides and ketones have previously been used to enhance the photodechlorination of polychlorobenzene (PCB) congeners in aqueous solutions (Chu & Javert, 1994; Hawari *et al.*, 1991). Hawari *et al.* (1992) reported that the photolysis of Arochlor 1254 under solar radiation for 20 hours, resulted in only 25% dechlorination. In the presence of phenothiazine sensitizer, Arochlor was completely dechlorinated in 4 hours, and in 1 hour at 350 nm with a relatively higher quantum yield ($\Phi = 2.33$).

Neevel *et al.* (1993, 1990) reported on the photodegradation of azo dye by using biacetyl as sensitizer. In aerobic aqueous solutions, biacetyl followed an oxidative pathway, which is presented in a general manner for 1-phenylazo-2-naphthol in the following Scheme 2.4:

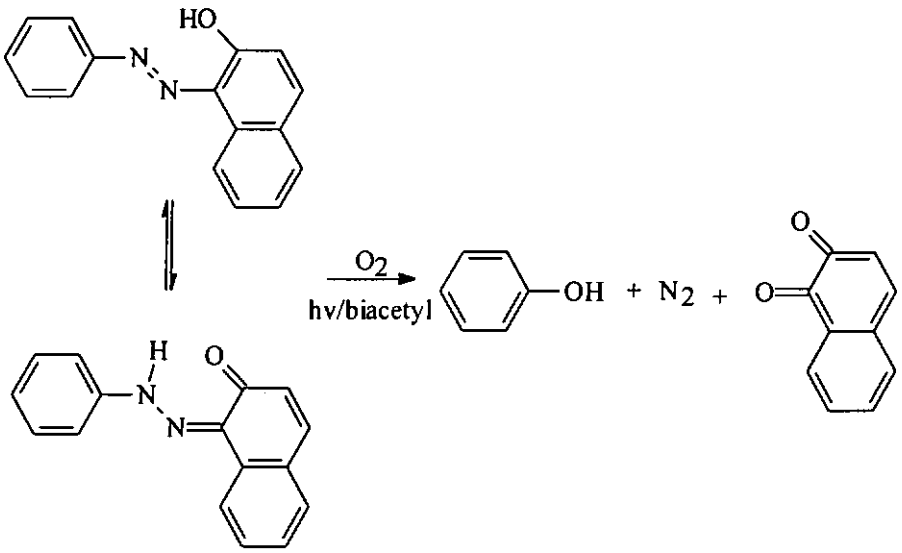

Scheme 2.4: Photodegradation of azo dye in the presence of biacetyl sensitizer

Obviously, the photosensitizer must possess sufficient energy to bring about the desired transition. Ketones or carbonyl groups are often used as the absorbing chromophore in UV photoinitiator system and have proved very popular for triplet sensitization studies, because triplet yields in carbonyl compounds are high, and the triplets of many acceptors lie lower in energy than carbonyl triplets and can therefore be populated efficiently in an exothermic energy transfer process (Isaacs, 1995).

For example, the quantum yield for the direct photolysis at 313 nm of ethyl pyruvate is 0.17 in benzene solution. However, in the presence of benzophenone sensitizer, the quantum yield for ethyl pyruvate removal is 0.32. It is thought that the triplet state of pyruvate is produced by energy transfer from triplet benzophenone, and dissociation occurs. The transfer is energetically favorable (triplet energies for benzophenone and ethyl pyruvate are 289 kJ mol^{-1} and 272 kJ mol^{-1}, respectively); it is interesting that 2-

acetonaphthone, with a triplet energy (247 kJ/mol) below that of the pyruvate, is ineffective as a sensitizer (Wayne, 1988).

Jolanta (1998) claimed that the presence of a ketone sensitizer like benzophenone accelerates the photofading of dyes, confirming that hydrogen abstraction is responsible for their degradation and the photolysis wavelength influence the process significantly. Jockusch and co-workers (1996) reported on the mixtures of cationic dyes in a ternary ketone (benzophenone, BP)-amine (triethanol amine)-dye systems that continuously irradiated at 365 nm. After the intersystem crossing $^{3}BP^{*}$ was produced and essentially reacts with the amine to form α-amino and ketyl radicals resulting in the bleaching of dyes.

Disperse dye is a substantially water-insoluble dye having one or more hydrophobic substituents on its molecule, and usually applied from aqueous dispersion (Waring & Hallas 1990), which is found to be difficult to degrade photochemically. The nature of the dye substituents will influence its photochemical behavior. For instance, electron withdrawing/donating groups and intramolecular hydrogen bonding are especially important to determine the photodecay rates of anthraquinone chromophores (Allen 1994). Yang *et al.* (1998), Chu and Ma (1997) stated that the solubility of dyestuff is the dominant factor for determining the rate of photodegradation in solution; therefore, the limited solubility of disperse dye hinders the efficiency of photodegradation. Chu and Tsui (1999) demonstrated that the photodegradation of azo disperse dye is enhanced in aqueous ketone solution,

indicating that the indirect photodegradation (photosensitization, in this case) is a useful approach to overcome the low performance of direct photolysis for hydrophobic dyes.

2.4.2 The Mechanisms of Photosensitization

Generally, the process of photosensitization are initiated by a sensitizer (Sens) that absorbs light energy (hv), transforms it into chemical energy and under favorable conditions transfers this energy to otherwise photochemically inert substances (X). This mechanism can be formulated as Eq. 2.5 - 2.6, where X^* is able to carry out further chemical reaction resulting in the degradation of its molecular structure and the sensitizer is regenerated after the energy transfer is complete, which makes the recycling feasible.

$$Sens + h\nu \rightarrow Sens^* \quad (2.5)$$

$$Sens^* + X \rightarrow X^* + Sens \quad (2.6)$$

It is important to note that the sensitization may proceed through a singlet, triplet or electron transfer mechanisms, a feature of the reaction which is dependent on the energy relationship between the sensitizer and substrate. Galadi and Julliard (1996) reported the photosensitized degradation of pesticides in acetonitrile/water mixture as a solvent with anthraquinone as a photosensitizer, while the presence of photosensitizer significantly increases the rate of photodegradation through the mechanism of electron-transfer and helps to completely remove the pollutant.

The photolysis of Arochlor 1254 in alkaline 2-propanol solution at $\lambda > 300$ nm in the presence of ACE was described by Hawari *et al.* (1991) proceeding with exceptionally high quantum yield. They also hypothesized that the high quantum yield was interpreted in terms of a free radical chain reaction and was suggested in which ACE triplet, T_1 (n,π^*) abstracts H-atom from 2-propanol to give the ketyl radical, $(CH_3)_2\dot{C}OH$, which after losing a proton to the alkaline medium gives the ketyl radical anion, $(CH_3)_2CHO^{\cdot-}$. The Aroclor in turn reacted with the latter species through an electron-transfer process giving unstable aryl radical anion, which cleaves releasing the chloride anion, Cl^- and the aryl radical, $Ar^{\cdot}$.

2.4.3 Quenching by Energy Transfer: Stern-Volmer Equation

The deactivation of the electronically excited state (singlet and/or triplet) to the ground state or lower state, is described generally as quenching. Quenching process (Gak *et al.*, 1998; Yasui *et al.*, 2000) can occur through energy transfer resulting in the generation of the excited state of the other molecule:

$$X^* + Q \rightarrow X' + Q^* \qquad (2.7)$$

where X′ is the ground state or another excited state of X, and Q is the quencher.

Quenching processes can be induced by a variety of compounds including oxygen, humic acids, nitrobenzene, butylhydroxy-toluene, dodecanethiol, and methyl iodine. This may be unfavorable for the achievement of photochemical reactions in that the excited reactant is returned to its ground state and the light energy lost. Hawari *et al.*

(1991) found that the presence of O_2 severely quenched the ACE sensitized photodechlorination process and no dechlorination was observed in the presence of oxygen. They indicated that oxygen effectiveness in quenching the reaction might due to the trapping of ACE triplet or other intermediate triplets in the chain reaction. Encinas *et al.* (1994) also reported on the quenching of excited states during the photoinitiation of fluorenone/triethylamine system in the polymerization processes, resulting in the retardation of polymerization rate.

However, quenching may also be desirable, for example, by the introduction of a quencher, either a singlet or a triplet state of the excited reactant can be selectively removed in order to bring about the desired reaction of the unaffected state (Nakamura *et al.*, 1997).

Quenching effects normally can be studied through classic Stern-Volmer analysis (Logan, 1996; Turro, 1978). A Stern-Volmer analysis of photochemical kinetics postulates that a reaction mechanism involves a competition between decay of pollutant (or probe molecule) in the excited state (D^*) and a bimolecular quenching reaction involving D^* and the quencher, Q. The kinetics are modeled with the steady-state approximation, where the excited intermediate is assumed to exist at a steady-state concentration:

$$\frac{d[D_1^*]}{dt} = 0 \qquad (2.8)$$

Possible reaction mechanisms of the photodegradation of a probe molecule, D, within an aqueous solution in the presence of quencher, Q and hydrogen source, HS, can be broken down in the following complex series of kinetic expressions:

	Rate	Process	
$D_0 + h\nu \rightarrow D_1^*$	fI	Sensitization	(2.9)
$D_1^* \rightarrow D_0 + \text{heat}$	$k_{d1}[D_1^*]$	Deactivation of singlet	(2.10)
$D_1^* \rightarrow D_0 + h\nu'$	$k_f[D_1^*]$	Fluorescence	(2.11)
$D_1^* \rightarrow D_3^*$	$k_{isc}[D_1^*]$	Intersystem crossing	(2.12)
$D_3^* \rightarrow D_0 + h\nu''$	$k_p[D_3^*]$	Phosphorescence	(2.13)
$D_3^* \rightarrow D_0 + \text{heat}$	$k_{d3}[D_3^*]$	Deactivation of triplet	(2.14)
$D_3^* + Q \rightarrow D_0 + Q^*$	$k_q[D_3^*][Q]$	Quenching of triplet	(2.15)
$D_3^* + HS \rightarrow \text{Product}$	$k_r[D_3^*][HS]$	Chemical reaction	(2.16)

The involvement of too many sub-reactions in a rate law makes the expression irresolvable. Several assumptions may be made based on earlier observations or hypotheses regarding the specific mechanisms of transformation, resulting in consideration simplification of the kinetic expression. Since the significant reactive intermediate is likely the long-lived triplet state for photochemical reaction, therefore, if intersystem crossing is effective compared with all other singlet processes, a simplified mechanism for the quenching may be proposed:

	Rate	Process	
$D_0 + h\nu \rightarrow D_1^*$	fI	Absorption	(2.17)
$D_1^* \rightarrow D_0 + h\nu'$	$k_f[D_1^*]$	Fluorescence	(2.18)
$D_1^* \rightarrow D_0$	$k_d[D_1^*]$	Radiationless deactivation	(2.19)
$D_1^* + Q \rightarrow D_0 + Q_1^*$	$k_q[D_1^*][Q]$	Fluorescence quenching	(2.20)

Based on the steady-state approximation, the net rate of formation of D_1^* (singlet) as,

$$\frac{d\,[D_1^*]}{dt} = fI - k_f[D_1^*] - k_d[D_1^*] - k_q[D_1^*][Q] = 0 \tag{2.21}$$

where I is the illuminating intensity, f is the efficiency of light absorption, k_f is the rate of fluorescence processes, and k_d is the rate of all deactivation processes, and k_q is the rate for bimolecular quenching process. Further information can be obtained by utilizing the concept of quantum yields, ϕ. For the purpose of discussion, fluorescence may be used (although similar expression for all other processes may be derived), in which the quantum yields is defined as the ratio of the process responsible for fluorescence to the initial illumination. That is,

$$\phi = \frac{k_F[P_1^*]}{fI} = \frac{k_F[P_1^*]}{[P_1^*](k_F + k_d + k_q[Q])} = \frac{k_F}{k_F + k_d + k_q[Q]} \tag{2.22}$$

In the absence of quencher (i.e., [Q] = 0), Equation (2-22) becomes to,

$$\phi' = \frac{k_F}{k_F + k_d} \tag{2.23}$$

The ratio of quantum yield ϕ' in the absence of quencher to the value of ϕ in its presence is given by:

$$\frac{\phi'}{\phi} = 1 + \frac{k_q}{k_F + k_d}[Q] \tag{2.24}$$

This is known as the Stern-Volmer equation. If the proposed mechanism is corrected, it gives a linear relation between ϕ'/ϕ values and quencher concentration with a slope equal to $k_q/(k_f+k_d)$. In the absence of a quencher, the mean lifetime τ of the excited singlet, the fluorescence lifetime, is given by $(k_f + k_d)^{-1}$. Thus the equation is sometimes written as,

$$\frac{\phi'}{\phi} = 1 + k_q \tau [Q] \tag{2.25}$$

and it implies that a plot of ϕ'/ϕ against the concentration of quencher will give a linear relation, with an intercept of one and the slope equal to $k_q\tau$. If τ can be measured in separate experiments then the value of k_q can be obtained. Frequently, it lies close to the diffusion-controlled limit.

CHAPTER 3 MATERIALS AND METHODS

3.1 Experimental Approach

As evidence from the literature review presented in Chapter 2, many fundamental scientific and engineering questions remain unanswered regarding the photosensitization reaction of organic dyes. Investigations into the possible use of sensitizer as initiator of dye degradation and also as solvent medium, in which to carry out photochemical decay of the solubilized organic dyes were limited. More specifically, there is a general lack of information in the literature on the photodegradation of organic dyes in a cocktail solution (i.e. mixture of sensitizer and hydrogen source). In addition, the potential quenching effects resulted from the presence of hydrogen sources remain largely unknown. Hence, in this research the focus has been in the following areas:

3.1.1 Investigations on the Photodegradation of Hydrophobic Disperse Dye

Photosensitization of Hydrophobic Disperse Dye

The photodecolorization of two typical disperse dyes with different chromophores was investigated in the presence of ACE at 253.7 nm. In this study, ACE performs not only as a photosensitizer, but also as a solvent to increase the solubility of the disperse dyes. The concentration of dye in solution was quantified by the high pressure liquid chromatography (HPLC). The decay kinetics of dye

photodegradation by UV on different initial pH and solvent system (i.e. ACE/H_2O ratio) were examined. In order to calculated the reaction quantum yields, the molar absorptivity of disperse dyes was determined by UV/Vis Spectrophotometer.

Applicability of the ACE Photosensitization Process

Respect to the impact of photoproducts on the environment, the applicability of this process was evaluated with the BOD_5/COD ratio of the final solution. In addition, purging method was selected for accessing the efficiency of ACE recovery at room temperature and the potential to increase the dissolved oxygen was also studied.

Additional Hydrogen Source

In order to enhance the decay rates, the cocktail photodegradation performance of a typical anthraquinone disperse dye was explored by adding two additives at the same time (ACE as the photosensitizer and triethylamine (TEA) as the hydrogen source) in the process. The enhancements were defined by the comparison of the relative quantum yields at different concentration of TEA through a pseudo first-order decay rate expression. Furthermore, the reaction mechanisms of the cocktail photodegradation process were proposed while the enhancing and quenching effects resulting from the hydrogen source were described through Stern-Volmer analysis.

3.1.2 Investigations on the Photodegradation of Hydrophilic Reactive Dye

Photodegradation of Reactive Dye

The photodegradation of azo reactive dye in the presence of ACE or TEA via the indirect photolysis was investigated. In order to define the function of additives in photodecolorization and to optimize the photodegradation of dyes in aqueous solution, the concentration of the additives was evaluated. The impact of pH was also examined since pH of the system is another important factor for photochemical reactions. The determination of the reaction rates has been conducted for all experiments.

The reaction mechanisms of indirect photolysis of reactive dye were examined. The optimized ACE solution containing the selected reactive dye was irradiated at 253.7 and the rates of decayed dye were quantified by HPLC. Consequently, the change of inorganic ions in the solution was determined by ion chromatography (IC).

Photodegradation of Reactive Dye in a Cocktail-Sensitization System

The modeling of photodecolorization of a nonbiodegradable azo reactive dye, in the cocktail mixture of ACE and TEA was investigated. The effects of TEA concentration and the light intensity on the photolytic ACE solution were evaluated. Since the dye photodegradation processes were found to be kinetically controlled, a quantitative estimation of dye in the cocktail photosensitization system was also studied. The system of differential equations has been solved by

numerical integration to calculate the concentration of RR2 as a function of time. A mathematical cocktail model was proposed and the predicted data was compared with the experiments. Furthermore, the sensitivity of the proposed cocktail model was analyzed.

3.2 Materials

3.2.1 Dyestuffs and Chemicals

Three different commercial available textile dyestuffs were used in the study including two hydrophobic disperse dyes (DY7 and DO11) and one hydrophilic reactive dye (RR2). Those selected dyestuffs are commonly used in today's dye house and regarded as dye contaminants in the discharged effluent. The dyestuffs were purchased from Aldrich Chemical Co. and used without further purification. The molecular structure of the dyes are shown in Figure 3.1 and also, their respective characteristics are given in Table 3-1.

ACE, TEA and acetonitrile were reagent or HPLC grade, they were used without further purification and purchased from Aldrich, or Farco. Powdered form of sodium carbonate and sodium bicarbonate were obtained from BDH for preparation of inorganic stock solutions during the inorganic ion analysis. Deionized distilled water was used throughout this study for chemical and dye solution preparation. The pH level of the solutions was adjusted by diluted sulphuric acid or aqueous sodium hydroxide solution.

Table 3-1: The physical and chemical characteristics of selected dyestuffs (Color Index 1974, 1987).

Generic Name	Abbrev.	Commercial Name	Purity (%)	Dye Class[a]	Chromophore	F. W.	Solubility[b] ($g\ L^{-1}$)	Molar Absorptivity[c]	λ_{max} (nm)
C.I. Disperse Yellow 7	DY7	Dianix Yellow 5R	95	Disperse	Anthraquinone	316.37	<<1	22970	387
C.I. Disperse Orange 11	DO11	Supracet Orange R	95	Disperse	Diazo	237.26	<<1	584	486
C.I. Reactive Red 2	RR2	Procion Red MX-5B	50	Reactive	Monoazo	615.34	~100	28560	538

[a] Based on the substitute groups added to the dye molecules.

[b] The solubility in water (Chu & Ma, 1997; Peter & Freeman, 1996).

[c] Molar absorptivity at 253.7 nm, $\varepsilon_{253.7}$ ($mol\ L^{-1}\ cm^{-1}$).

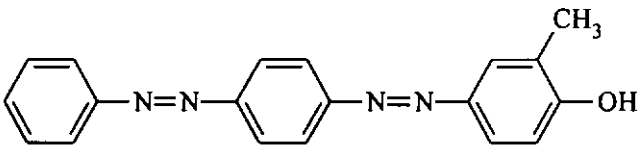

C. I. Disperse Yellow (DY7)

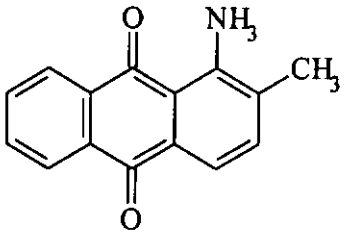

C. I. Disperse Orange 11 (DO11)

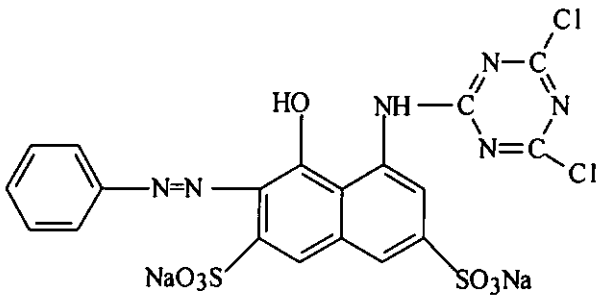

C. I. Reactive Red 2 (RR2)

Figure 3.1: The molecular structures of the three selected dyes used in this study.

3.3 METHODS

3.3.1 Photochemical Reactor

All photochemical experiments were carried out in a Rayonet™ photochemical reactor RPR-200, manufactured by The Southern New England Ultraviolet Company. The photoreactor basically consisted of a merry-go-round apparatus, 5-mL cylindrical quartz cuvettes with internal diameter 10 mm, and phosphor-coated low-pressure mercury lamps. A schematic drawing of the photoreactor was shown in Figure 3.2.

The reactor holds up to 16 lamps around the outside and up to 8 cylindrical quartz or pyrex cuvettes in the merry-go-round in the center. Two to twelve phosphor-coated low pressure mercury lamps were used as light sources that emitted monochromatic lights at 253.7 nm. The incident UV intensity at 3.81 cm from each lamp was about 2100 watt/cm^2 (equivalent to 1.5×10^{-6} Einstein L^{-1} s^{-1}). The merry-go-round apparatus rotated at a constant speed of 5 rpm throughout the experiments to make sure all the cuvettes receive same amount of light exposure. A ventilation fan was installed at the bottom of the photoreactor in order to prevent heat accumulation.

3.3.2 Experimental Procedures

In the photolysis experiment, each quartz curvette was filled with 4-ml aqueous solution containing identical concentration of dye solution and additive (ACE or TEA). The initial dye concentration utilized was 20 mg L^{-1}. The cuvette was sealed with Teflon-lined caps to minimize the volatilization effect and was irradiated in the

photoreactor at room temperature (18-20°C). Control experiments were also conducted at the same conditions without the addition of additives. At given irradiation time intervals, the reacted samples were collected from the photoreactor and the extent of dye degradation was quantified at its respective maximum absorption wavelength, λ_{max} by high performance liquid chromatography (HPLC). The wavelength of the maximum absorption for RR2 was determined by monitoring UV/VIS spectrum in the range of 200-700 nm. The production of inorganic ions during photodecolorization process measured by the ion chromatography.

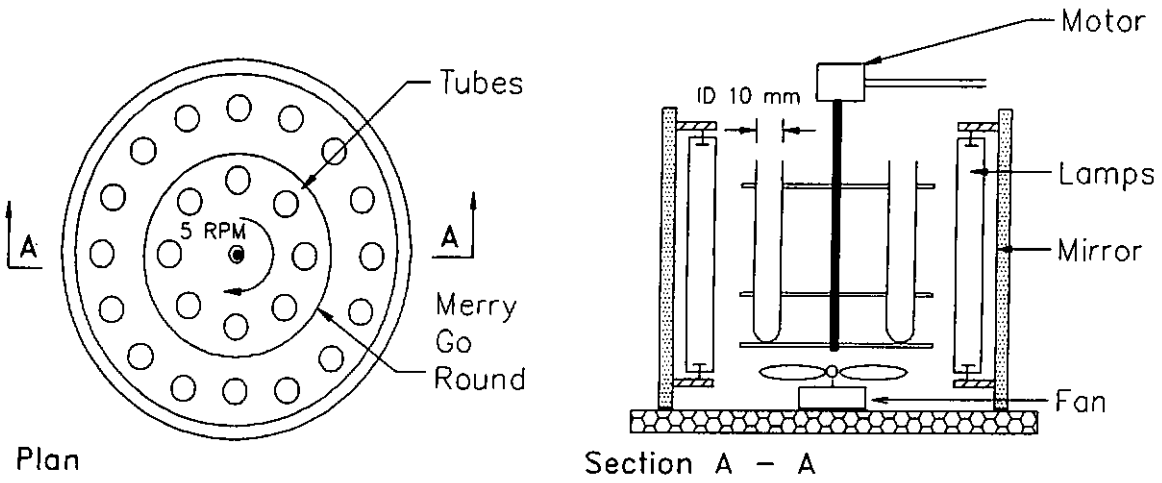

Figure 3.2: The plan view and sectional view of the photochemical reactor.

3.3.3 Analytical Measurements

High Pressure Liquid Chromatography (HPLC)

The irradiated samples were collected from each quartz cuvette at a prefixed time, and then they were analyzed by HPLC. The chromatographic system consisted of

an ISCO Model 2350 pump, a Water™ 486 tunable absorbance detector operated at the dye maximum absorbance wavelength and an ISCO valve injector with a 100-μL loop. The chromatographic separations were performed on the stainless steel Restek column: 5μm 4.6 mm ID × 250 mm Pinnacle™ Octyl Amine column. Mobile phase compositions were a mixture of acetonitrile and deionized distilled water (refer to Table 3-2), and the flow rate was set to be 1-ml min^{-1}. After the samples were exposed to the UV light, 150 to 200 μL of exposed mixtures were injected directly into a 100 μL loop. Peak identity confirmation of the probe dyes was achieved by retention time matching of those injected standards. Total run time for one sample was 10 to 25 minutes. The scanning and absorbance determination of the dye solution was pre-determined by the Spectronic Genseys 2 UV-Visible Spectrophotometer.

Standard Calibration Curve: The calibration curve is a standard curve of area against dye concentration at its λ_{max} and is plotted from readings of a series of freshly prepared standards. A known concentration of dye solution was prepared by dissolving *x* g of dye powder in 50 ml deionized distilled water (for hydrophilic dye, RR2) or in ACE (for hydrophobic dyes, DY7 and DO11). Then, 25 ml of this solution are transferred to another volumetric flask and diluted with deionized distilled water to 50 ml final volume. Further dilution was done for twice. After mixing, the readings of area from HPLC analysis at the dye's λ_{max} were taken.

Table 3-2: The mobile phase compositions of HPLC analysis

Dye	Mobile phase compositions (Acetonitrile : water, v/v)	Retention Time (min ± 0.1)
DY7	70 : 30	10.0
DO11	60 : 40	8.0
RR2	45 : 55	2.1

UV-Visible Spectrophotometer

The spectrophotometer Spectronic Genesys 2 was used to scan the dye spectra, define the dye's maximum wavelength absorbance λ_{max} and determine the molar absorptivity of each dye at 253.7 nm.

Molar Absorptivity at 253.7 nm: A known concentration of dye solution was prepared by dissolving *x* g of dye powder in deionized distilled water (hydrophilic dye, RR2) or in ACE (for hydrophobic dyes, DY7 and DO11). After the mixing, the dye solution was then transferred to a 1 cm ID quartz cell and the reading of absorbance at 253.7 nm was determined immediately by using deionized distilled water or ACE as the reference.

According to the practical expression of Beer's law in the form (Suppan, 1994),

$$I_0 / I_t = 10^{-A} \qquad \text{with} \quad A = \varepsilon_{253.7}\, c\, l \tag{3.1}$$

where A is defined as the absorbance at 253.7 nm, c is the molar concentration of dye solution, l is the optical pathlength in cm and $\varepsilon_{253.7}$ is the dye molar extinction coefficient (molar absorptivity) in mol L^{-1} cm^{-1}.

Ion Chromatography

The inorganic anions released from the photoreduction of RR2 were performed by ion chromatography equipped with a Alltech ERIS^{TM} 1000HP autosuppressor and a BIO-RAD Model HPCM conductivity monitor. A 4.6 mm ID × 150 mm Allsep anion separator column was used and the eluant solution was a mixture of 0.85 mmol L^{-1} sodium bicarbonate and 0.9 mmol L^{-1} sodium carbonate solution. Peak identity confirmation of the released inorganic anions was achieved by retention time matching of those injected standards.

BOD_5/COD

BOD_5 tests and COD tests were also accomplished to examine the quantity of the organic content of the treated samples. Pretreatment of the UV-exposed samples was carried out by heating them in a water bath at about 70°C for 10 minutes, ensuring that all of the ACE was vaporized. The laboratory procedures of BOD_5 and COD test (dichromate reflux method) were based on the Standard Methods (Lenore *et al.*, 1995).

Purging Method

To examine the recycling of ACE, a simple gas stripping system (*i.e.* an aeration stone connected to an air pump and flowmeter) was used to regenerate the ACE in treated effluent, as shown in Figure 3.3. The air flow rate was kept at 0.5 l/min. During the stripping, the change of sample volume was recorded and the variation of dissolved oxygen was determined by a YSI Model 58 DO meter.

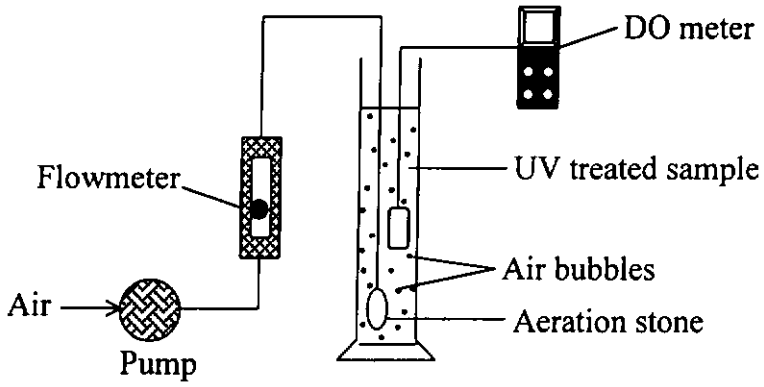

Figure 3.3: Diagram of purging system for ACE recovery.

3.3.4. Summary of Experiments

All experiments that were performed in this research are summarized in Table 3-3 and Table 3-4, and all experiment data are complied in the Appendix.

Table 3-3: Experiments performed on hydrophobic disperse dyes (DY7 & DO11).

Exp. No.[a]	Probe Cpd.[b]	ACE/H_2O Ratio (v/v)	Initial pH[c]	Remarks
DYA/W01[d]	DY7	0 : 1.00	7	
DYA/W02	DY7	1 : 2.33	7	
DYA/W03	DY7	1 : 2.13	7	
DYA/W04	DY7	1 : 2.00	7	Effect of ACE/H_2O
DYA/W05	DY7	1 : 1.78	7	ratio
DYA/W06	DY7	1 : 1.00	7	
DYA/W07	DY7	2 : 1.00	7	
DYA/W08	DY7	3 : 1.00	7	
DYpH01	DY7	1 : 2	4	
DYpH02	DY7	1 : 2	5.5	Effect of pH
DYpH03	DY7	1 : 2	9	
DYpH04	DY7	1 : 2	11	
DYCOD01	DY7	1 : 2	9	COD test
DYBOD01	DY7	1 : 2	9	BOD_5 test
ReACE01		1 : 2		Recovery of ACE
DOA/W01[d]	DO11	0 : 1	9	
DOA/W02	DO11	1 : 5	9	
DOA/W03	DO11	1 : 4	9	Effect of ACE/H_2O
DOA/W04	DO11	1 : 3	9	ratio
DOA/W05	DO11	1 : 2	9	
DOA/W06	DO11	1 : 1.5	9	
DOpH01	DO11	1 : 4	3	
DOpH02	DO11	1 : 4	5	Effect of pH
DOpH03	DO11	1 : 4	7	
DOpH04	DO11	1 : 4	11	

Exp. No.	Probe Cpd.	TEA/ACE[e] Ratio (v/v)	Initial pH	Remarks
DOT/A01	DO11	1 : 644	9	Define the function of TEA in cocktail solution
DOT/A02	DO11	1 : 385	9	
DOT/A03	DO11	1 : 297	9	
DOT/A04	DO11	1 : 256	9	
DOT/A05	DO11	1 : 227	9	
DOT/A06	DO11	1 : 192	9	
DOT/A07	DO11	1 : 154	9	
DOT/A08	DO11	1 : 148	9	
DOT/A09	DO11	1 : 142	9	
DOT/A10	DO11	1 : 138	9	
DOT/A11	DO11	1 : 135	9	
DOT/A12	DO11	1 : 128	9	

[a] All sample solutions were determined at 253.7 nm in the Rayonet photoreactor with light intensity was equivalent to 1.5×10^{-5} Einstein L^{-1} s^{-1}.

[b] The concentration of dye was set at 20 mg L^{-1} for each experimental run.

[c] pH adjustment ± 0.1.

[d] Control experiments were prepared by dissolving the hydrophobic dye in deionized distilled water and shaken in a mechanical rotary shaker at 20°C for 24 hours to ensure dye saturation.

[e] For Exp. No. DOT/A01 – 12, the ACE/H_2O ratio was 1: 4 (v/v).

Table 3-4: Experiments performed on hydrophilic reactive dye (RR2[a]).

Exp. No.	[ACE], mol L^{-1}	[TEA], mol L^{-1}	Initial pH[b]	Light intensity, (Einstein L^{-1} s^{-1})	Remarks
RRACE01	-	-	11	1.5×10^{-5}	Effect of ACE
RRACE02	0.003	-	11	1.5×10^{-5}	
RRACE03	0.008	-	11	1.5×10^{-5}	
RRACE04	0.014	-	11	1.5×10^{-5}	
RRACE05	0.027	-	11	1.5×10^{-5}	
RRACE06	0.054	-	11	1.5×10^{-5}	
RRACE07	0.081	-	11	1.5×10^{-5}	
RRACE08	0.108	-	11	1.5×10^{-5}	
RRACE09	0.135	-	11	1.5×10^{-5}	
RRACE10	0.162	-	11	1.5×10^{-5}	
RRACE11	0.216	-	11	1.5×10^{-5}	
RRApH01	0.108	-	3	1.5×10^{-5}	Effect of pH
RRApH02	0.108	-	5	1.5×10^{-5}	
RRApH03	0.108	-	7	1.5×10^{-5}	
RRApH04	0.108	-	8.5	1.5×10^{-5}	
RRAN01	0.108	-	11	3.0×10^{-5}	Anion determination
RRTEA01	-	0.005	11	1.5×10^{-5}	Effect of TEA
RRTEA02	-	0.01	11	1.5×10^{-5}	
RRTEA03	-	0.02	11	1.5×10^{-5}	
RRTEA04	-	0.03	11	1.5×10^{-5}	
RRTEA05	-	0.04	11	1.5×10^{-5}	

RRTEA06	-	0.05	11	1.5×10^{-5}	
RRTEA07	-	0.06	11	1.5×10^{-5}	
RRTEA08	-	0.07	11	1.5×10^{-5}	
RRTpH01	-	0.04	3	1.5×10^{-5}	
RRTpH02	-	0.04	5	1.5×10^{-5}	Effect of pH
RRTpH03	-	0.04	7	1.5×10^{-5}	
RRTpH04	-	0.04	8.5	1.5×10^{-5}	
RRCT01	0.108	0.005	11	1.5×10^{-5}	
RRCT02	0.108	0.01	11	1.5×10^{-5}	
RRCT03	0.108	0.02	11	1.5×10^{-5}	Cocktail photo-sensitization
RRCT04	0.108	0.03	11	1.5×10^{-5}	
RRCT05	0.108	0.04	11	1.5×10^{-5}	
RRCT06	0.108	0.05	11	1.5×10^{-5}	
RRCTLI01	0.108	0.02	11	3.0×10^{-5}	
RRCTLI02	0.108	0.02	11	6.0×10^{-5}	
RRCTLI03	0.108	0.02	11	9.0×10^{-5}	Effect of light intensity
RRCTLI04	0.108	0.02	11	1.2×10^{-5}	
RRCTLI05	0.108	0.02	11	1.8×10^{-5}	

[a] Initial dye concentration utilized was 1.8×10^{-5} mol L^{-1}.

[b] pH adjustment ± 0.1.

3.4 DATA ANALYSIS

In order to quantitatively characterize the photochemical reactions, several mathematical procedures were performed as follows:

(1) Determination of kinetic rate constants (by integrated rate equations) and decay quantum yields;

(2) Stern-Volmer analysis of photochemical kinetics (rate enhancement and quenching effect on DO11 by TEA).

(3) Sensitivity analysis of the cocktail model.

3.4.1 Integrated Rate Equations

Pseudo First-order Reaction

From previous studies (Naomi *et al.*, 2000; Aranyosi *et al.*, 1999; Bandara *et al.*, 1996), under constant temperature, light intensity and illumination wavelength, the initial decay rates of the dyes in solution were generally postulated to follow the pseudo first-order reaction and could be determined by the integrated first-order decay expression:

$$\frac{d[D]}{dt} = -k_D[D] \quad \text{or} \quad [D]_t = [D]_0 e^{-k_D t} \tag{3.2}$$

where D_t = the concentration of dye at time t, mol L^{-1}

D_0 = the concentration of dye at time zero, mol L^{-1}

k_D = the first order decay rate constant, s^{-1}

Zero-order Reaction

Apart from the first-order decay reaction, unusual case of zero-order kinetic behavior might observe during the degradation process (Luis *et al.*, 2000; Wolfgang *et al.*, 1999). A zero-order reaction yields a linear plot of concentration versus time, the slope being equal to –k. It is evident that a zero-order rate constant has the units of rate, for example, mol L^{-1} s^{-1}.

$$d[D]/dt = -k \quad \text{or} \quad [D] = [D]_0 - kt \tag{3.3}$$

3.4.2 Quantum Yield Determination

Probably the most important concept in photochemical kinetics is that of the quantum yield Φ_D and it is defined as the efficiency of the photochemical reaction, that is, the number of dye molecules being decomposed per photon absorbed (Horspool, 1992; Choudhry & Webster, 1985):

$$\Phi_D = \frac{\text{No. of molecules reacted (or produced)}}{\text{No. of photons of light absorbed}} \tag{3.4}$$

The pseudo first-order decay rate constant of the dye, k_D under the monochromatic light source can be used for the calculation of its reaction quantum yield by the following Eq. 3.5 (Chu & Jafvert, 1994; Horspool, 1992):

$$\Phi_D = \frac{k_D}{2.303 \times I_{0,\lambda} \times \varepsilon_{D,\lambda} \times \ell} \tag{3.5}$$

where Φ_D is the reaction of quantum yield (dimensionless), $I_{0,\lambda}$ is the intensity of the incident light at 253.7 nm (Einstein L^{-1} s^{-1}), $\varepsilon_{D,\lambda}$ is the molar absorptivity of the dye at 253.7 nm (L mol^{-1} cm^{-1}) and ℓ is the cell path length (1 cm).

3.4.3 Sensitivity Analysis

Sensitivity analysis is a powerful tool for the understanding of the relevant chemistry by focusing the attention on the most significant reactions and guiding future research to reduce critical uncertainties. Sensitivity analysis of kinetic model permits an estimation of the effects of parameter variations, can help assess uncertainties, and distinguishes important from unimportant model features (Eisenberg *et al.*, 1998).

Such analysis often provides important clues as to the dominant mechanisms occurring in complex system. This technique has been extensively used to study photochemical chemistry (Alberto & Russell, 2000; Yang *et al.*, 1997). Sensitivity analysis quantifies the effect that single parameter (or independent variables, α_j) variations have on model outputs (or dependent variables, y) (Vuilleumier *et al.*, 1997):

$$y_{a_j} = \partial y / \partial \alpha_j \approx \left[y(\alpha_j + \Delta\alpha_j) - y(\alpha_j) \right] / \Delta\alpha_j \qquad (3.6)$$

which enables the study of the interactions, within the frame of the model, among all kind of parameters used (e.g. initial concentrations or reaction rate parameters).

CHAPTER 4 RESULTS AND DISCUSSION I : PHOTODEGRADATION OF HYDROPHOBIC DYE

4.1 Acetone-Photosensitization Of Disperse Dye

To optimize the photodegradation of dyes in aqueous ACE solutions and reduce the potential cost of ACE used as a sensitizer and solvent in a large quantity, the adjustment of ACE/H_2O ratios was necessary. The photodegradation of a typical disperse dyes (DY7 and DO11) with different chromophores in the aqueous ACE solution was studied by a series of experiments.

4.1.1 Photolysis at Different Ratios of ACE/H_2O

The photodegradation of DY7 and DO11 in various ratios of aqueous ACE solution and in water alone are shown in Figure 4.1 and Figure 4.2 respectively. Control experiments (*i.e.* direct photolysis of selected dyes in distilled water) were also carried out at the same conditions in the absence of ACE. Results indicate that the photodegradation (or photodecolorization) reactions mainly followed pseudo first-order kinetics, with the exception of the water sample. The rate expression can be expressed as:

$$\frac{d[D]_t}{dt} = -k_A[D]_t \qquad (4.1)$$

where the k_A is the pseudo first-order rate constant and $[D]_t$ is the concentration of the disperse dye in the solution.

According to the decay quantum yields as shown in Table 4-1, the quantum yield of direct photolysis of DY7 measured in the water phase was very low (9.03×10^{-5}), and the decay quantum yield of DO11 was undetectable because of the low solubility of disperse dye in water (normally much less than 1g L^{-1}). If the direct photolysis quantum yields were compared to that of optimal conditions in Table 4-1, more than ten times of performance increments were observed after the addition of ACE to the solution. The difference was likely because the photodecolorization of disperse dye in water could only go through the slower direct-photolysis mechanism, rather than the faster photosensitization process.

Theoretically in a photosensitization process, after the photo-sensitizer (ACE) exposes to UV, it absorbs the light energy (hv) and will be transformed from its ground-state into its excited-state (Horspool, 1992). The intermolecular interactions between the excited triplet ACE (ACE^*) and the dye molecule (D) then will initiate an energy transfer between the two molecules. Dye in such excited states (D^*) are more reactive and short lived, and will either decay back to their ground states by losing their excitation energy in some physical ways or undergo chemical reactions and lead to the decay of the dye, as shown in following Scheme 4.1.

$$ACE \xrightarrow{hv} ACE^*$$

$$D + ACE^* \rightarrow D^* + ACE$$

$$\downarrow$$

$$decayed\ \ dye$$

Scheme 4.1

In the photodegradation process, the chromophore of the dye molecule can be broken down by abstracting hydrogen atoms from the solution (Horspool, 1992). For azo type disperse dyes such as DY7, the reductive cleavage of the azo group (-N=N-) is likely the dominant mechanism because the electrons of these π-bonds are comparatively more diffusive than the other parts within the molecule. Therefore, the chromophore of the azo dyes can be reduced and converted to its corresponding amines involving the hydrogen atom abstraction from the aqueous solution and is described by Eq. 4.2. For anthraquinone disperse dyes, such as DO11, photoreduction is most likely attributed to the carbonyl group (9- and 10- positions) which can be reduced to the colorless leuco form of hydroquinone in the presence of hydrogen sources as shown in Eq. 4.3. ACE, in addition to act as a photosensitizer, may also serve as a hydrogen source for color removal in these cases, since there is no other hydrogen sources available in the solution.

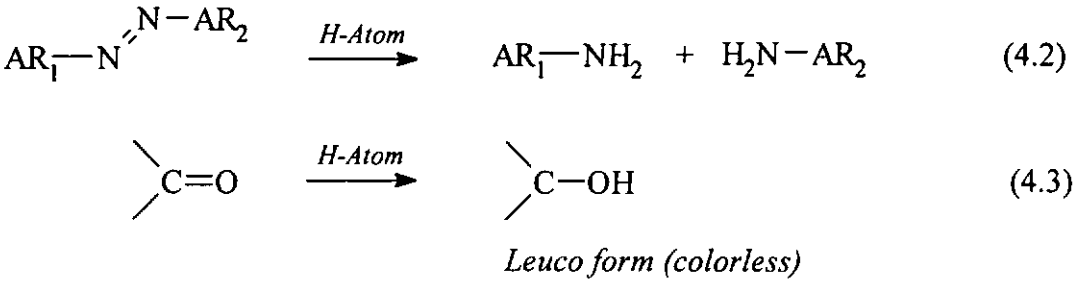

From Table 4-1, the decay quantum yields normally increase with the ACE/H_2O ratios, and are optimized at the ratios of 1:2 and 1:4 (v/v) for DY7 and DO11, respectively. It is important to note that the re-crystallization of the dye molecules in the aqueous phase was observed if the ACE/H_2O ratio dropped below the optimal ratios, which caused a decrease in the overall photodecay rate. This was apparently

because some of the dye molecules now resided in the hydrophilic aqueous phase, not the hydrophobic phase (*i.e.* the phase of aqueous ACE). In the aqueous phase, only the direct-photolysis mechanism was available for dye decay, so, the overall performance of the photodecay was reduced. It is interesting to see that the further increase of ACE/H_2O ratio above 1:2 (v/v) would lower the rate of photosensitization, too. This could be because the ACE itself can consume photons emitted from UV lamps and giving off the energy in the forms of heat, phosphorescence or fluorescence. If the concentration of ACE is too high in the solution, the acetone becomes a light barrier and will absorb and consume most of the photons without contributing to the sensitization reaction (the molar absorptivity of ACE at 253.7nm is 11 M^{-1} cm^{-1} (Chu & Jafvert, 1994)), which indirectly causes the attenuation of light intensity available for dye degradation. An ACE/H_2O ratio of 1: 2 for DY7 and 1: 4 for DO11 (v/v) were therefore suggested and used for further investigation in this study.

Table 4-1: Decay quantum yields of DY7 and DO11 in different ACE/H_2O ratios at 253.7 nm[a].

	DY7[b]			**DO11**[c]	
ACE/H_2O (v/v)	$k_{A,DY}$ (s^{-1})	Φ_{DY7}	ACE/H_2O (v/v)	$k_{A,DO}$ (s^{-1})	Φ_{DO11}
0 : 1.00	7.15×10^{-5}	9.03×10^{-5}	0 : 1	Nil.	≈ 0
1 : 2.33	5.40×10^{-4}	6.81×10^{-4}	1 : 5	1.14×10^{-3}	5.65×10^{-2}
1 : 2.13	6.80×10^{-4}	8.57×10^{-4}	1 : 4	1.44×10^{-3}	7.13×10^{-2}
1 : 2.00	1.13×10^{-3}	1.42×10^{-3}	1 : 3	1.35×10^{-3}	6.69×10^{-2}
1 : 1.78	7.12×10^{-4}	8.97×10^{-4}	1 : 2	1.15×10^{-3}	5.70×10^{-2}
1 : 1.00	6.78×10^{-4}	8.55×10^{-4}	1 : 1.5	0.97×10^{-3}	4.80×10^{-2}
2 : 1.00	6.43×10^{-4}	8.11×10^{-4}			
3 : 1.00	6.40×10^{-4}	8.07×10^{-4}			

[a] Decay rate constants and quantum yields were determined at 253.7 nm in the Rayonet reactor with light intensity = 1.5×10^{-5} Einstein L^{-1} s^{-1}.

[b] Molar absorptivity of DY7 at 253.7 nm = 22970 L mol^{-1} cm^{-1} and the initial solution pH = 7.

[c] Molar absorptivity of DO11 at 253.7 nm = 584 L mol^{-1} cm^{-1} and the initial solution pH = 9.

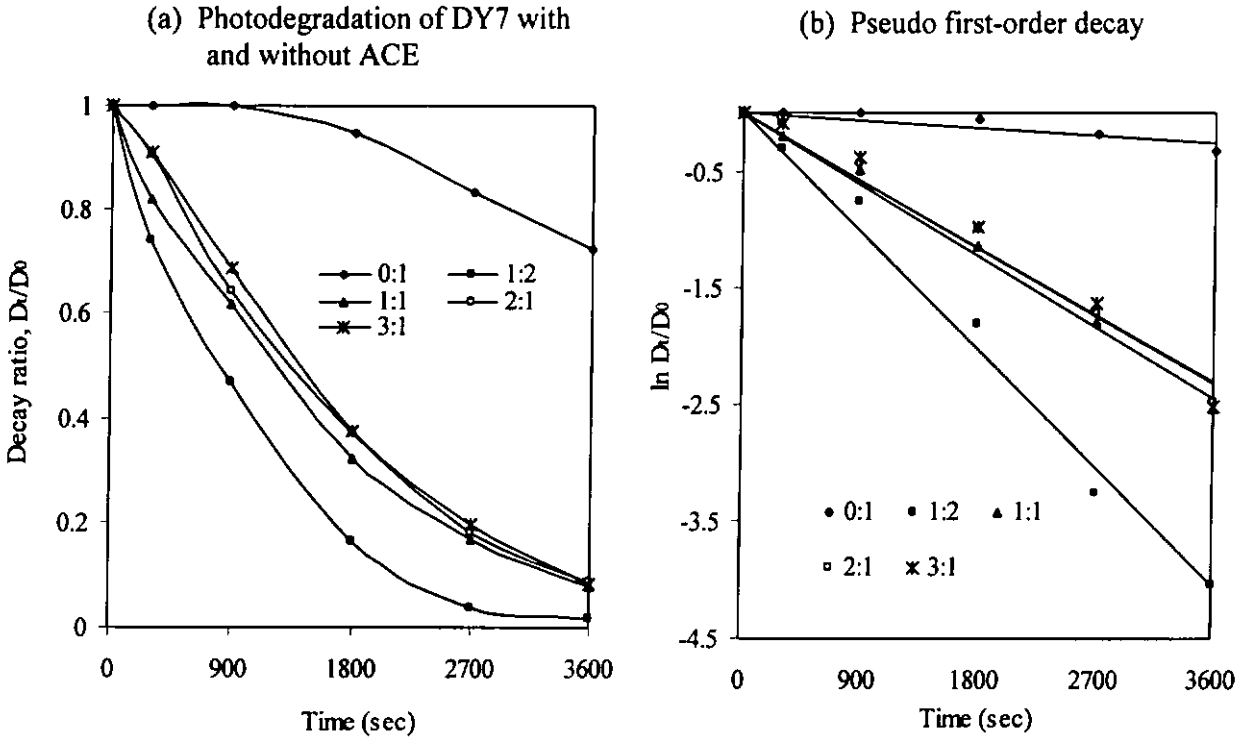

Figure 4.1: The photodegradation of DY7 in different ACE/H_2O (v/v) ratios at 253.7 nm and initial pH 7.

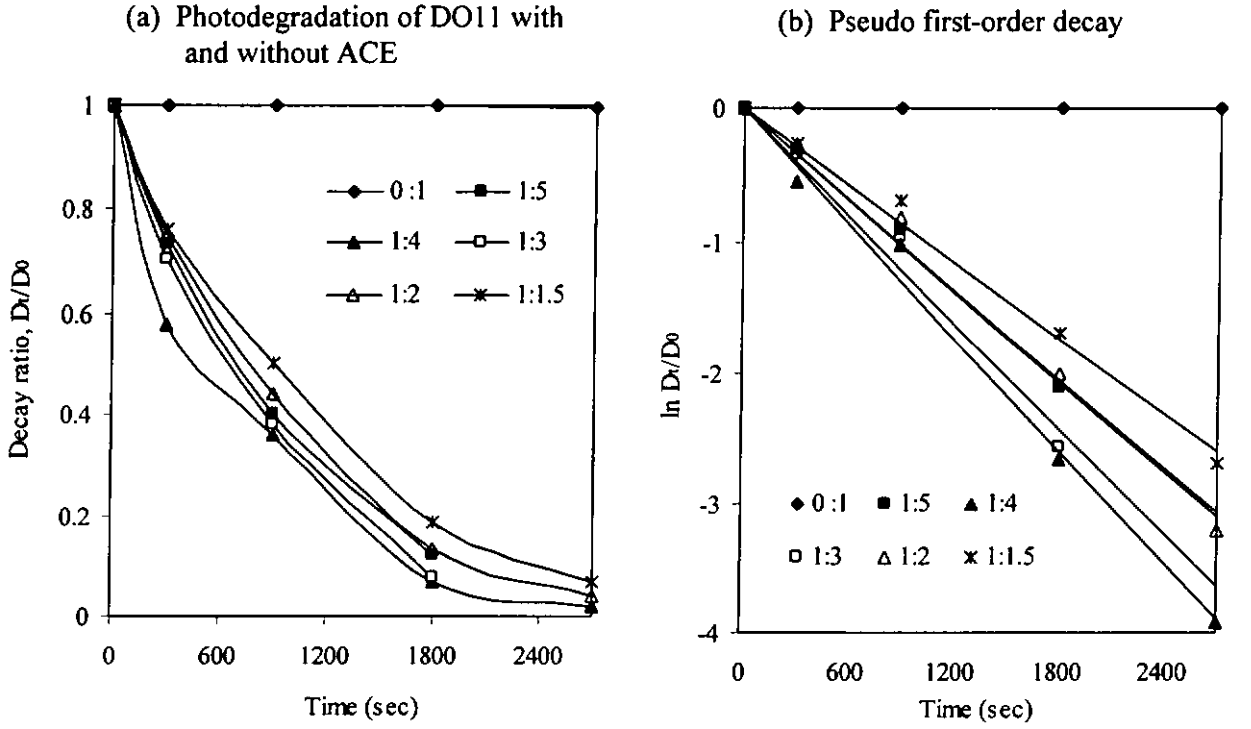

Figure 4.2: The photodegradation of DO11 in different ACE/H_2O (v/v) ratios at 253.7 nm and initial pH 9.

4.1.2 Effect of Initial pH

Figure 4.3 demonstrates the photosensitization of DY7 and DO11 at different initial pHs as the ACE/H_2O ratio is at its optimum (1: 2 and 1: 4 (v/v) respectively). The photodecay of disperse dyes in aqueous ACE solution at different initial pHs follow pseudo first-order kinetics. The pseudo first-order rate constants and reaction quantum yields at various initial pHs are summarized in Figure 4.5 and Table 4-2, respectively. The experimental data fit the pseudo first order kinetics quite well, as the correlation coefficient, r^2, ranged from 0.9833 to 0.9986.

It is important to point out that the solution pH decreases during the photolysis process, as shown in Figure 4.4. Comparing Figures 4.3 and 4.4, the decline in pH is accompanied by a reduction in dye concentration, which suggests that the proton is one of the major end products of the photosensitization reaction. In addition, the proton generated in the reaction is counter-proportional to the decay rates, *i.e.* the higher the proton formation, the lower the reaction rate (see the comparison in Table 4-2), which strongly implies that the generation of protons may inhibit the photodegradation process.

According to the experimental observations, the overall photosensitization rates increased as the initial pH increased, as shown in Figure 4.3. The results showed that the photosensitization rate of DY7 and DO11 increased from 0.09×10^{-3} s^{-1} at pH 4 to 1.29×10^{-3} s^{-1} at pH 11 and from 1.27×10^{-3} s^{-1} at pH 3 to 1.44×10^{-3} s^{-1} at pH 9 respectively. The relatively low photosensitization rates in the acidic solution were

probably retarded by the high proton (H^+) concentration that was originally introduced to the solution. In an alkali condition, the hydroxide ion (OH^-) in the original solution might neutralize the acidic products of photodegradation, and therefore accrete the forward reaction (*i.e.* the dye decay and proton producing), in which the highest photosensitization rate was observed.

On the other hand, hydroxyl and hydroperoxyl radicals will be generated when UV is absorbed by water in the presence of oxygen at high pH (Chu & Ma, 1998). It is very likely that the photodecolorization of disperse dye is partly contributed by free radical reaction in which the hydroxyl and hydroperoxyl radicals are involved. Therefore, the rate law of the dye decolorization solely due to free radical reaction at elevated pH might be expressed as Eq. 4.4.

$$\frac{d[D]}{dt} = -\left(k_{OH}[OH\bullet] + k_{OOH}[OOH\bullet]\right)[D] \tag{4.4}$$

where $[OH\cdot]$ is the concentration of hydroxyl radicals, $[OOH\cdot]$ is the concentration of hydroperoxyl radicals, and k_{OH} and k_{OOH} are the respective kinetic rate constants. By combining the photosensitization pathway (Eq. 4.1) and free radical pathway (Eq. 4.4), the overall rate law of the dye decay will be:

$$\frac{d[D]}{dt} = -\left(k_{OH}[OH\bullet] + k_{OOH}[OOH\bullet] + k_A\right)[D] \tag{4.5}$$

Since the formation of the free radicals OH· or OOH· solely depends on the UV light absorption, the concentration of free radicals in the solution are assumed to close to a

constant (*i.e.* at steady state) as excess photons can be absorbed by aqueous phase during the reaction. The Eq. 4.5 could be further simplified as follows:

$$\frac{d[D]}{dt} = -k_{Overall}[D] \tag{4.6}$$

where the $k_{Overall}$ is the overall (pseudo first-order) rate constant. Therefore, the photodecay of hydrophobic disperse dye DY7 or DO11 at high pH follows pseudo-first-order reaction in which the photosensitization and free radical reactions are involved.

It is interesting to find that at extreme high pH levels (*i.e.* at initial pH 11) the photodecay rate of DO11 significantly decreases to the lowest measurement of 1.01×10^{-3} s^{-1} (Figure 4.5), and the pattern of solution pH throughout the photolysis is different from the other pHs (Figure 4.4), indicating that another mechanism is involved. The retardation of photodegradation at pH 11 is likely due to the structural change of anthraquinone dye.

Allen (1994) stated that at high pH levels, substituents of an electron-donating group such as amino groups in the α-positions (*e.g.* 1-, 4-, 5- or 8-) to the carbonyl group on the anthraquinone chromophore are capable of forming an intramolecular hydrogen bond (Scheme 4.2), which is theoretically more chemically stable than the molecules without hydrogen bonds (*i.e.* at lower pH levels). Upon the absorption of light energy, the dye structure changes from a stable keto form in the ground state to a less stable enol form in the excited state. This enol form will mostly give off its absorbed

energy rapidly in the form of heat and return to the keto form, thus preserving the dye structure intact (Rys & Zollinger, 1972) and therefore reducing the photodegradation rates.

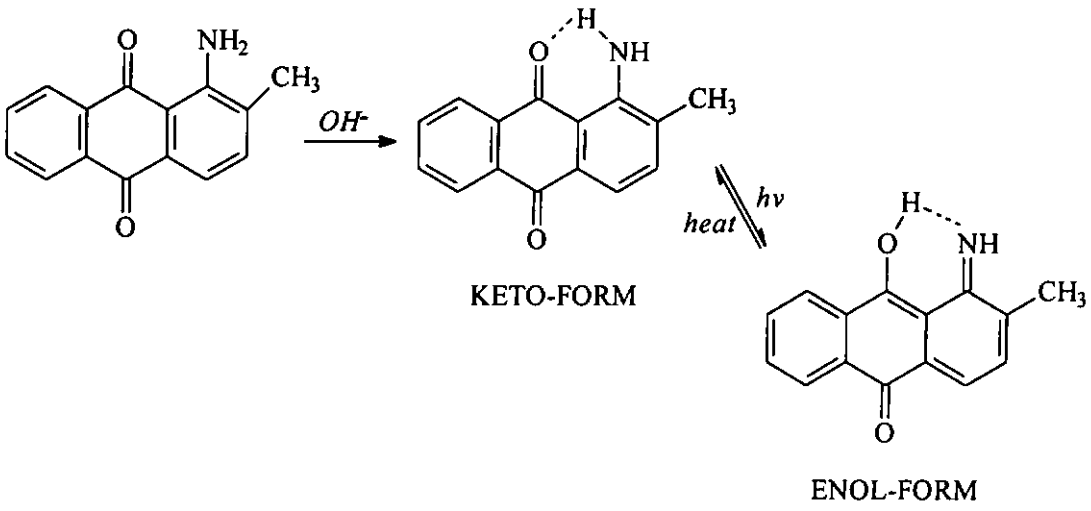

Scheme 4.2

Table 4-2: Regression results of decay of DY7 and DO11 in ACE/H_2O solution at different pH according to the pseudo first-order kinetics.

Initial pH	Final pH	$[H^+]$ generated, mol/L	Quantum Yield Φ	r^2 for rate constant
		DY7 (1:2 v/v)		
4.0	3.7	1.24×10^{-4}	1.06×10^{-3}	0.9934
5.5	4.2	6.76×10^{-5}	1.30×10^{-3}	0.9898
7.0	4.3	5.61×10^{-5}	1.43×10^{-3}	0.9879
9.0	4.5	3.16×10^{-5}	1.56×10^{-3}	0.9970
11.0	5.2	6.31×10^{-6}	1.63×10^{-3}	0.9986
		DO11 (1:4 v/v)		
3.0	2.7	7.91×10^{-4}	6.29×10^{-2}	0.9969
5.0	3.2	6.23×10^{-4}	6.49×10^{-2}	0.9833
7.0	3.8	1.51×10^{-4}	6.93×10^{-2}	0.9935
9.0	3.9	1.32×10^{-4}	7.13×10^{-2}	0.9907
11.0	7.0	1.02×10^{-7}	5.00×10^{-2}	0.9961

[a] The final pHs were measured after 2700 sec. of UV irradiation.

[b] Decay rates and quantum yields were determined at 253.7 nm in the Rayonet reactor with light intensity = 1.5×10^{-5} Einstein L^{-1} s^{-1}.

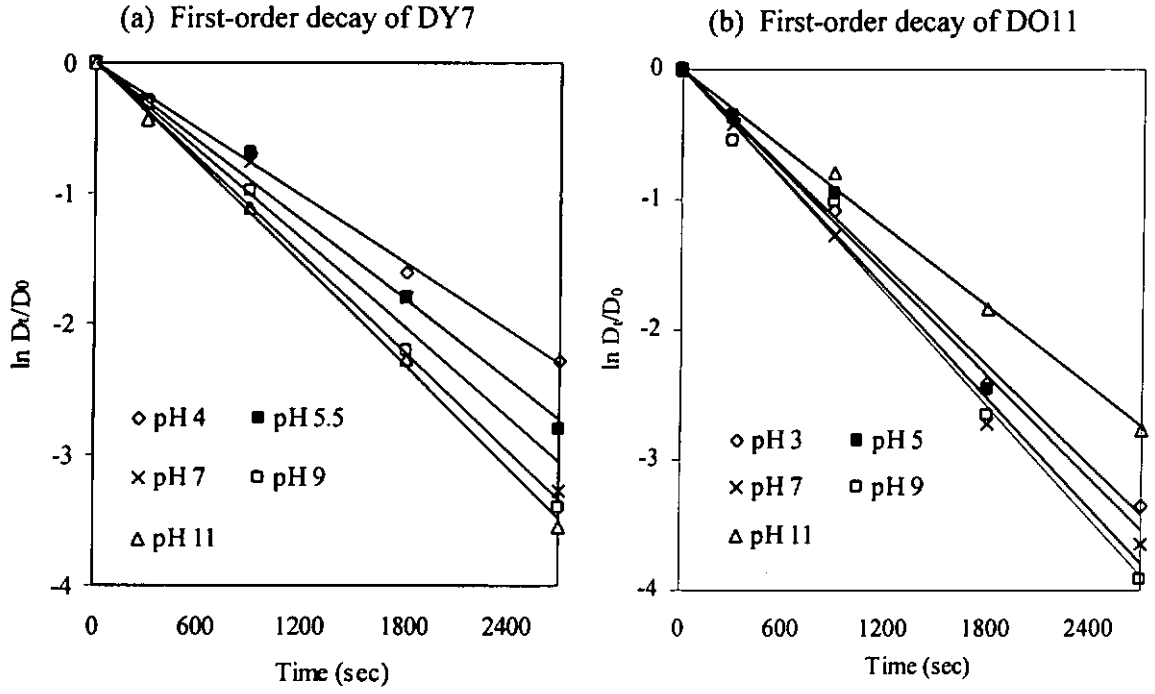

Figure 4.3: First-order decay of DY7 and DO11 in 1:2 and 1:4 (v/v) respectively ACE/H_2O solution at different initial pHs.

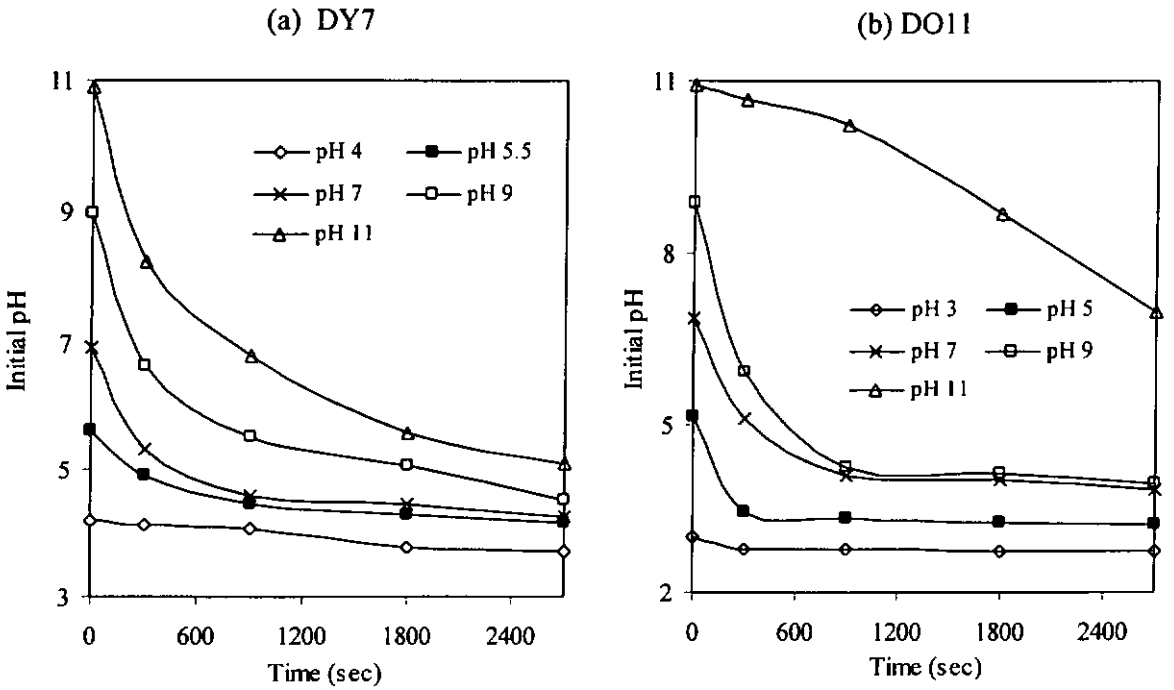

Figure 4.4: The change of solution pH throughout the photosensitization process at different initial pH levels.

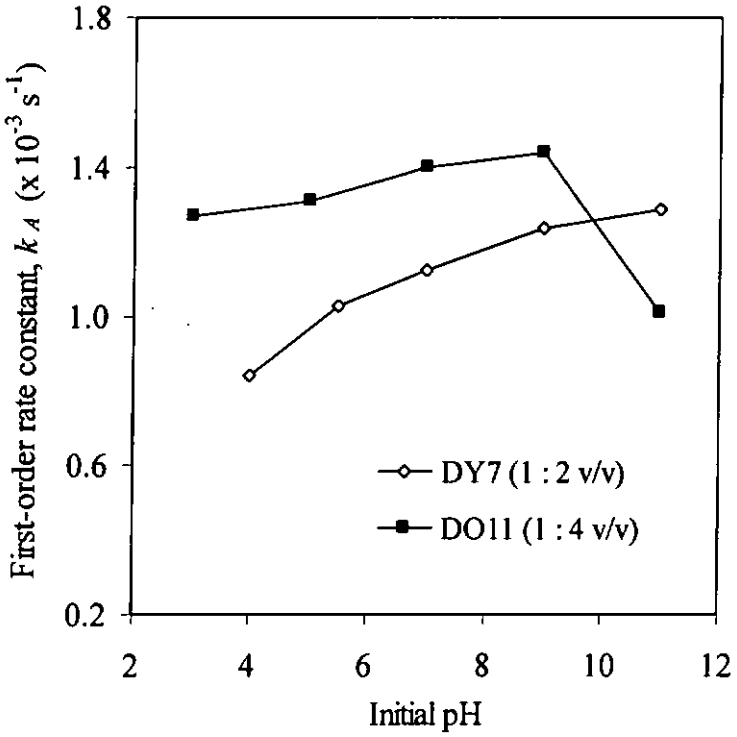

Figure 4.5: The effect of initial pH to the pseudo first-order decay rate constants.

4.1.3 Applications

During photochemical degradation, the large dye molecules can be split into smaller fragments (Ince, 1999; Liu *et al.*, 1999; Tratnyek *et al.*, 1994). For the azo disperse dye such as DY7 the electrons of the π-bonds (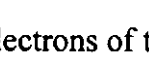) are more diffuse, so the cleavage would probably take place on those bonds. Figure 4.6 shows that the photoproducts contributed a higher COD content than their parent compound (*i.e.* DY7), indicating that the photolysis of dyes was quite effective and complete. The BOD_5/COD ratio was also investigated, and it was found to increase from 0.207 before treatment to 0.438 after 5400 seconds of photolysis. The increase of the BOD_5/COD ratio after UV-photolysis indicated that the final products of the photosensitization process became more biodegradable. Therefore, the treatment performance of biological units (*e.g.* activated sludge process) that generally follows photodegradation will be greatly improved.

For field application, it is suggested recovering the ACE after the photolysis process to reduce chemical costs and minimize the impact on the environment. ACE is among the solvents which have comparatively low acute and chronic toxicity, so the purging method was selected for ACE recovery at room temperature, due to its moderate Henry's constant (2.5×10^{-5} atm·m^3/mol), low boiling point (56°C), and the potential to increase the dissolved oxygen for ensuring biological treatment. Figure 4.7 demonstrates that more than 95% ACE recovery can be achieved with respect to the quantity of air applied. The dissolved oxygen in the solution reached saturation after 60% of the ACE was recovered, which might be a critical control boundary for

system design. A high performance device (such as stripping tower) was suggested to recover the first 60% of the ACE, with the remaining 30 to 35% of ACE recovered during the ensuing aerobic biological process, where aeration is also available, so that the total air consumption can be minimized.

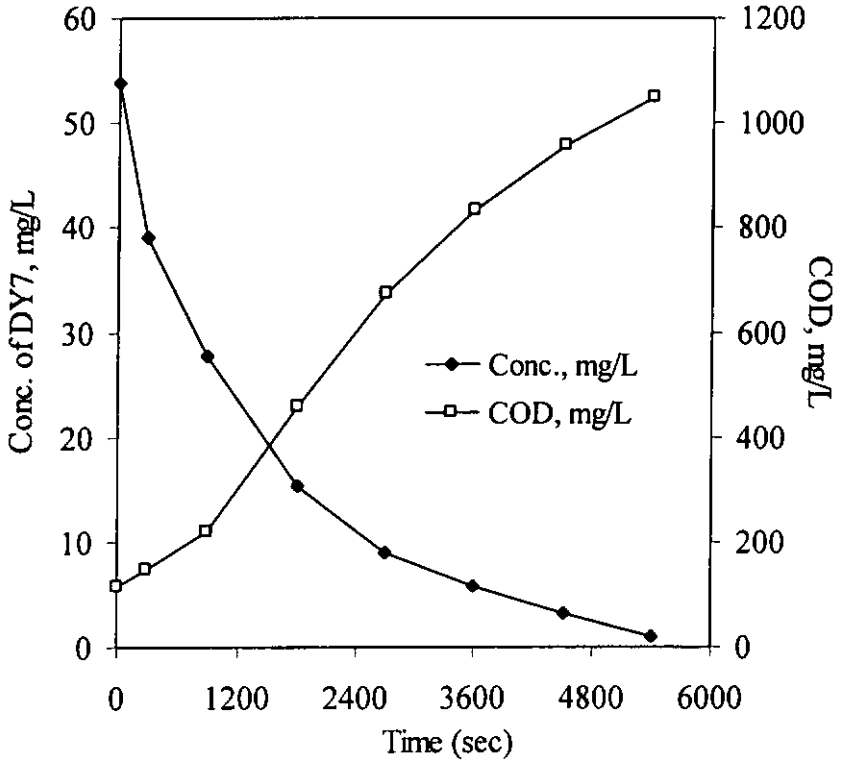

Figure 4.6: The variation of COD with the degradation of DY7 in aqueous ACE (1 : 2 v/v) at 253.7 nm.

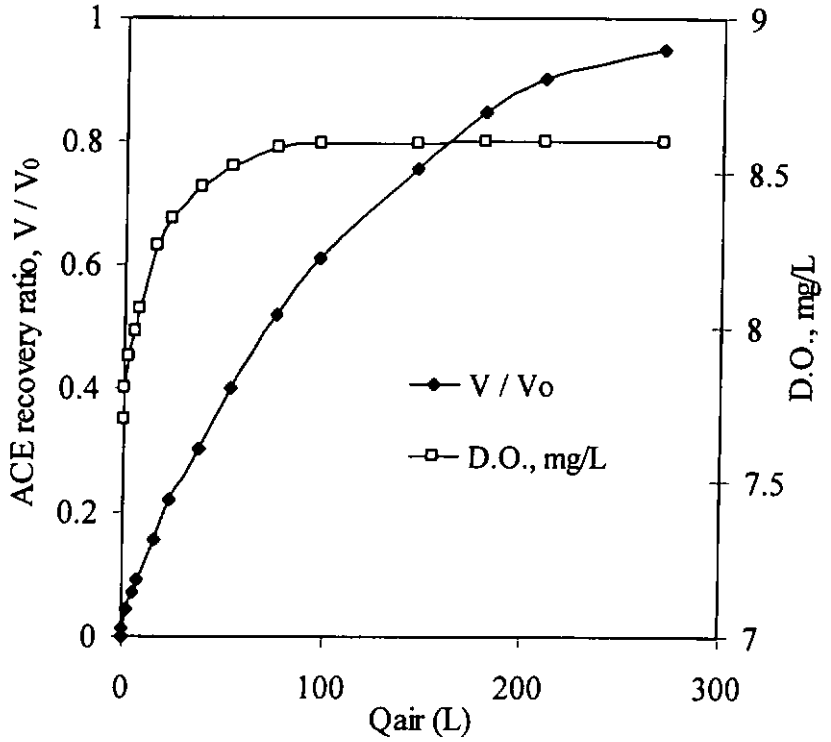

Figure 4.7: The rate of ACE recovery and variation of dissolved oxygen (D.O.) at 0.5 L min^{-1} of air flowrate, where V is the ACE recovery volume and V_0 is the initial ACE volume.

4.2 Cocktail-Photodegradation Of Disperse Dye

The photodegradation (at λ = 253.7 nm) of a typical anthraquinone disperse dye (DO11) in an aqueous ACE solution and in the presence of triethylamine (TEA) is investigated. Anthraquinone disperse dyes are known to have very low photodegradation rates in the natural environment because of their low solubility. The importance of ACE in the photosensitization of hydrophobic dyes has been proven in Chapter 4.1 that it acts not only as a solvent to increase the dye's solubility but also as a photosensitizer to enhance the dye's decay rate. Since the photoreduction reaction is found to be the dominant for dye-decolorizing, it is possible that photosensitization can be further enhanced if an additional hydrogen source (*i.e.* electron donors) is co-existent in the solution.

4.2.1 Photosensitization Process in the Presence of Hydrogen Source

Though the photodegradation rates of anthraquinone disperse dye are greatly increased in aqueous ACE solutions, the adding of additional hydrogen source may further promote the reaction. The photolysis of DO11 at different TEA concentrations (in ACE/H_2O ratio of 1:4 and at an initial pH of 9) was investigated. The decay rate constants (k_D) were found firstly to increase with [TEA], however after reaching a maximum rate at 5.21×10^{-3} s^{-1}, more TEA addition inhibited the photolysis rates (Figure 4.8). At low [TEA] concentrations, the increase of the decay rates is mainly due to two reasons. First, TEA may neutralize the acidic end product (protons, which have a retardation effect on the photolysis reaction) out of the

solution and enhance the photolysis reaction, since the nitrogen center of the TEA molecule exerts an exposed lone pair electron that can receive a proton (Eq. 4.7). As shown in Table 4-3, the total proton generation of the reactions gradually decreased as [TEA] increased. Therefore, in this mechanism, TEA acts as a proton acceptor and a rate enhancement of over 27% was observed compared to that without the addition of TEA.

$$CH_3CH_2-\ddot{N}(C_2H_5)_2 \;+\; \underset{\text{(proton generated from photolysis)}}{H^+} \longrightarrow CH_3CH_2-\overset{H}{\overset{\uparrow}{N}}(C_2H_5)_2 \qquad (4.7)$$

Secondly, TEA is a good electron donor and/or hydrogen source as well, previous studies having suggested that aliphatic amine might assist in photodechlorination (Chu & Jafvert, 1994), photoinitiation (Encinas *et al.*, 1994) and photoreduction (Säuberlich *et al.*, 1997) reactions. In the photoreduction of DO11 with the presence of TEA, as shown in Scheme 4.3, one hydrogen atom is transferred from TEA to the excited dye D^*, creating an iminium ion derivative and a reduced dye, the colorless leuco form, DH_2 (Kagan, 1993). Scheme 4-3 illustrates that the major function of TEA at low concentration is as a hydrogen source, and therefore rate enhancement of the photoreduction of anthraquinone dye with higher quantum yields is observed at low [TEA].

$$D_{\text{insoluble}} \xrightarrow{ACE} D_{\text{soluble}}$$

$$\left.\begin{aligned} ACE + h\nu &\longrightarrow ACE^{*} \\ D + ACE^{*} &\longrightarrow D^{\bullet} + ACE \end{aligned}\right\} \textit{Photosensitization}$$

$$\left.\begin{aligned} CH_3CH_2-\ddot{N}(C_2H_5)_2 + D^{*} \rightarrow\ & CH_3CH_2-\overset{+\bullet}{\ddot{N}}(C_2H_5)_2 + D^{\bullet-} \\ & \downarrow \\ & CH_3\dot{C}H-\ddot{N}(C_2H_5)_2 + \dot{D}H \\ & \downarrow \\ & CH_3CH=\overset{+}{N}(C_2H_5)_2 + {}^{-}DH \\ & \text{(iminium ion)} \qquad \downarrow \\ & DH_2 \\ & \text{(reduced leuco form)} \end{aligned}\right\} \text{Photoreduction}$$

Scheme 4-3: The photochemical reaction of excited dye (D^{*}) in the presence of TEA as an electron donor (or hydrogen source).

As the [TEA] is overdosed, inhibition of reaction is observed. The photoreduction rate of DO11 reaches a maximum value of 1.83×10^{-3} s^{-1} at the TEA/ACE molar ratio of 1:192 and decreases gradually at higher ratios (Figure 4.8). Similar observations have been reported by Encinas *et al.* (1994) on the photoinitiation of a fluorenone/TEA system in the polymerization process, indicating that TEA is possibly a quencher on deactivation of the excited states. TEA functioning as both a hydrogen source to promote the photoreaction and a quencher to retard the photoreaction is very important for environmental applications. Its reaction mechanisms, therefore, are proposed and examined in the following section.

Table 4-3: The photolysis of DO11 in ACE aqueous solution[a] at pH 9 in the presence of TEA.

TEA/ACE, M/M	Final pH[b]	$[H^+]$ generated, mol L^{-1}	Decay rate[c], $\times 10^{-3}$ s^{-1}	Quantum Yield Φ
0 : 1 (no TEA)	3.89	1.29×10^{-4}	1.44	0.0713
1 : 644	4.23	5.89×10^{-5}	1.53	0.0756
1 : 385	4.30	5.01×10^{-5}	1.68	0.0830
1 : 297	4.45	3.55×10^{-5}	1.78	0.0882
1 : 256	4.56	2.75×10^{-5}	1.80	0.0891
1 : 227	4.60	2.51×10^{-5}	1.82	0.0903
1 : 192	4.64	2.29×10^{-5}	1.83	0.0906
1 : 154	4.80	1.58×10^{-5}	1.82	0.0901
1 : 148	4.87	1.35×10^{-5}	1.74	0.0862
1 : 142	5.01	9.77×10^{-6}	1.61	0.0796
1 : 138	5.32	4.79×10^{-6}	1.58	0.0782
1 : 135	5.54	3.98×10^{-6}	1.55	0.0770
1 : 128	6.96	1.10×10^{-7}	1.53	0.0758

[a] The ACE/H_2O ratio was 1:4 (v/v).

[b] The final pH was measured at 1800 sec. of UV irradiation.

[c] Decay rates were determined at 253.7 nm in the Rayonet merry-go-round reactor.

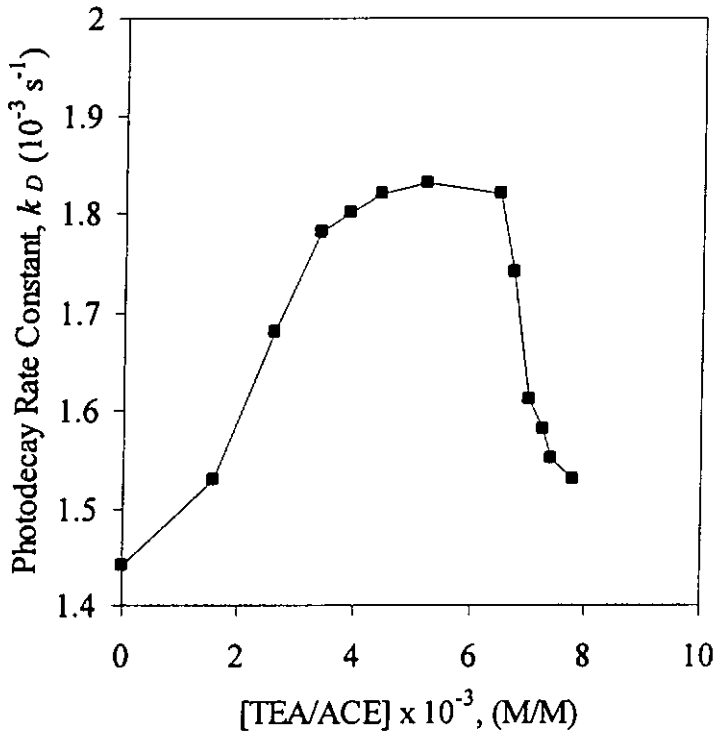

Figure 4.8: Rate constant of the photodegradation of DO11 within 1:4 (v/v) ACE/H_2O ratio at pH 9 at different TEA concentrations.

4.2.2 Proposed Reaction Models Involving TEA

Quenching effects normally can be studied through the classic Stern-Volmer analysis, which postulates that a reaction mechanism involves a competition between decay of the probe molecule in the excited state (D^*) and a bimolecular quenching reaction involving D^* and the quencher (TEA). In this study, this technique was also used to predict the bimolecular rate-enhancing reaction involving D^* and the hydrogen source (TEA). The photodegradation of DO11 (D) within the aqueous ACE in the presence of hydrogen source and/or quencher (TEA) may result in the following complex series of kinetic expressions:

Sub-Reactions	Rate	Process	
$ACE + hv \rightarrow ACE_1^*$		Irradiation	(4.8)
$ACE_1^* \rightarrow ACE_3^*$	$k_{isc}[ACE^*]$	Intersystem crossing	(4.9)
$D_0 + ACE_3^* \rightarrow D_1^* + ACE$	fI	Sensitization	(4.10)
$ACE_1^* + TEA \rightarrow ACE_1 + TEA_3^*$	$k_a[D_1^*][TEA]$	Quenching of sensitizer	(4.11)
$D_1^* \rightarrow D_0 +$ heat	$k_{d1}[D_1^*]$	Deactivation of singlet	(4.12)
$D_1^* \rightarrow D_0 + hv'$	$k_f[D_1^*]$	Fluorescence	(4.13)
$D_1^* \rightarrow D_3^*$	$k_{isc}[D_1^*]$	Intersystem crossing	(4.14)
$D_3^* \rightarrow D_0 + hv''$	$k_p[D_3^*]$	Phosphorescence	(4.15)
$D_3^* \rightarrow D_0 +$ heat	$k_{d3}[D_3^*]$	Deactivation of triplet	(4.16)
$D_3^* + TEA \rightarrow D_0 + TEA_3^*$	$k_q[D_3^*][TEA]$	Quenching of triplet	(4.17)
$D_3^* + TEA \rightarrow$ Product	$k_r[D_3^*][TEA]$	Chemical reduction	(4.18)

Scheme 4.4

The inclusion of all sub-reactions in developing a model would lead to an extremely complex kinetic expression, which would be difficult to be verified. Therefore, several assumptions may be made based on earlier observations or hypotheses regarding the specific mechanisms of transformation, which result in considerable simplification of the kinetic expression. If the intersystem crossing is efficient compared with all other singlet processes, a simplified Scheme 4.5 can be proposed:

Sub-Reactions	Rate	Process	
$D_0 + h\nu \rightarrow D_1^* \rightarrow D_3^*$	$\alpha f I$	Sensitization / Intersystem crossing	(4.19)
$D_3^* + TEA \rightarrow$ Product	$k_r[D_3^*][TEA]$	Chemical reduction reaction	(4.20)
$D_3^* \rightarrow D_0$	$k_d[D_3^*]$	Triplet deactivation / Phosphorescence	(4.21)
$D_3^* + TEA \rightarrow D_0 + TEA_3^*$	$k_q[D_3^*][TEA]$	Quenching of triplet	(4.22)

Scheme 4.5

where I is the illuminating intensity, f is the efficiency of light absorption and α is the intersystem crossing efficiency.

I. Modeling the Rate Enhancement by TEA as a Hydrogen Source

At low [TEA], quantum yield Φ_D increases with the increase of [TEA], indicating that the quenching effect is insignificant. Therefore, Eq. 4.22 can be neglected from Scheme 4.5 and only Eq. 4.19-4.22 will be used to develop the model. Since the D_3^* is short-lived that it does not accumulate to an appreciable level in the solution, a steady-state approximation can be made (Espenson 1981),

$$\frac{dD_3^*}{dt} = \alpha fI - k_d\left[D_3^*\right][TEA] = 0 \qquad (4.23)$$

therefore,

$$\alpha fI = (k_r[TEA] + k_d) \times \left[D_3^*\right] \qquad (4.24)$$

Since the concerned quantum yield (Φ_D) of our concern is the chemical decay (reduction) of D, the quantum yield can therefore be defined in Eq. 4.26, which actually is merged from Eqs. 3.5 and 4.24,

$$\Phi_D = \frac{k_r[D_3^*][TEA]}{fI} = \frac{k_r\alpha[TEA]}{k_r[TEA] + k_d} \qquad (4.25)$$

Taking the reciprocal of Eq. 4.25 results in a linear rate-enhancing model with an intercept of $1/\alpha$ and a slope of $k_d/k_r\alpha$.

$$\frac{1}{\Phi_D} = \frac{1}{\alpha} + \frac{k_d}{k_r\alpha} \times \frac{1}{[TEA]} \qquad (4.26)$$

When the [TEA] is lower than 1.19×10^{-2} mol L^{-1}, a plot of $1/\Phi_D$ vs. $1/[TEA]$ in Figure 4.9 shows a very good correlation ($r^2 = 0.9903$, only the lowest five [TEA] concentrations are used for correlation), which verifies the major function of TEA as a

hydrogen source if the TEA concentration is low. Beyond this low [TEA] range, the Eq. 4.26 will over estimate the Φ_D (*i.e.* the highest two [TEA] points in Figure 4.9), indicating the involvement of triplet quenching by TEA becoming perceptible.

II. Modeling the Retardation Effect of TEA as a Quencher

At high [TEA], where the hydrogen source is abundant, it is reasonable to assume that the TEA concentration remains a constant throughout the reaction, therefore Eq. 4.20 can be modified to:

$$D_3^{\bullet} + HS \rightarrow produuct \qquad Rate = k_r'[D_3^{\bullet}] \qquad (4.27)$$

where $$k_r' = k_r[TEA] \qquad (4.28)$$

Considering the Eqs. 4.19, 4.21, 4.22 and 4.27, and again according to the steady-state assumption,

$$\frac{dD_3^{\bullet}}{dt} = \alpha \text{fI} - k_r'[D_3^{\bullet}] - k_d[D_3^{\bullet}] - k_q[D_3^{\bullet}][TEA] = 0 \qquad (4.29)$$

The quantum yield (Φ_D) of the dye decay can be reformulated as:

$$\Phi_D = \frac{k'_r[D_3^{\bullet}]}{\text{fI}} = \frac{k'_r \alpha}{k'_r + k_d + k_q[\text{TEA}]} \qquad (4.30)$$

Taking the reciprocal of the Eq. 35, a linear quenching model is resulted:

$$\frac{1}{\Phi_D} = \frac{k_r' + k_d}{k_r'\alpha} + \frac{k_q}{k_r'\alpha}[TEA] \qquad (4.31)$$

Eq. 4.31 indicates a linear correlation between $1/\Phi_D$ and [TEA] with an intercept of $(k_r' + k_d)/k_r'\alpha$ and a slope of $k_q/k_r'\alpha$. When the [TEA] dose is at higher range (above 1.75×10^{-2} mol L^{-1}), a plot of $1/\Phi_D$ vs. [TEA] is shown in Figure 4.10 with a r^2

of 0.9016, indicating the quenching effect due to high [TEA] dominating the overall reaction.

The three rate constants, k_q, k_r, k_d, and one coefficient α, can be solved mathematically by the four slopes and intercepts in Eqs. 4.26 and 4.31. However, the intercept of Eq. 4.31 is physically meaningless because it only occurs at [TEA] equals to zero which conflicts to our initial assumption (*i.e.* high [TEA]). Usually for exothermic quenching, it is frequently assumed that the rate of quenching is controlled by the diffusion rate (Horspool, 1976), therefore the quenching rate, k_q, can be evaluated from the modified Debye Huckel expression:

$$k_q = \frac{8RT}{3000\eta} \quad (\text{L mol}^{-1}\text{sec}^{-1}) \tag{4.32}$$

where η is the viscosity of the solution in poise, R is the universal gas constant. For aqueous solution at room temperature (*i.e.* T = 298K), k_q is resolved to be 6.5×10^9 L mol^{-1} s^{-1}. From the regression results of Figures 4.9 and 4.10, k_r, k_d and α therefore can be solved as follows:

$$1/\alpha = 9.8788 \tag{4.33}$$

$$\frac{k_d}{k_r \alpha} = 0.0142 \tag{4.34}$$

$$\frac{k_q}{k'_r \alpha} = 627.56 \tag{4.35}$$

From Eq. 4.33, the value of α is calculated to be 0.1012. At optimal quantum yield (*i.e.* [TEA] is 1.40×10^{-2} mol L^{-1}), k_r and k_d are determined to be 7.29×10^9 L $mol^{-1}s^{-1}$ and 1.05×10^7 s^{-1} respectively. At high [TEA] levels, k'_r is solved to be 1.02×10^8 s^{-1}

from Eq. 4.35, since $k_r' = k_r[TEA]$, we can foresee that the k_r and k_d both will depend on the [TEA] as shown in Eqs. 4.36 and 4.37,

$$k_r = \frac{1.02\times10^{8}}{[TEA]} \quad (\text{L mol}^{-1}\ \text{s}^{-1}) \tag{4.36}$$

$$k_d = \frac{1.47\times10^{5}}{[TEA]} \quad (\text{s}^{-1}) \tag{4.37}$$

Rate constants of k_r and k_d, at high [TEA] were therefore plotted in Figure 4.11. The magnitude of the photodecay rate constant k_r, are about three logs higher than the triplet deactivation rate constant, k_d, suggesting the triplet deactivation process is less significant in determine the overall reaction rates. Because the quenching rate (k_q) is a constant and is independent to the [TEA] concentration, therefore, as the [TEA] is overdosed in the solution, the k_r reduced and directly results in the reduction of quantum yields, which confirms with the observed quenching effect.

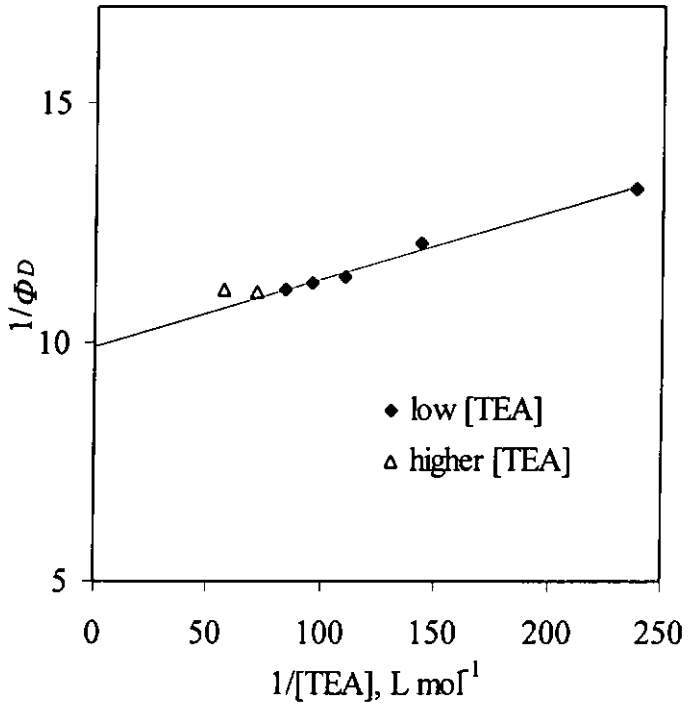

Figure 4.9: Plot of Φ_D^{-1} against $[TEA]^{-1}$ for the photolysis of DO11 with TEA in aqueous ACE.

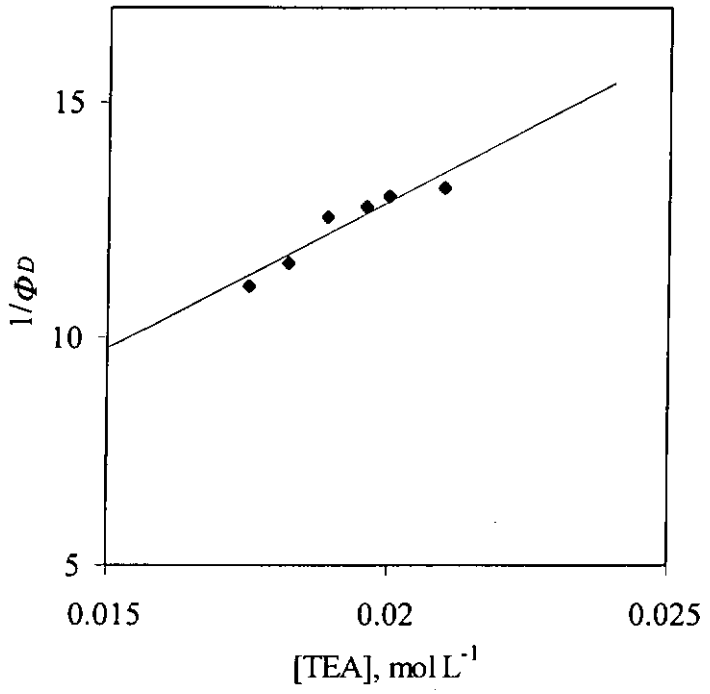

Figure 4.10: Plot of Φ_D^{-1} against [TEA] for the photolysis of DO11 with TEA in aqueous ACE.

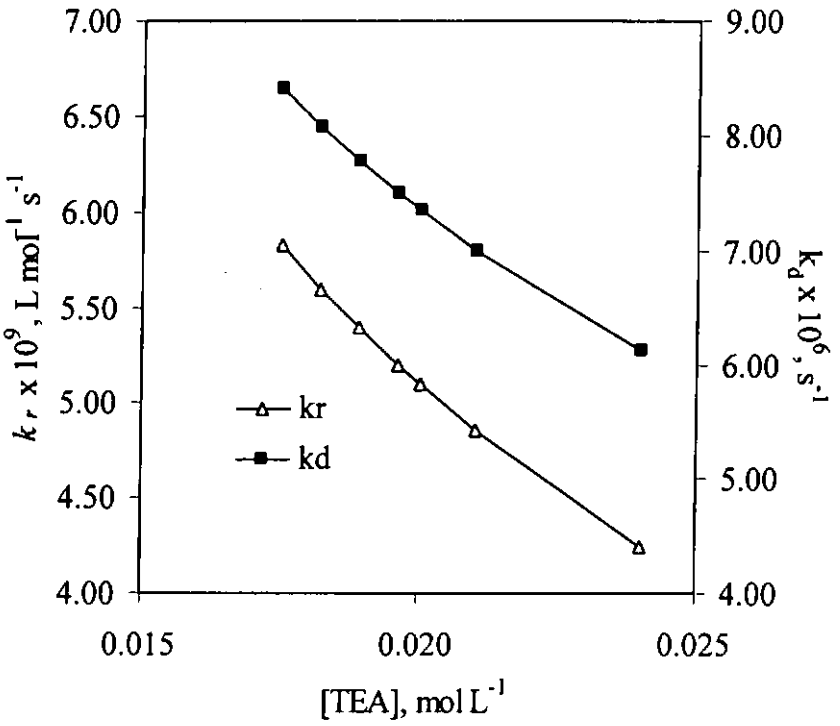

Figure 4.11: Rate constant of k_r and k_d at high TEA concentrations.

CHAPTER 5 RESULTS AND DISCUSSION II : PHOTODEGRADATION OF HYDROPHILIC DYE

5.1 Photodecolorization In The Presence Of Additives

The photodegradation of hydrophilic dye (RR2) in the presence of ACE or TEA via the indirect photolysis is investigated. Such indirect photodegradation processes provide attractive routs to treat or pretreat dye pollutants by using UV light. The primary interest of this Chapter is to explore the photodegradation performance of a typical chlorinated reactive dye RR2 by adding different types of additives mineralization related to the reaction pathways through the degradation of RR2.

5.1.1 Reaction Kinetics and Photodegradation Rates

The photodegradation kinetics of RR2 within various concentrations of ACE or TEA were investigated, as shown in Figure 5.1 where the pseudo first-order and zero-order kinetics were observed in the presence of ACE and TEA, respectively. The decay rates of RR2 at various concentrations of ACE and TEA were reported in Table 5-1, in which the r^2 of regression lines ranged from 0.9997 to 0.9758. For the first-order photodegradation of RR2 by using ACE, another way to further examine the photolysis performance is the use of quantum yield, Φ_D (refer to Eq. 3.4 – 3.5).

As shown in Table 5-1, by using 0.108 mol L^{-1} of ACE, the pseudo first-order rate constants increased 75 times from 0.03×10^{-2} (without using ACE) to 2.26×10^{-2} s^{-1},

while the use of 0.07 mol L^{-1} of TEA in the solution, the zero-order rate constants increased 20 times from 0.20×10^{-8} (without using TEA) to 4.00×10^{-8} mol L^{-1} s^{-1}. In general, the decay rates of RR2 were normally increased with the increment of ACE and TEA concentrations. However, it is interesting to note that further increasing of [ACE] results in gradual decline of the reaction rates. This is most likely due to the light attenuation by excess ACE in the solution. High concentration of ACE may act as a light filter, which has been discussed in Chapter 4.1.1.

Table 5-1: Photodegradation kinetics of RR2 in different concentrations of ACE or TEA at 253.7nm[a].

Presence of ACE (pseudo first-order kinetic)[b] $D_t = D_0\, e^{-k_A}$ or $\frac{dD_t}{dt} = -k_A D_t$			**Presence of TEA** (zero-order kinetic)[b] $D_t = D_0 - k_T t$ or $\frac{dD_t}{dt} = -k_T$	
[ACE], mol L^{-1}	k_A, 10^{-2} s^{-1}	Φ_D, 10^{-3}	[TEA], mol L^{-1}	k_T, 10^{-8} mol L^{-1} s^{-1}
0.000	0.03	0.30	0.000	0.20
0.003	0.17	1.72	0.005	1.90
0.008	0.57	5.78	0.010	2.50
0.014	0.71	7.20	0.020	2.80
0.027	1.23	12.47	0.030	3.20
0.054	1.62	16.42	0.040	3.30
0.081	1.92	19.46	0.050	3.40
0.108	2.26	22.91	0.060	3.50
0.135	1.94	19.66	0.070	4.00
0.162	1.85	18.75		
0.216	1.46	14.80		

[a] Incident light intensity is 1.5×10^{-5} Einstein L^{-1} s^{-1} within the Rayonet photoreactor; initial pH of the solutions were 11.0 ± 0.1.

[b] D_0 and D_t are the concentration of RR2 at time zero and t respectively; k_A and k_T are the pseudo first-order and zero-order decay rate constants, respectively.

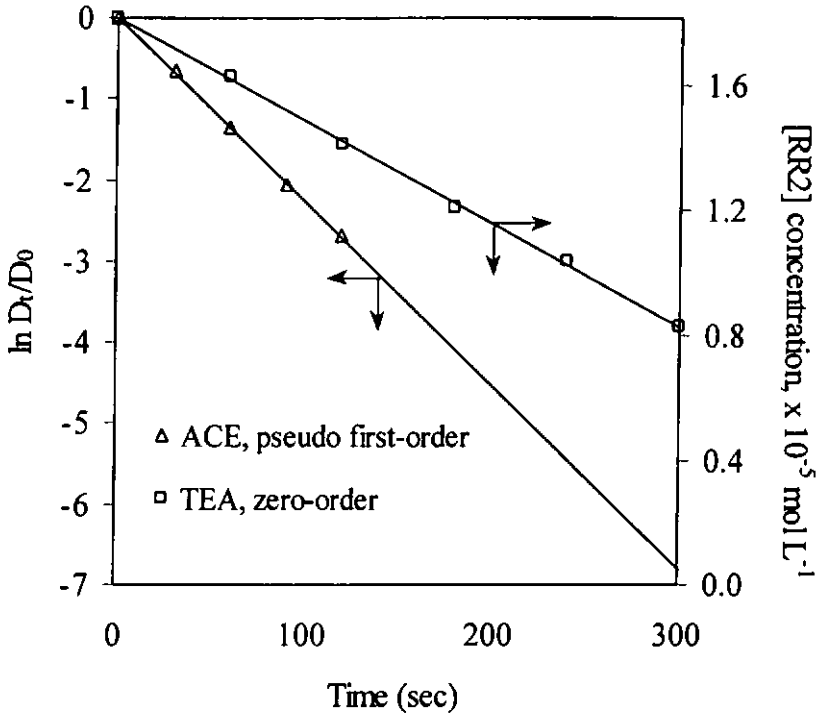

Figure 5.1: Pseudo first-order and zero order decay of RR2 in the presence of ACE and TEA respectively. (The [ACE] = 0.108 mol L^{-1}, [TEA] = 0.04 mol L^{-1})

5.1.2 Effect of Initial pH

The photodecolorization of RR2 in the presence of ACE or TEA at various initial pHs was also examined as shown in Figure 5.2. The concentration of ACE and TEA used for this study was 0.108 mol L^{-1} and 0.04 mol L^{-1} respectively. Results showed that the photodecolorization of RR2 was more favorable at higher pH levels. The pseudo first-order rate constants of photodegradation of RR2 in ACE aqueous solution increased from 1.15×10^{-2} s^{-1} at pH 3 to 2.26×10^{-2} s^{-1} at pH 11, and the solution pH decreased gradually throughout the reaction of dye decay. Since no major product peaks were founded in the HPLC analysis, the chance of forming organic acids in the solution and depressing the pH level is low. Proton apparently is the only source or photo-product causing the drop of the pH level. In the alkali medium, the generated proton is consumed by OH^- in the solution, possibly resulting in a positive enhancement of forward reaction (*i.e.* the dye decay), in which higher decay rate was observed. This explanation also justifies that the proton may inhibit or retard the photodegradation process, which consists with the observations of lower rates at lower initial pH levels.

In the TEA aqueous solution, the rate enhancement due to the pH change at low to medium level (pH < 8.5) is less significant, however at pH level of 11, the decay rate suddenly increases 8 times than that at pH 8. There are several reasons that may account for this. First, with respect to the chemical structure of TEA, the nitrogen center of the TEA molecule exerts an exposed lone pair electron. When additional protons are introduced in the solution (*i.e.* lower pH levels), the TEA molecule will be

deactivated through protonation, resulting in a weakened hydrogen source (Eq. 5.1), and the rate improving becomes insignificant.

$$(CH_3CH_2)_3-\ddot{N} \xrightarrow{H^+} (CH_3CH_2)_3-\overset{H}{\overset{\uparrow}{N}} \qquad (5.1)$$

At high pH level of 11, the TEA becomes a active hydrogen source to promote the photoreaction, in addition, the TEA (a Lewis base) may neutralize the acidic end product (proton, which have a retardation effect on the photolysis reaction) that generates from the photolysis process and therefore promote the reaction rates.

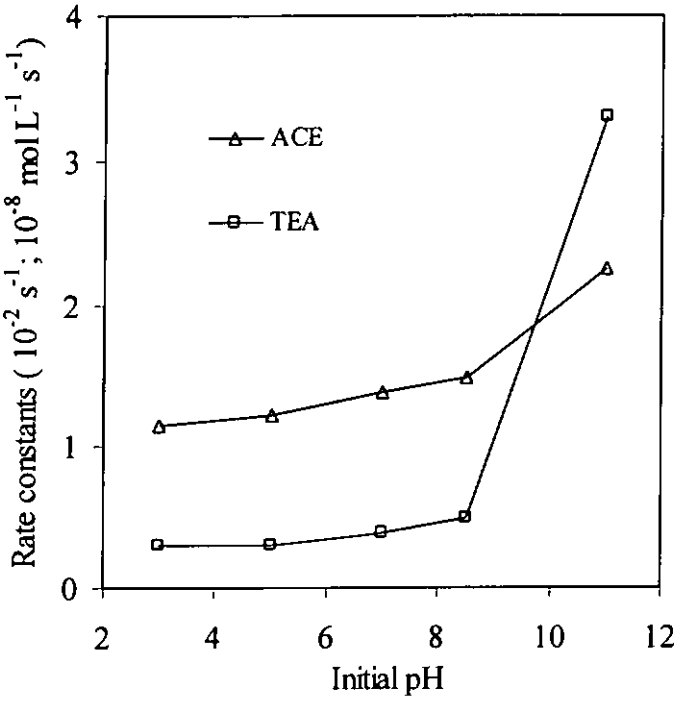

Figure 5.2: Variation of decay rate constants at different initial pH.

5.1.3 Function of Additives in Photodecolorization

The indirect photodecolorization of azo reactive dye RR2 in solutions containing ACE or TEA and the control experiment without using any additive (direct photolysis) were reported in Figure 5.3. Results demonstrated that direct photolysis of RR2 in water alone was a slow and an insignificant process. However, over seventy to twenty times of rate increments were observed after the addition of ACE and TEA to the solution, respectively. The results were summarized in Table 5-1, where the decay rates of direct photolysis in water were compared to that of indirect photolysis in solutions containing various doses of ACE and TEA. Apparently, the rate improvement is solely contributed by the use of ACE or TEA.

In the presence of ACE that has high triplet energy property makes the photosensitization process the likely dominant mechanism. The photoreduction of RR2 is initiated by excitation of the photo-sensitizer, ACE into its triplet state (ACE_3^*). Since the excited ACE_3^* is co-exist with the dye molecules in the liquid phase, inter-reaction of the ACE_3^* with RR2 will trigger energy transfer. The transferred energy can then be converted into chemical energy which is capable of inducing dissociation, intramolecular rearrangement, reduction-oxidation, or other photochemical reactions and results in the photoreductive fading of the dye. In such a complex photochemical process, the mechanisms of ACE react via their excited state with the dye molecules can be simplified by the following proposed Eqs. 5.2 – 5.5:

Excitation and intersystem crossing (ISC):

$$ACE_0 \xrightarrow{h\nu} ACE_1^* \xrightarrow{ISC} ACE_3^* \quad (5.2)$$

Sensitization:

$$RR2_0 + ACE_3^* \longrightarrow RR2_1^* + ACE_0 \quad (5.3)$$

Intersystem crossing of the excited dye molecule (Peters and Freeman, 1996):

$$RR2_1^* \xrightarrow{ISC} RR2_3^* \quad (5.4)$$

Chemical reduction by abstracting a hydrogen atom:

$$RR2_3^* + H\bullet \longrightarrow photo-products \quad (5.5)$$

On the other hand, judging from the reaction rates and kinetic orders, the photolysis of RR2 by adding TEA apparently has a different route from that in ACE solution. TEA is a known electron donor and/or hydrogen source, there are some discussion in literatures on the photoreduction, photodechlorination and photoinitiation reactions that it mediates (Sauberlich *et al.*, 1997, Encinas *et al.*, 1994). When dye molecules absorb photons, the energy of UV will be transferred to the dye molecules and the electronic configurations of dyes are excited to their singlet or triplet states. In the presence of hydrogen source, TEA for example, one hydrogen atom can be transferred from TEA to the excited dye D^*, creating an iminium ion derivative and resulted in the reduction of the dye, as illustrated in Eqs. 5.6 and 5.7.

Irradiation and intersystem crossing (ISC):

$$RR2_0 \xrightarrow{h\nu} RR2_1^* \xrightarrow{ISC} RR2_3^* \quad (5.6)$$

Electron transfer and photoreduction:

$$(C_2H_5)_3\ddot{N} + RR2_3^* \rightarrow (C_2H_5)_3\overset{+\bullet}{N} + RR2^{\bullet -} \rightarrow$$

$$(C_2H_5)_2\ddot{N}\text{–}CH_3\dot{C}H + R\dot{R}2 - H \rightarrow (C_2H_5)_2\overset{+}{N}=CH_3CH + RR2 - H^- \quad (5.7)$$

(iminium ion) *(decayed dye)*

If the hydrogen sources in the solution are abundant, bond breaking of chromophores is another possible photochemical mechanism of RR2. The azo bond *(-N=N-)* in RR2, which often acts as a designative point of reaction in photochemical process because these π-bond electrons are comparatively more diffusive than the other parts within the molecule (see Eq. 4.2).

Also as noted in Figure 5.3, it was observed that the decay rates of RR2 slowly declined (*i.e.* tailing) after 90-95% removal of the RR2 in the presence of ACE and TEA. The tailing may be due to several reasons: (a) some of the photoproducts may act as internal light filters that significantly reduce the light available for RR2 degradation; (b) the photoproducts may act as quenchers to interfere with photoreaction; (c) the depletion of available hydrogen sources in the solution, and (d) minor pathways such as photodechlorination and photodesulphonation reactions, as will be discussed later, may result in the tailing because such pathways have no contribution to the decay of the original RR2 molecules.

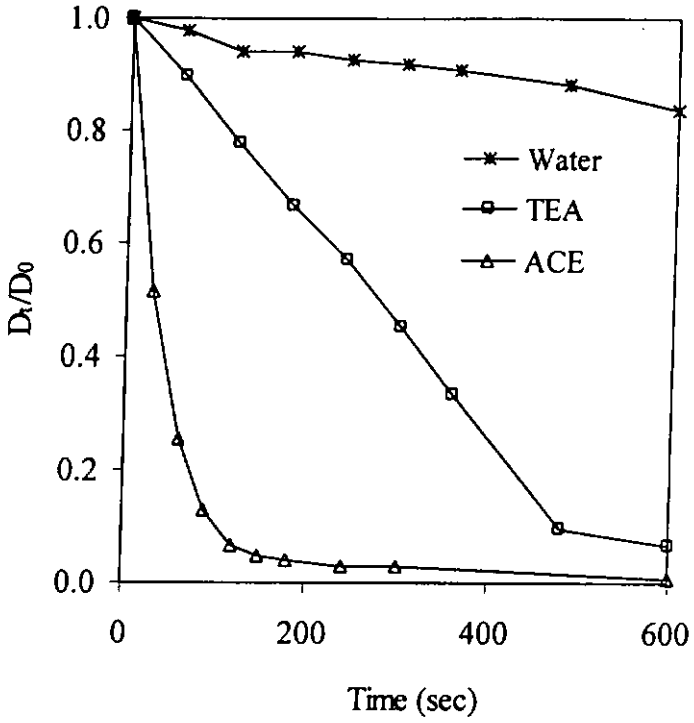

Figure 5.3: The photodegradation of RR2 in aqueous solution at 253.7 nm. The initial pH is 11 and light intensity is 1.5 x 10^{-5} Einstein L^{-1} s^{-1}. Control experiments were conducted at the same conditions in deionized distilled water.

5.1.4 Reaction Mechanism of Indirect Photolysis

As previously mentioned, the solution pH generally drops during the photolysis process, in order to identify the dominant reaction mechanisms in this process, the concentration change of inorganic ions in the solution are consequently investigated. RR2 was irradiated in aqueous solution containing 0.108 mol L^{-1} ACE at 253.7 nm with light intensity 3.0×10^{-6} Einstein L^{-1} s^{-1}.

Regarding to the dye structure in Chapter 3, there are two chlorides (Cl^-) in RR2 linking to the 1,3,5-triazine ring, and two sulphonate (SO_3^-) groups connecting to the naphthalene ring. The typical formation curves of Cl^-, SO_3^-, and degradation curve of RR2 are shown in Figure 5.4, in which the dechlorination process (releasing Cl^-) was observed as the decolorization (breaking chromophore) initiated. The concentration of chloride ions in solution increased rapidly at the first 600 sec and then gradually leveled off. On the other hand, the desulphonation (releasing SO_3^-) did not occur until 60% of the dye was degraded. Obviously, the indirect photolysis of RR2 is initiated by photodecolorization and photodechlorination simultaneously, then followed by the photodesulphonation at a later stage. About 70% of Cl^- and 45% of SO_3^- will be mineralized before the dye is fully decolorized.

It is evident that bond cleavages occur at the azo linkage, chloro-triazine group and sulphonate-naphthalene ring and are substituted by a hydrogen coming from the hydrogen source in the system, while an equivalent amount of proton will be released to the solution to maintain charge balance (Chu & Jafvert, 1994). Assuming close to

unity activity coefficients, the generation of proton could be calculated and compared with all other anions as shown in Figure 5.5. The overall molar balance of the parent compound (RR2-assume to be 1) and the final products including cation (H^+) and anions (Cl^- and SO_3^-) is in approximately stoichiometric. Therefore, it can be conclude that the photodecolorization, photodechlorination and photodesulphonation are likely the dominant reaction mechanisms in the indirect photodegradation of RR2 as a clean process, while the decay of RR2 generates proton, chloride and sulphonate ions as the end photoproducts.

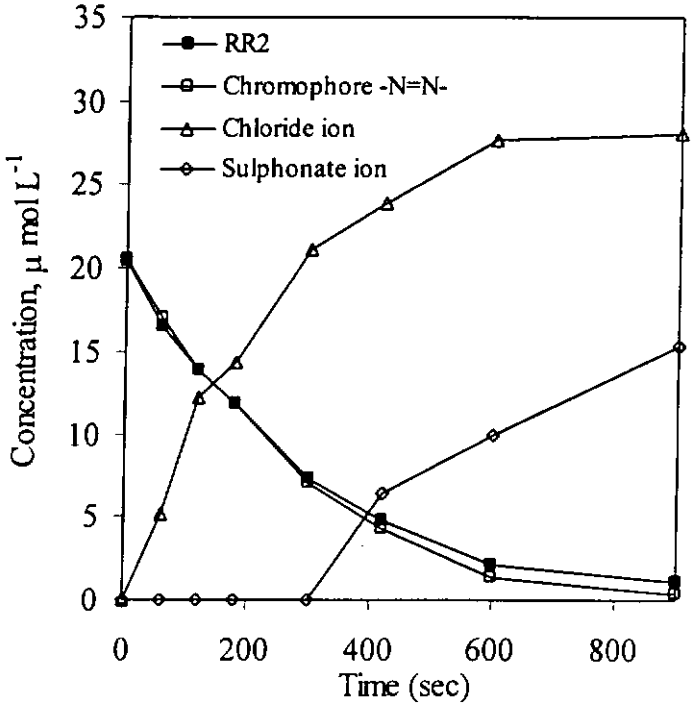

Figure 5.4: Photodegradation of 2.05 x 10^{-5} mol L^{-1} RR2 within 0.108 mol L^{-1} ACE solution at 253.7 nm and the formation of final products Cl^-, SO_3^- ions throughout the reaction. The initial pH is 11 and light intensity is 3.0 x 10^{-6} Einstein L^{-1} s^{-1}.

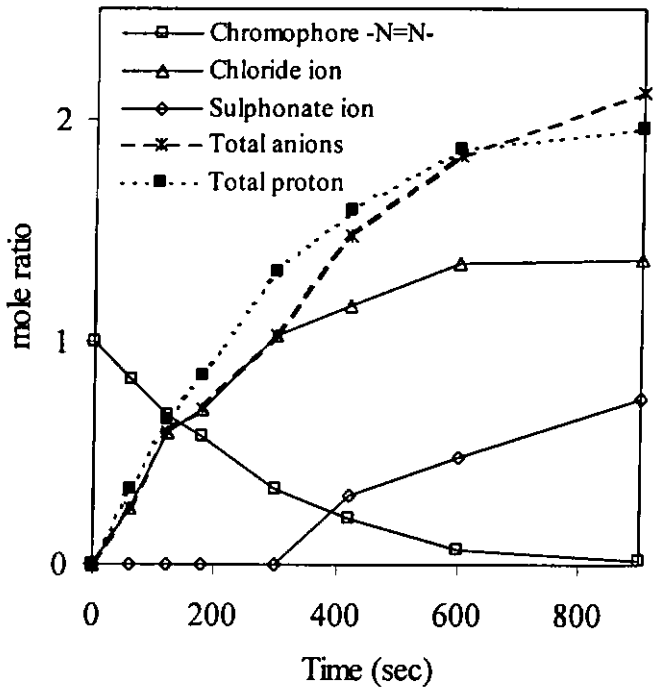

Figure 5.5: Molar balance of the photodegradation of RR2 and generation of H^+, Cl^- and SO_3^- in aqueous ACE solution.

5.2 Cocktail Photolysis System

The presence of hydrogen source or photosensitizer in a photodegradation process is a critical factor in increasing the decay rate of hydrophilic reactive dye. Tests were conducted in aqueous solutions containing TEA and ACE, where zero- and first-order kinetics were observed respectively as discussed in detail in Chapter 5.1. Wolfgang *et al.* (1999) proposed a kinetic model of the degradation of TCE and cis-DCE by combining zero- and first-order kinetics. Therefore, the primary interest of this study was to explore the possibility of rate enhancement by photolyzing a typical reactive azo dye in a cocktail system, in which the auxiliary hydrogen source (TEA) and photosensitizer (ACE) are both present. In addition, the experimental data will be further analyzed and used to develop a mathematical model for such a cocktail system.

5.2.1 Cocktail Photolysis System

Results in Figure 5.6 illustrated that the overall photodecolorization performance was further enhanced through the proposed cocktail photolysis process if both ACE and TEA were co-existed in the system. The cocktail photolysis of RR2 was further examined at an optimal concentration of ACE of 0.108 M (from our previous study) at various concentrations of TEA. The overall photodegradation kinetic of RR2 was close to the pseudo first-order reaction as shown in Figure 5.7. It is interesting to note that the decolorization curves of RR2 in cocktail photolysis system can be clearly divided into three distinct stages. A lag phase as the photochemical reaction was initiated, then followed by a rapid decolorization (with a rate k_S), and a tailing stage at

the end of photolysis (see Figure 5.7(a)). The decay rates (k_L) of lag phase at different concentrations of TEA are quite similar (around 4.487×10^{-3} s^{-1}), suggesting the decay rates in lag phase are less-dependent on the concentration of TEA. Because no lag phase was evident for the photodegradation assisted by optimal ACE concentration, the lag phase is apparently solely resulted from the presence of TEA.

The lag phase was terminated after 15 – 24 seconds of UV illumination and followed by a rapid decay of RR2. The duration of the lag phase t_L and the initial dye concentration of RR2 of second stage (D_L) at t_L could be determined from the intercept of the two rate curves by the known slopes of k_L and k_S for each initial TEA concentration, as shown in Figures 5.7(b) and 5.8. The figures illustrated that the t_L was reduced as the TEA concentration increased from 0.005M to 0.03M and remained at 15 seconds even if more TEA was used. The D_L, on the contrary, shows a perfect matching of counter-proportional character to the duration of t_L, which justified the previous observation that the decay rates in lag phase was independent to the concentration of TEA.

The observed lag phase implied that the cocktail photolysis process has a complex nature, meaning the mixing and/or interfering of various reaction mechanisms are likely involved. Originally, the main function of TEA in the photodegradation of dye is a hydrogen source, and ACE is a photosensitizer. As both of them are add together in the cocktail photolysis process, the TEA is likely to quench the excited ACE* (Eq. 5.9) resulting in a lower initial reaction rate (the lag phase), the ability of TEA in

behaving as a potential quencher has been reported previously (Jockusch *et al.*, 1996; Encinas *et al.*, 1994).

$$ACE_1^* + TEA \longrightarrow ACE_1 + TEA_3^* \qquad (5.9)$$

But the lag phase will be terminated soon (in less than 24 seconds), because the ACE concentration is two to ten times higher than the available TEA in the solution, so the photosensitization pathway contributed by those unquenched acetone molecules become dominant in the solution quickly. TEA although partly quenches the excited acetone, however, it should not quit from offering the hydrogen source to the reaction even at the beginning of the reaction. This presumption can be justified by the duration of lag phase, which is evidenced to be shorter at higher TEA concentration. After the quenching effect is embedded by accumulated ACE* concentration in the solution, the TEA contributes to the photodegradation reaction as an additional hydrogen source, therefore, the overall decay rate of dye is largely increased (the rapid decay stage) because the involvement of two reaction mechanisms, *i.e.* the cocktail process - photosensitization in the help of additional hydrogen source.

From Figure 5.7(b), the photodecolorization rates (slopes) of the second-stage reactions are increased significantly with the increment of initial concentration of TEA and more than 90% of the total color was reduced in 60 seconds of UV-irradiation. The pseudo first-order rate constants at different initial concentration of TEA for the second stage (k_S) were summarized in Table 5-2. It was astonished to find that the low dose of TEA could improve the decay rate of RR2 by 2.62 times than

that without TEA, but overdose of TEA would result in a reverse of the rate and eventually quench the reaction.

To study the complicated cocktail photolysis system, it is necessary to investigate the possible reaction mechanisms involved in the reaction. In the presence of both photosensitizer ACE and hydrogen source TEA in the solution, the reduction of RR2 is initiated by excitation of the unquenched photosensitizer ACE into its triplet state ($ACE_0 \rightarrow ACE_3^*$), followed by an energy transfer from the triplet ACE to the dye molecule. In succession, one hydrogen atom is abstracted from TEA to the excited dye, forming an iminium ion derivative and a reduced dye in the colorless leuco-structure. The reaction sequence and the functions of ACE and TEA in the cocktail photolysis system of dye RR2 can be described by the following Eqs. 5.10 – 5.13:

Excitation and intersystem crossing of the sensitizer:

$$ACE_0 \xrightarrow{h\nu} ACE_1^* \xrightarrow{ISC} ACE_3^* \qquad (5.10)$$

Sensitization:

$$RR2_0 + ACE_3^* \longrightarrow RR2_1^* + ACE_0 \qquad (5.11)$$

Intersystem crossing of the excited dye molecule (Peters & Freeman, 1996):

$$RR2_1^* \xrightarrow{ISC} RR2_3^* \qquad (5.12)$$

Electron transfer and photoreduction due to hydrogen source (or electron donor) TEA (Kagan, 1993):

$$(C_2H_5)_3\ddot{N} + RR2_3^{\bullet} \rightarrow (C_2H_5)_3\overset{+\bullet}{N} + RR2^{\bullet -} \longrightarrow$$
$$(C_2H_5)_2\ddot{N}\text{–}CH_3\dot{C}H + R\dot{R}2-H \rightarrow (C_2H_5)_2\overset{+}{N}=CH_3CH + RR2-H^{-} \quad (5.13)$$
(iminium ion) (decayed dye)

Apart from the above photoreduction mechanisms, reductive cleavage of the dye chromophore is another possible feature involved in the photodegradation of dye molecules.

However, as shown in Table 5-2, the RR2 decay gradually slows down after reaching a maximum rate at 0.03 M of TEA. This evidence suggests that high concentration of TEA can also perform as a quencher to retard the photoreaction through the deactivation of the excited dye molecules. Similar observation was also discussed by Encinas *et al.* (1994) on the photoreaction process of fluorenone and TEA, where the TEA is capable to quench the excited states. Additionally, a rate-quenching model proposed in Chapter 4.2.2 further justify the quenching mechanism of dye molecule by TEA:

$$RR2_3^{\bullet} + TEA \longrightarrow RR2_0 + TEA_3^{\bullet} \quad (5.15)$$

As noted in the decay curves in Figure 5.7(a), after 90-95% of RR2 was removed in the cocktail solutions, the decay rates of RR2 declined into a tailing stage. The reasons of forming tailing stage in a photoreduction process have been discussed previously (Chu & Jafvert, 1994).

Table 5-2. Decay rate constants of RR2 in second stage of the cocktail photosensitization systems with different initial concentration of TEA.

0.108 M [ACE] + different [TEA] mol L^{-1}	**Second stage decay rate constants** $k_S \times 10^{-2}$ s^{-1}
0.000	2.26
0.005	4.39
0.010	5.28
0.020	5.91
0.030	6.03
0.040	5.84
0.050	4.40

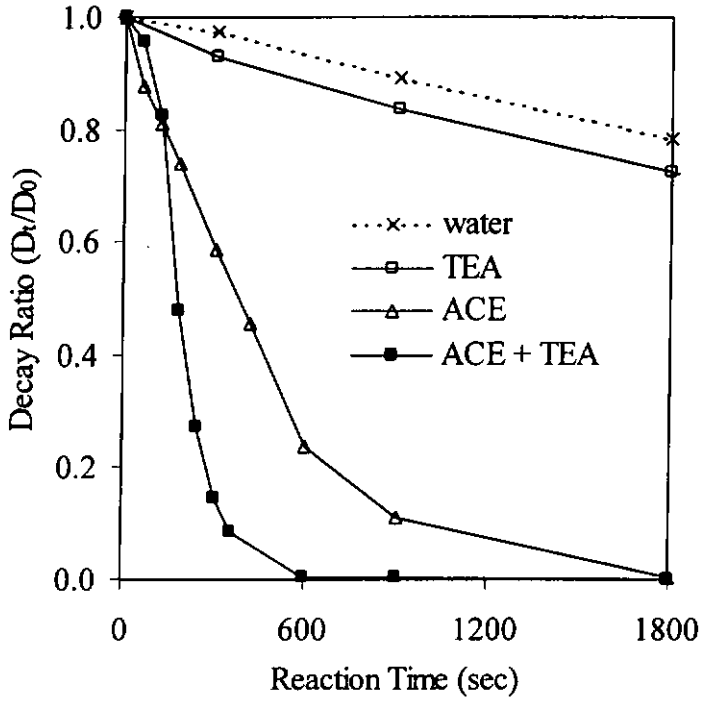

Figure 5.6: The photodegradation of RR2 in aqueous solution at 253.7 nm. Experiments were performed at initial pH 11 with light intensity 3.0 × 10^{-6} Einstein L^{-1} s^{-1}. The initial concentration of [TEA] and [ACE] are 0.02 mol L^{-1} and 0.108 mol L^{-1} respectively. Control experiments were conducted at the same condition with deionized distilled water only.

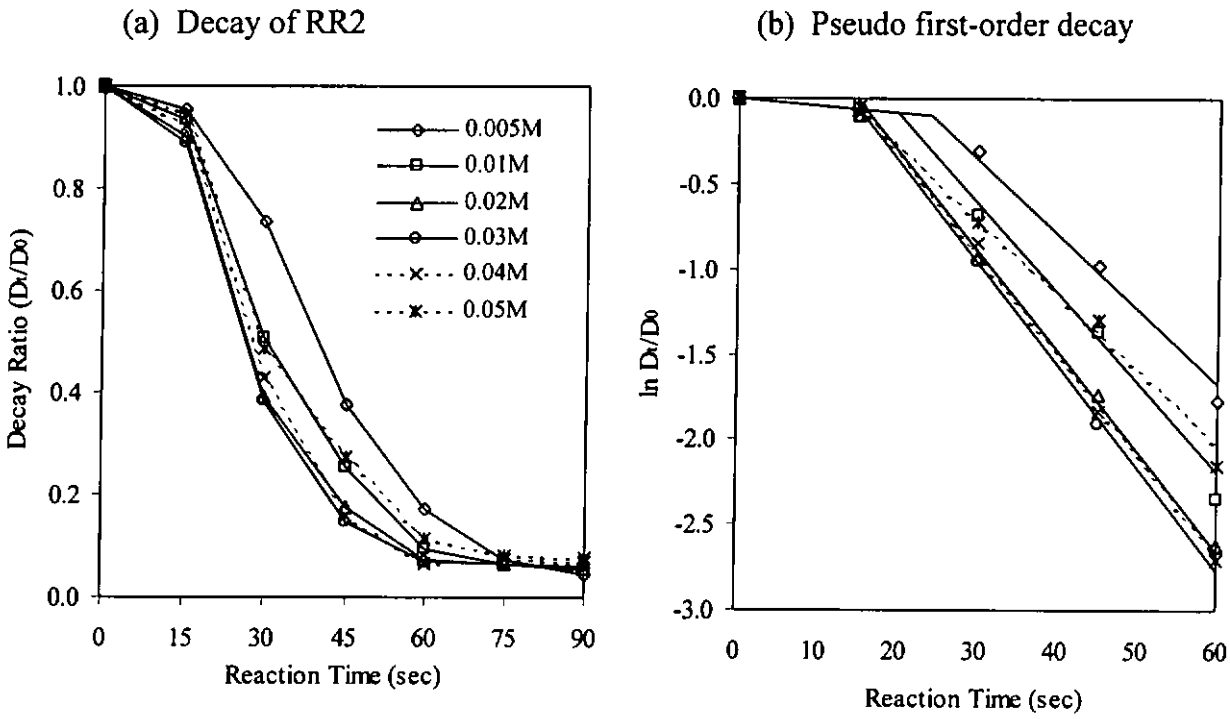

Figure 5.7: (a) Decolorization of RR2 in cocktail photosensitization system (0.108 mol L^{-1} ACE with different [TEA]). In all cases, the light intensity is 1.5×10^{-5} Einstein s^{-1} L^{-1} at 253.7 nm. (b) The first two stage of pseudo first-order decay of cocktail photosensitization reactions. The solid line indicates the enhancement of reaction, and dashed line indicates the retardation in the second stage.

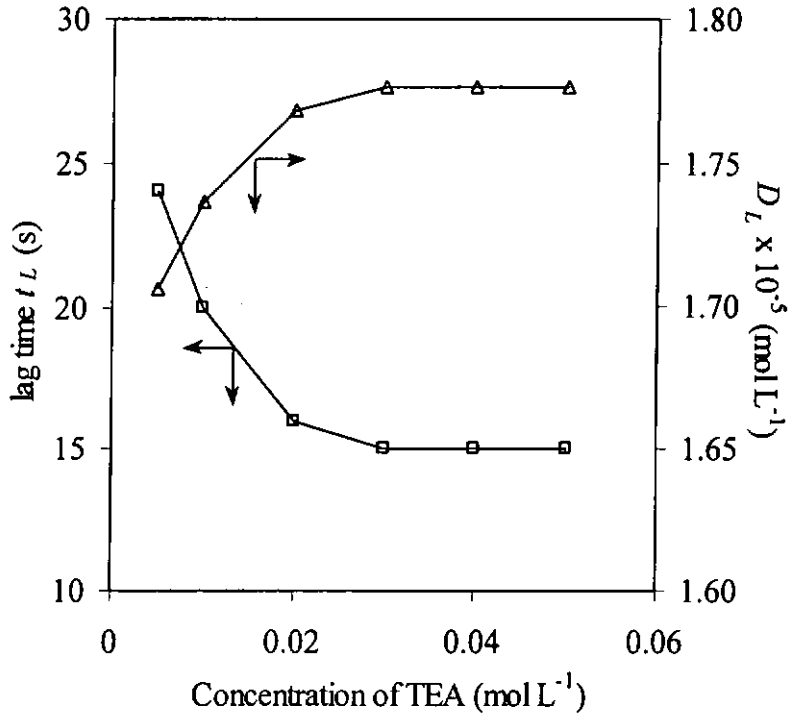

Figure 5.8: The concentrations of RR2 at its corresponding lag time of the cocktail photosensitization system within different TEA concentration.

5.2.2 Effects of Incident Light Intensity

Figure 5.9 presented the cocktail photodegradation of RR2 as a function of six different light intensities; the corresponding reaction rate constants at different irradiation light intensity were also shown. The tests were conducted in a mixture of 0.108 mol L^{-1} ACE and 0.02 mol L^{-1} TEA aqueous solution with the same initial dye concentration while the light intensities were ranged from 3.0×10^{-6} to 1.8×10^{-5} Einstein L^{-1} s^{-1} (by changing the number of lamps). A good linear correlation was resulted, in which the higher the light intensity, the faster the reaction rates on dye photodegradation. To investigate the "dye decay/UV-intensity" performance, the quantum yield (Φ_s) was used:

$$\Phi_s = \frac{k_s}{2.303 \times \varepsilon_{c,\lambda} \times I_\lambda \times \ell} \qquad (5.16)$$

where k_S is the pseudo first-order constant of cocktail photodecay of RR2 at the second stage (s^{-1}) , I_λ is the intensity of the incident light at 253.7nm (Einstein L^{-1} s^{-1}), $\varepsilon_{c,\lambda}$ is the molar absorptivity of RR2 at 253.7nm (L mol^{-1} cm^{-1}), and ℓ is the cell path length (cm).

From Figure 5.9, at low intensity levels, the reaction Φ_s was found to be counter-proportional to the decay rates. This indicated that optical-dense conditions was occurred where the limited photons were almost completely consumed by the solutes in the cocktail solution (i.e. $I_{in} >> I_{out}$). Nevertheless, at high intensity levels, the amount of photons is abundant, and it is reasonable to see that the values of Φ_s tend to

reach a constant. This suggests that the photochemical performance becomes independent to the incident light intensity and resulting in a constant Φ_s at high incident light intensities.

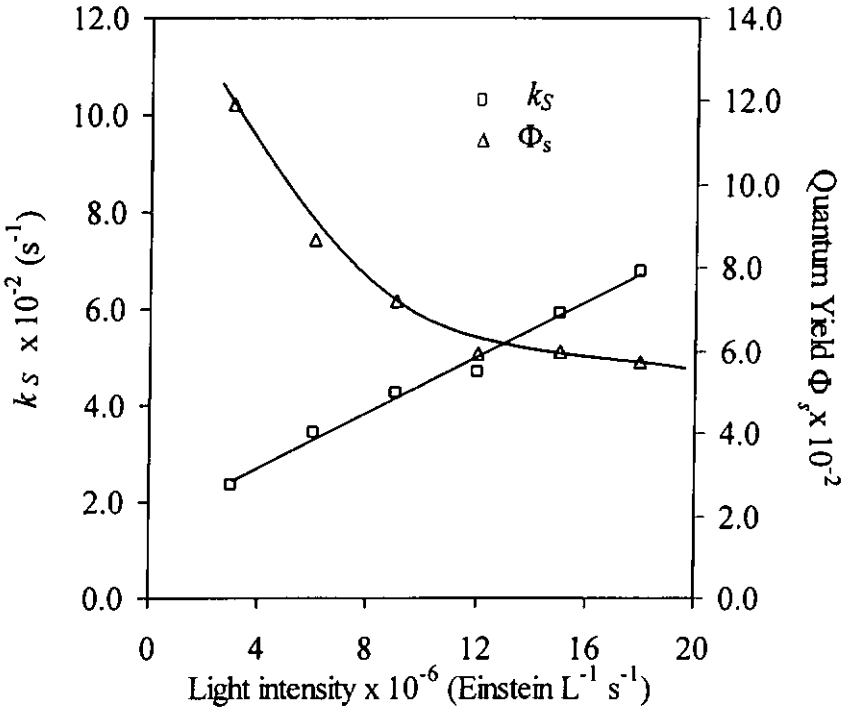

Figure 5.9: Decay rates and quantum yields of the cocktail photodegradation of RR2 by exposing at different incident light intensity. ([ACE] = 0.108 mol L^{-1}; [TEA] = 0.02 mol L^{-1}).

5.2.3 Quantitative Prediction

Previous literatures showed that the photodegradation of organic dyes in aqueous solutions were found to be kinetically controlled (Chu & Tsui, 1999; Herrera *et al.*, 1999; Chu & Ma, 1998). The photodegradation of RR2 in 0.108 mol L^{-1} aqueous ACE solution follows pseudo first-order decay kinetic with a decay rate of 0.0226 s^{-1}, while zero-order reactions are observed in sole TEA-assisted solutions. Table 5-1 demonstrated those zero-order rate constants of RR2 decay in different concentrations of TEA at 253.7 nm, and the r^2 were ranged from 0.9994 to 0.9920.

In principal, the cocktail photolysis system is assumed to be consisted of two parallel irreversible pseudo first-order and zero order reactions. The differential rate equations are:

In ACE solution: $$\frac{dD_t}{dt} = -k_A D_t \quad (5.17)$$

In TEA solution: $$\frac{dD_t}{dt} = -k_T \quad (5.18)$$

where k_A (s^{-1}) and k_T (mol L^{-1} s^{-1}) are the kinetic rate constants for the photodegradation of RR2 in aqueous ACE and TEA solution respectively, and D_t represents the concentration of probe dye at time t. Mathematically, by combining Eq. 5.17 and Eq. 5.18, the concentration of RR2 in the cocktail photolysis system can be rewritten as Eq. 5.19:

$$\frac{dD_t}{dt} = -k_A D_t - k_T \quad (5.19)$$

Rearranging of Eq. 5.19:

$$\frac{dD_t}{dt} + k_A D_t = -k_T \tag{5.20}$$

and by applying the general integration formulas (5.21) – (5.23):

$$\frac{dy}{dt} + P(t)y = q(t) \tag{5.21}$$

$$y = y_0\, e^{-r(t)} + e^{-r(t)} \int_0 e^{r(t)} q(t)\, \mathrm{dt} \tag{5.22}$$

where $$r(t) = \int_0 P(t)\, dt \tag{5.23}$$

By substituting Eq. 5.20 into the integration formulas, the concentration of RR2 at time t can be represented by:

$$D_t = D_L\, e^{-k_A(t-t_L)} - k_T\, e^{-k_A(t-t_L)} \int_0 e^{k_A(t-t_L)}\, dt \tag{5.24}$$

therefore, the cocktail model can be solved as follow:

$$D_t = D_L\, e^{-k_A(t-t_L)} - \frac{k_T}{k_A}\left[1\text{-}e^{-k_A(t-t_L)}\right] \tag{5.25}$$

where t_L is the duration of lag phase of the cocktail system (s) and D_L is the concentration of RR2 in solution at the completion of lag phase. After the substitution of those rate constants in the cocktail model, the predicted curve and experimental data were illustrated in Figure 5.10 for comparison. It is clearly to see that the proposed model underestimates the performance of cocktail system as well as the decay of RR2 at 253.7 nm. It is likely that the bias come from the over-simplification of the model, where no "add-on effect" due to the mutual rate-boost between ACE and TEA is considered. Therefore, add-on effect should be involved in the cocktail system and the proposed model can be modified into a more practical format for the overall performance prediction by inputting factors that reflect the levels of add-on

effect. So the "cocktail original model" can be restated by multiplying the rate constants by the factors, and the proposed "cocktail corrected model" was derived as:

$$D_t = D_L\, e^{-\alpha k_A (t-t_L)} - \frac{\beta k_T}{\alpha k_A}\left[1-e^{-\alpha k_A (t-t_L)}\right] \qquad (5.26)$$

where α and β are the respective factors of add-on effect for k_A and k_T. The coefficients α and β were easily solved by the following procedures: (1) assignation of two different reaction times t, (2) determination of the concentration of RR2 at t by k_S, (3) substitution of those known variables (D_t, D_L , k_A, k_T, t and t_L) in the proposed cocktail corrected model, and (4) solving the two equations.

Therefore, the respective factors α and β were solved for each set of cocktail test in a fixed ACE concentration with varying TEA concentration and was plotted in Figure 5.11. The predicted values derived from the cocktail original model and the corrected model were compared with the experimental data in Figure 5.10. In addition, the corrected model and the add-on factors were applied to the full ranges of data, and the results were shown in Figure 5.12. Apparently, the proposed corrected model could predict the RR2 decay in a cocktail photolysis process quite well in the presence of ACE and TEA by the help of using add-on factors α and β.

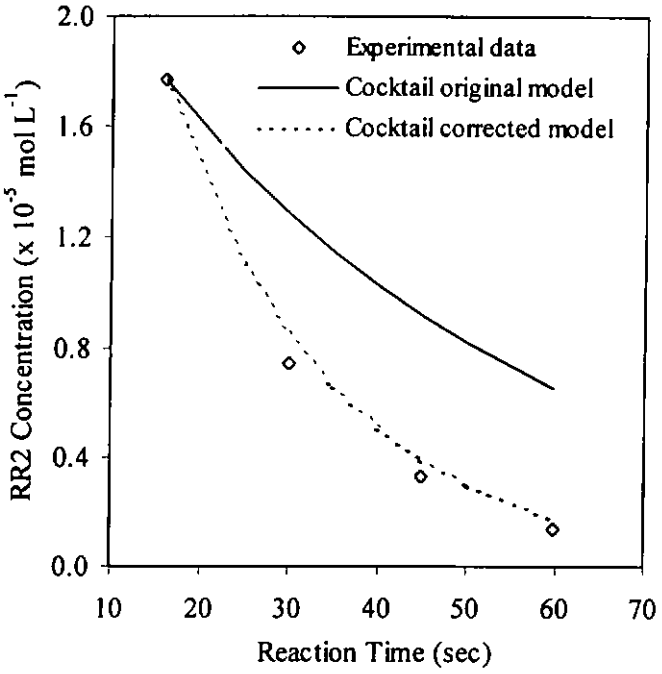

Figure 5.10: The comparisons of experimental results and the proposed cocktail models for the photodecolorization system of RR2 within 0.108 mol L^{-1} ACE and 0.02 mol L^{-1} TEA aqueous solution at 253.7 nm. (The dash line represents the proposed Cocktail corrected model with $\alpha = 2.31$ and $\beta = 1.69$).

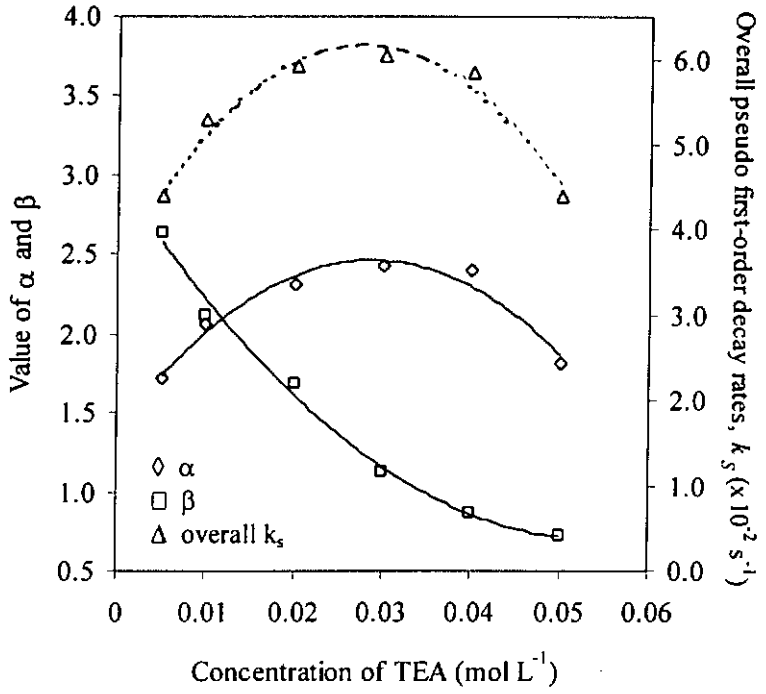

Figure 5.11: The variations of the coefficients α and β and the overall performance of the cocktail system in terms of the pseudo first-order decay rates as a function of different concentration of TEA.

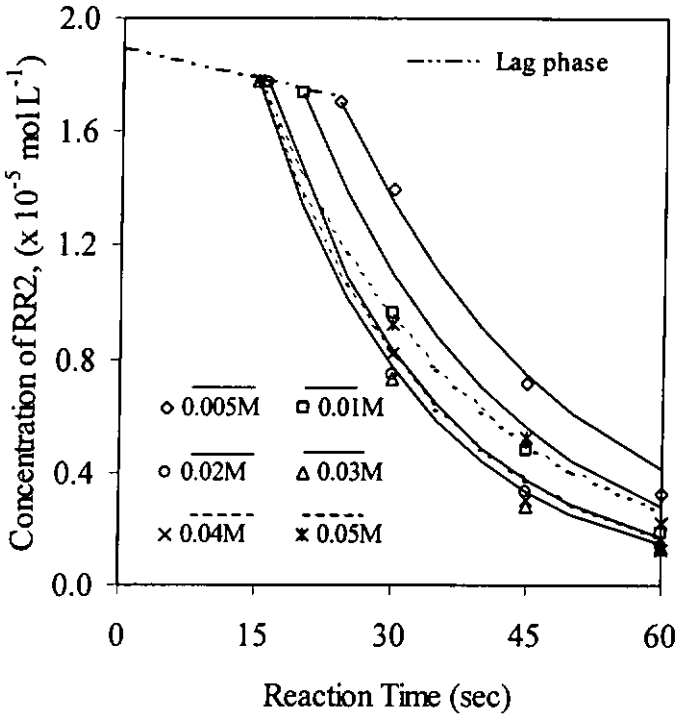

Figure 5.12: Performance prediction of the cocktail photosensitization system of RR2 at 0.108 mol L^{-1} ACE concentration with different concentration of TEA by the Cocktail corrected model. The markers indicate the experimental data, and the lines indicate the modeling values.

5.2.4 Sensitivity Analysis of Cocktail Corrected Model

Figure 5.11 shows that the overall pseudo first-order decay rates k_S have a similar trend with the value of α, which is gradually increased to a maximum point at 0.03 mol L^{-1} TEA and then decreased at higher TEA concentrations, while β is counter-proportional to the increment of TEA concentration. This suggests that the cocktail corrected model is more depended on the coefficient α and the ACE photosensitization mechanism is likely the dominant mechanism in the cocktail system. As for β, its values become less than one at higher TEA concentration, this confirms that overdose of TEA may cause the adverse effects for the photodegradation of RR2, i.e. quenching reaction between the TEA and excited dye, as explained previously.

To verify this observation, the sensitivity analysis of the factors α and β was conducted to determine the dominant mechanism occurring in the cocktail photolysis system (Jahan *et al.*, 1999; Seefeld & Stockwell, 1999). From Figure 5.12, the optimal photodegradation of RR2 by using cocktail photolysis was observed in a mixture of 0.108 mol L^{-1} ACE and 0.02 mol L^{-1} TEA, so it was selected as a typical case for the sensitivity analysis at a specific reaction time of 45 seconds, as shown in Figure 5.13. It is clear to note that the proposed cocktail corrected model is mainly dependent on the magnitude of α, and the coefficient β has less contribution to the proposed model. Since Figures 5.11 and 5.13 both suggest that the factor β contribute less than that of α within the tested range, it is confidence to conclude that the photosensitization (resulted from ACE) is the dominant reaction mechanism in the cocktail photolysis

system. The hydrogen source (TEA) though does not contribute a major decay pathway in the system, it can promote the reaction rate of photosensitization by offering the add-on effect.

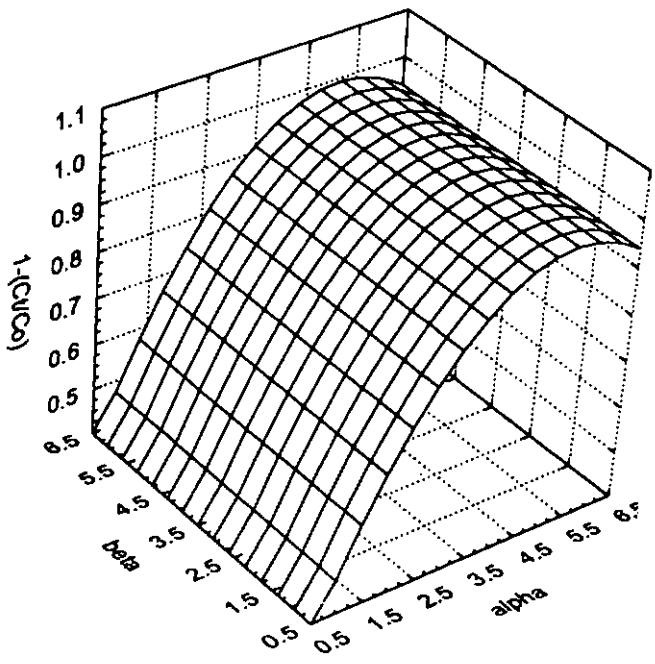

Figure 5.13: The sensitivity analysis of coefficients α and β to the Cocktail corrected model

CHAPTER 6 CONCLUSIONS AND RECOMMENDATIONS

6.1 Conclusions

The performances of the ACE-sensitized photochemical reaction of hydrophobic disperse dyes (DY7 and DO11) and hydrophilic reactive dye (RR2) was investigated using a Rayonet™ photoreactor with 253.7 nm UV illumination.

The role of the ACE was not only to act as the photo-sensitizer, but also as a solvent for the hydrophobic disperse dye. The ACE-photosensitization of the dye molecule is pH dependent. Inhibition of the rate was observed at lower pH. The addition of hydroxide ions to the solution may have neutralized the acidic products that were generated from the photolysis, and have therefore improved the photosensitization process. The free radical pathway may also partly contribute to the dye decay at high pH. The ACE-photosensitization of disperse dyes follow the pseudo first-order kinetics, and the final products of the process become more biodegradable than the parent dye. The recycling of ACE is feasible, and more than 95% ACE recovery can be achieved using a simple purging system.

Investigations of the cocktail-photodegradation of anthraquinone disperse dye (DO11) was conducted in aqueous ACE solution in the presence of TEA. The use of TEA together with ACE sensitizer can further promote the dye degradation reaction by consuming the acidic products that generated from the photosensitization and by

acting as an additional hydrogen source. At optimal [TEA], 27% of further rate improvement DO11 decay was achieved. Although the possible sub-reactions involved in such cocktail reactions are extremely complicated, the assumptions made in the proposed Scheme 4.5 are proven valid, which effectively simplifies the reaction mechanisms and makes the process predictable. The proposed rate-enhancing model and rate-quenching model based on the simplified reaction mechanisms have good correlation suggesting that triplet deactivation, triplet quenching by TEA, and TEA-enhanced photodegradation are the major sub-reactions in this process and capable of describing the overall reaction successfully. Therefore, the initial hypothesis regarding the neglect of all singlet processes is valid.

The use of additional hydrogen source or sensitizer to aid the indirect photodegradation of RR2 at 253.7 nm is a successful process. Both ACE and TEA showed a good treatment performance on the photodecolorization of RR2. The kinetics of RR2 photodegradation in aqueous ACE or TEA solution followed pseudo first-order and zero-order decay respectively. The RR2 decay rates are dependent on both the retardation effects coming from the proton generation and the initial pH levels. The photodegradation of RR2 via photoreduction was the main decay pathway, in which photodecolorization, photodechlorination and photodesulphonation were observed. In addition, the mineralized products of anions including Cl^- and SO_3^- are also presented approximately in stoichiometric amounts with the formation of proton in the solution.

Investigations of the cocktail photolysis of azo dye (C.I. Reactive Red 2, RR2) was conducted in a aqueous mixture of ACE and TEA at 253.7 nm monochromatic ultraviolet (UV) lamps. ACE acts as a photosensitizer to initiate the degradation of RR2, and the use of TEA as an additional hydrogen source can further aid the photodegradation of RR2 and promote the rates. The cocktail photolysis of RR2 can be clearly divided into three distinct stages: a slow lag-phase, a rapid decolorization, and a tailing. The possible reasons of such phenomena have been discussed.

The cocktail photolysis process involves a series of complex reactions that mainly consist of two parallel irreversible reactions caused by the presence of ACE and TEA: a pseudo first-order and a zero order reaction, respectively. Quantitative estimation of the cocktail photolysis system of azo dye was studied through the examination of reaction kinetics in the decolorization process. A cocktail model corrected by the add-on effect was proposed and successfully quantified the dye decomposition in the cocktail photolysis system at any predetermined reaction time.

6.2 Recommendations

Based on the experimental results, ACE-photosensitization process has been proven to be an effective means for the degradation of both disperse and reactive dyes. In fact, the addition of hydrogen source TEA in the ACE-photosensitization process showed a significant enhancement on the decolorization rate. Therefore, further studies should be extended to the application of this technique in different types of dyestuffs and examined on the photodecolorization of actual dyeing wastewater to solve the real world problem. Furthermore, a continuous pilot scale reactor for the dye removal by the cocktail photolysis system is needed as a next step to further develop.

In this thesis, the use of UV light for degradation of organic dyes in the cocktail system is a promising method. Apart from this, there is still much room to explore the utilizing of the cheaper visible light sources or to use a greater quantity of the inexhaustible visible sunlight for treating dyeing wastewater.

REFERENCE:

Alberto M.D. and Russell A.G. "Iteratuve inverse modeling and direct sensitivity analysis of a photochemical air quality model". *Environmental Science and Technology*, vol. 34, pp. 4974–4981. (2000)

Allen N.S. "Photooxidation and photoreduction of dyes in polymers". In *Photochemistry of dyed and pigmented polymer*, Applied Science Publishers, London. (1980)

Allen N.S. "Photofading and light stability of dyed and pigmented polymers". *Polymer Degradation and Stability*, vol. 44, pp. 357-374. (1994)

Aranyosi P., Czilik M., Rémi E., Parlagh G., Vig A. and Rusznák I. "The light stability of azo dyes and azo dyeings IV. Kinetic studies on the role of dissolved oxygen in the photofading of two heterobifunctional azo reactive dyes in aqueous solution". *Dyes and Pigments*, vol. 43, pp. 173-182. (1999)

Arslan, I. and Akmehmet B.I. "Degradation of commercial reactive dyestuffs by heterogenous and homogenous advanced oxidation processes: A comparative study". *Dyes and Pigments*, vol. 43, pp. 95-108. (1999)

Aspland J.R. "A series on dyeing: Chapter 9: The structure and properties of disperse dyes and related topics". *Textile Chemists and Colorists.*, vol. 25, pp. 21-25. (1993)

Bandara J., Mielczarski J.A. and Kiwi J. "Photosensitized degradation of azo dyes on Fe, Ti, and Al oxides. Mechanism of charge transfer during the degradation". *Langmuir*, vol. 15, pp. 7680-7687. (1999)

Bandara J., Morrison C., Kiwi J., Pulgarin C. and Peringer P. "Degradation/decoloration of concentrated solutions of Orange II. Kinetics and

quantum yield for sunlight induced reactions via Fenton type reagents". *Journal of Photochemistry and Photobiology A: Chemistry,* vol. 99, pp. 57-66 (1996)

Baughman G.L. and Weber E.J. "Transformation of dyes and related compounds in anoxic sediment: kinetics and products". *Environmental Science and Technology,* vol. 28, pp. 267-276. (1994)

Beltrán F.J., González M. and González J.F. "Industrial wastewater advanced oxidation. Part 1. UV radiation in the presence and absence of hydrogen peroxide". *Water Research,* vol. 31, pp. 2405-2414. (1997)

Beydilli M.I., Pavlostathis S.G. and Tincher W.C. "Decolorization and toxicity screening of selected reactive azo dyes under methanogenic conditions". *Water Science and Technology,* vol. 38, pp. 224-232

Bolton J.R. and Cater S.R. "Homogeneous photodegradation of pollutants in contaiminated water: An introduction". In Helz G.R., Zepp R.G. and Crosby D.G., eds., *Aquatic and Surface Photochemistry,* Lewis Publisher, pp. 467-490. (1994)

Bunce N.J. "Photolysis of aryl chlorides with aliphatic amines". *Journal of Organic Chemistry,* vol. 47, pp. 1948-1955. (1982)

Bunce N.J. and Challacher J.C. "Photolysis of aryl chlorides with dienes and with aromatic amines", *Journal of Organic Chemistry,* vol. 47, pp. 1955-1958. (1982)

Carr C.M. *Chemistry of the textiles industry.*, Blackie Acdemic & Professional, 1st ed., London; New York. (1995)

Chang J.S. and Lin Y.C. "Fed-batch bioreactor strategies for microbial decolorization of azo dye using a Pseudomonas luteola strain". *Biotechnology Progress,* vol. 16, pp. 979-985. (2000)

Chaudhuri S.K. and Sur B. "Oxidative decolorization of reactive dye solution using fly ash as catalyst". *Journal of Environmental Engineering*, vol. 126, pp. 583-594. (2000)

Choudhry G.G. and Webster G.R. "Environmental Photochemistry of PCDDs. Part I. Kinetics and Quantum Yields of the Photodegradation of 1,2,3,4,7-Penta-and 1,2,3,4,7,8-Hexachlorodibenzo-p-Dioxin in Aqueous Acetonitrile". *Chemosphere*, vol. 14, pp. 9-26. (1985)

Chu W. and Choy W.K. "The study of lag phase and rate improvement of TCE decay in UV/surfactant system". *Chemosphere*, vol. 41, pp. 72-82. (2000)

Chu W. and Ma C.W. "Quantitative prediction of direct and indirect dye ozonation kinetics". *Water Research.*, vol. 34, pp. 3153-3160. (2000)

Chu W. and Ma C.W. "Reaction kinetics of UV-decolourization of dye materials". *Chemosphere*, vol. 37, pp. 961-974. (1998)

Chu W. and Ma C.W. "Effect of UV-decolorizing of aromatic dyes with different chemical structures." *Toxicological and Environmental Chemistry*, vol. 63, pp. 247-255. (1997)

Chu W. and Jafvert C.T. "Photodechlorination of polychlorobenzene congeners in surfactant micelle solutions". *Environmental Science and Technology*, vol. 28, pp. 2415-2422. (1994)

Chu W. and Tsui S.M. "Photo-Sensitization of Diazo Disperse Dye in Aqueous Acetone". *Chemosphere*, vol. 39, pp. 1667-1677. (1999)

Colour Index. *Journal of Society of Dyers and Colourists*. Bradford. (1974, 1987)

Cook M.M. "Sodium borohydride dye reduction in wastewater". In *Environmental Chemistry of Dyes and Pigments*, Reife A. and Freeman H.S., eds., John Wiley & Sons, Inc. New York, pp. 33-41. (1996)

Cooper P. "Environmental legislation for the United Kingdom textile industry". *Indian Textile Journal*, vol. 102, pp. 30-36. (1992)

Cooper P. "Removing color from dyehouse waste waters – a critical review of technology available". *Journal of Society of Dyers and Colourists.*, vol.109, pp. 97. (1993).

Davis A.P. and Huang C.P., "Removal of phenols from water by a photocatalytic oxidation process". *Water Science and Technology*, vol. 21, pp. 455-464. (1989)

Dávial-Jiménez M.M., Elizalde-González M.P., Gutiérrez-González A. and Peláez-Cid A.A. "Electrochemical treatment of textile dyes and their analysis by high-performance liwuid chromatography with diode array detection". *Journal of Chromatography A*, vol. 889, pp. 243-259. (2000)

Dhale A.D. and Mahajani V.V. "Reactive dye house wastewater treatment. Use of hybrid technology: membrane, sonication followed by wet oxidation". *Industrial and Engineering Chemistry Research*, vol. 38, pp. 2058-2064. (1999)

Eisenberg J.N.S., Bennett D.H. and Mckone T.E. "Chemical dynamics of persistent organic pollutants: a sensitivity analysis relating soil concentration levels to atmospheric emissions". *Environmental Science and Technology,* vol. 32, pp. 115-123. (1998)

Encinas M.V., Lissi E.A. Rufs A.M. and Previtali C.M. "Polymerization photoinitiated by carbonyl compounds. X. Methyl methacrylate polymerization

photoinitiated by fluorenone in the presence of triethylamine". *Journal of Polymer Science: Part A: Polymer Chemistry*, vol. 32, pp. 1649-1655. (1994)

Espenson J. H. *Chemical Kinetics and Reaction Mechanisms*, McGraw-Hill, New York. (1981)

Frederick A. and Line R.A. "Photodegradation of high molecular weight kraft bleachery effluent organochloine and color". *Water Research*, vol. 29, pp. 661-669. (1995)

Gak V.Y., Nadtochenko V.A. and Kiwi J. "Triplet-excited dye molecules (eosine and methylene blue) quenching by H_2O_2 in aqueous solutions". *Journal of Photochemistry and Photobiology A: Chemistry*, vol. 116, pp. 57-62. (1998)

Galadi A. and Julliard M. "Photosensitized oxidation degradation of pesticides". *Chemosphere,* vol. 33, pp. 1-15. (1996)

Galindo C., Jacques P. and Kalt A. "Photodegradation of Aminoazobenzene Acid Orange 52 by Three Advanced Oxidation Processes: UV/H_2O_2, UV/TiO_2 and VIS/TiO_2 Comparative mechanistic and kinetic investigations". *Journal of Photochemistry and Photobiology A: Chemistry,* 130, 35-47. (2000)

Ganesh R., Boardman G.D. and Michelsen D. "Fate of azo dyes in sludges, *Water Research,* vol. 28, pp. 1367-1376. (1994)

Grau P. "Textile industry wastewaters treatment". *Water Science and Technology*, vol. 24, pp. 97-103. (1991)

Habner K., Schmelz E. and Rossbach V. "Identification of potentially carcinogenic azo dyes by means of PADIS analysis system". *International Textile Reports,* vol. 78, pp. 161-164. (1997)

Hamada K., Nishizawa M., Yoshida D. and Mitsuishi M. "Degradation of an azo dye by sodium hypochlorite in aqueous surfactant solutions". *Dyes and Pigments*, vol. 36, pp. 313-322. (1998)

Hawari J., Demeter A., Greer C. and Samson R. "Acetone-induced photodechlorination of Arochlor 1254 in alkaline 2-propanol: Probing the mechanism by thermolysis in the presence of di-t-butyl peroxide". *Chemosphere,* vol. 22, pp. 1161-1174. (1991)

Hawari J., Demeter A. and Samson R. "Sensitized photolysis of polychlorobiphenyls in alkaline 2-propanol: Dechlorination of Arochlor 1254 in soil samples by solar radiation". *Environmental Science and Technology*, vol. 26, pp. 2022-2027. (1992)

Herrera F., Kiwi J., Lopez A. and Nadtochenko V. " Photochemical decoloration of Remozal Brilliant Blue and Uniblue A in the presence of Fe^{3+} and H_2O_2". *Environmental Science and Technology*, vol. 33, pp. 3145-3151. (1999)

Herrera F., Lopez A. and Kiwi J. "Photochemically activated degradation of reactive dyes: statistical modeling of the reactor performance". *Journal of photochemistry and photobiology A: Chemistry*, vol. 135, pp. 45-51. (2000)

Ho T.F.L. and Bolton J.R. "Toxicity changes during the UV treatment of pentachlorophenol in dilute aqueous solution". *Water Research,* vol. 32, pp. 489-497. (1998)

Horspool W.M. *Organic Photochemistry: a Comprehensive Treatment.* Ellis Horwood, New York. (1992)

Horspool W.M. *Aspects of Organic Photochemistry.* Academic Press, London. (1976)

Hsu Y.C., Yen C.H. and Huang H.C. "Multistage treatment of high strength dye wastewater by coagulation and ozonation". *Journal of Chemical Technology and Biotechnology*, vol. 71, pp. 71-76. (1998)

Ince N.H. "Critical effect of hydrogen peroxide in photochemical dye degradation". *Water Research*, vol. 33, pp. 1080-1084. (1999)

Isaacs N.S. *Physical organic chemistry*, Wiley & Sons, pp. 837-841. (1995)

Jahan K., Ahmed T. and Maier W.J. "Modeling the influence of nonionic surfactants on biodegradation of phenanthrene". *Water Research*, vol. 33, pp. 2181-2193. (1999)

Jockusch S., Timpe H.J., Schnabel W. and Turro N.J. "Photoreduction of organic dyes in ketone amine system". *Journal of Photochemistry and Photobiology A: Chemistry*, vol. 98, pp. 129-136. (1996)

Jolanta S.G. "Photodegradation of some 1:2 metal complexed azo dyes in an amide environment". *Dyes and Pigment*, vol. 36, pp.149-159. (1998)

Juang R.S., Tseng R.L., Wu F.C. and Lee S.H. "Adsorption behavior of reactive dyes from aqueous solutions on chitosan". *Journal of Chemical Technology and Biotechnology*, vol. 70, pp. 391-399. (1997)

Kagan J. *Organic photochemistry principles and applications*, Academic Press Inc., San Diego. (1993)

Kang S.F. and Chang H.M. "Coagulation of textile secondary effluents with Fenton's reagent". *Water Science and Technology.*, vol. 36, pp. 215-222. (1997)

Katsuda N., Omura T. and Takagishi T. "Photodegradation of an anthraquinone type disperse dye on polyester, diacetate, and triacetate fibers, and in solution". *Dyes and pigments*, vol. 34, pp. 147-157. (1997)

Kim S.M. and Vogelpohl A. "Degradation of organic pollutants by the photo-fenton-process". *Chemical Engineering Technology*, vol. 21, pp. 187-191. (1998)

Laszlo J.A. "Regeneration of dye-saturated quaternized cellulose by bisulfite-mediated borohydride reduction of dye azo groups: An improved process for decolorization of textile wastewaters". *Environmental Science Technology,* vol. 31, pp. 3647-3653. (1997)

Lenore S.C., Arnold E.F. and Trussell R.R. *Standard methods for the examination of water and wastewater.* American Public Health Association, Washington, D.C., 19th ed. (1995)

Liakou S., Kornaros M. and Lyberatos G. "Pretreatment of azo dyes using ozone". *Water Science and Technology,* vol. 36, pp. 155-163. (1997)

Lin S.H. and Lin C.M. "Treatment of textile waste effluents by ozonation and chemical coagulation". *Water Research*, vol. 27, pp. 1743-1748. (1993)

Lin Y., Gapta G. and Baker J. "Photodegradation of Aroclor 1254 using diethylamine and simulated sunlight". *Journal of Hazardous Materials,* vol. 45, pp. 259-264. (1996)

Lindfors B.E., Nieckarz G.F., Tyler D.R. and Glenn A.G. "Measurement of the cage effect in the photolysis of the $(\eta^5\text{-}C_5H_4(CH_2)_2N(H)C(O)(CH_2)_3CH_3)_2Mo_2(CO)_6$ complex". *Journal of Photochemistry and Photobiology A: Chemistry*, vol. 94, pp. 101-105. (1996)

Liu G.M., Wu T.X. and Zhao J.C. "Photoassisted degradation of dye pollutants. 8. Irreversible degradation of Alizarin Red under visible light radiation in air-equilibrated aqueous TiO_2 dispersions." *Environmental Science and Technology,* vol. 33, pp. 2081-2087. (1999)

Logan S.R. *Fundamentals of chemical kinetics.* Essex: Longman, pp. 212-217 (1996)

Luis M.A.R., John F.H., Arnold L.R., Louise M.L.S. and Ilia A.G. "Mechanistic studies of the Palladium-catalyzed amination of aryl halides and the oxidative addition of aryl bromides to $Pd(BINAP)_2$ and $Pd(DPPF)_2$: An unusual case of zero-order kinetic behavior and product inhibition". *Journal of American Chemical Society*, vol. 122, pp. 4618-4630 (2000)

Mack J. and Bolton J.R. "Photochemistry of nitrite and nitrate in aqueous solution: a review" *Journal of Photochemistry and Photobiology A: Chemistry*, vol. 128, pp. 1-13. (1999)

Marcì G., Sclafani A., Augugliaro V., Palmisano L. and Schiavello M. "Influence of some aromatic and aliphatic compunds on the rate of photodegradation of phenol in aqueous suspensions of TiO_2". *Journal of Photochemistry and Photobiology A: Chemistry*, vol. 89, pp. 69-74. (1995)

McCallum J.E.B., Madison S.A. Alkan S., Depinto R.L. and Rojas Wahl R.U. "Analytical studies on the oxidative degradation of the reactive textile dye Uniblue A". *Environmental Science and. Technology,* vol 34, pp. 5157-5164. (2000)

Meyer V., Carlesson F.H.H. and Oellermann R.A. "Decolourization of textile effluent using a low cost natural adsorbent materials". *Water Science and Technology,* vol. 26, pp. 1205-1211. (1992)

Miao X.S., Chu S.G. and Xu X.B. "Degradation pathways of PCBs upon UB irradiation in Hexane". *Chemosphere*, vol. 39, pp. 1639-1650. (1999)

Morais L.C., Freitas O.M., Gonçclves E.P., Vasconcelos L.T. and González Beça C.G. "Reactive dyes removal from wastewaters by adsorption on eucalyptus bark: varibles that define the process". *Water Research*, vol. 33, pp. 979-988. (1999)

Nakamura K., Kowaki T., Scully A.D. and Hirayame S. "Quenching of chlorophyll *a* fluorescence by oxygen in highly concentrated solutions and microdroplets". *Journal of Photochemistry and Photobiology A: Chemistry,* vol. 104, pp.141-149. (1997)

Namboodri C.G. and Walsh W.K. "Ultraviolet light/hydrogen peroxide system for decolorizing spent reactive dyebath waste water". *American Dyestuff Reporter*, Mar., pp. 15-25. (1996)

Naomi L.S., Peller J., Vinodgopal K. and Kamat P.V. "Combinative sonolysis and photocatalysis for textile dye degradation". *Environmental Science and Technology*, vol. 34, pp. 1747-1750. (2000)

Neevel J.G., Beek J.C.A. Ouden H.H.I. and Graaf B. "Photo-oxidation of azo dyes in the presence of biacetyl and oxygen". *Journal of Society of Dyers and Colorists*, vol 106, pp. 176-180. (1990)

Neevel J.G., Peereboon M. and Graaf B. "Kinetics of the biacetyl-sensitised photo-oxidation of CI Acid Orange 7". *Journal of Society of Dyers and Colorists*, vol 109, pp. 106-113. (1993)

Neumann M.G., Schmitt C.C., Previtali C.M. and Bertolotti S.G. "Photoreduction of resazurin in the presence of aliphatic amines". *Dyes and Pigments*, vol. 32, pp. 93-99. (1996)

O'Neill C., Hawkes F.R., Esteves S.R.R. Hawkes D.L. and Wilcox S.J. "Anaeroic and aerobic treatment of a simulated textile effluent". *Journal of Chemical Technology and Biotechnology,* vol.74, pp. 993-999. (1999)

O'Neill C., Hawkes F.R., Hawkes D.L., Lourenço N.D., Pinheiro H. and Delée W. "Colour in textile effluents – sources, measurement, discharge consents and

simulation: a review". *Journal of Chemical Technology and Biotechnology,* vol.74, pp. 1009-1018. (1999)

Patricio P.Z., Airton K., Sandra G.M., Ronaldo P. Patricia CM., Juan R. and Nelson D. "Degradation of reactive dyes I. A comparative study of ozonation, enzymatic and photochemical processes". *Chemosphere,* vol. 38, pp. 835-852. (1999)

Peter A.T., and Freeman H.S. *Physico-chemical principles of color chemistry*, Blackie Academic & Professional, London. (1996)

Pelegrini R., Peralta-Zamora P., Andrade A.R., Reyes J. and Durán N. "Electrochemically assisted photocatalytic degradation of reactive dyes". *Applied Catalysis B: Environmental*, vol. 22, pp. 83-90. (1999)

Philippe C.V., Roberto B. and Willy V. "Treatment and reuse of wastewater from the textile wet-processing industry: review of emerging technologies". *Journal of Chemical Technology and Biotechnology,* vol. 72, pp. 289-302. (1998)

Poulios I. and Tsachpinis I., " Photodegradation of the textile dye Reactive Black 5 in the presence of semiconducting oxides". *Journal of Chemical Technology and Biotechnology,* vol. 74, pp. 349-357. (1999)

Qu P., Zhao J., Shen T. and Hidaka H. "TiO_2-assisted photodegradation of dyes: a study of two competitive primary processes in the degradation of RB in an aqueous TiO_2 colloidal solution". *Journal of Molecular Catalysis A: Chemical,* vol. 129, pp. 257-268. (1998)

Reutergardh L.B. and Iangphasuk M. "Photocatalytic decolourization of reactive azo dye: a comparison between TiO_2 and CdS photocatalysis". *Chemosphere.* vol. 35, pp. 585-596. (1997)

Rys, P., and Zollinger, H. *Fundamentals of the chemistry and application of dyes*, Wiley-Interscience, New York. (1992)

Sarasa J., Roche M.P., Ormad M.P., Gimeno E., Puig A. and Ovelleiro J.L. "Treatment of a wastewater resulting from dyes manufacturing with ozone and chemical coagulation". *Water Research*, vol. 32, pp. 2721-2727. (1998)

Sato R., Kurihara T. and Takeishi M. "Rate enhancement of amines in the photopolmerization of methyl methacrylate under oxygen". *Polymer International*, vol. 47, pp. 159-164. (1998)

Säuberlich J., Brede O. and Beckert D. "Investigation of the photoreduction of anthraquinonedisulfonic acid by triethylamine with Fouries transform electron spin resonance". *Journal of Physical Chemistry. Part A*, vol. 101, pp. 5659-5665. (1997)

Schliephake K., Mainwaring D.E., Lonergan G.T., Jones I.K. and Baker W.L. "Transformation and degradation of the disazo dye Chicago Sky Blue by a purified laccase from Pycnoporus cinnabarinus". *Enzyme and Microbial Technology*, vol. 27, pp. 100-107. (2000)

Seefeld S. and Stockwell W.R. "First-order sensitivity analysis of models with time-dependent parameters: an application to PAN and ozone". *Atomspheric Environment*, vol. 33, pp. 2941-2953. (1999)

Shu H.Y. and Huang C.R. "Ultraviolet enhanced oxidation for color removal of azo dye wastewater". *American Dyestuff Reporter*, Aug., pp. 30-36. (1995)

Sopa C., Munsin T. and Thongchai P. "Anaerobic decolorization of reactive dyebath effluents by a two-stage UASB system with tapioca as a co-substrate". *Water Research*, vol. 34, pp. 2223-2232. (2000)

Suppan P. *Chemistry and light.* The Royal Society of Chemistry, pp. 51-54 (1994)

Tanaka K., Padermpole K and Hisanage T. "Photocatalytic degradation of commerical azo dyes". *Water Research*, vol. 34, pp. 327-333. (2000)

Tang W.Z. and Chen R.Z. "Decolorization kinetics and mechanisms ofcommerical dyes by H_2O_2/Iron powder system". *Chemosphere*, vol. 32, pp. 947-958. (1996)

Tratnyek P.G., Elovitz M.S. and Cloverson P. "Photoeffects of textile dye wastewaters: sensitization of singlet oxygen formation, oxidation of phenols and toxicity to bacteria". *Environmental Toxicology and Chemistry.* vol. 13, pp. 27-33. (1994)

Turro N.J. *Modern molecular photochemistry.* The Benjamin/Cummings Publishing Company, Inc., pp. 246-248. (1978)

Tünay O., Kabdasli I., Eremektar G. and Orhon D. "Color removal from textile wastewaters". *Water Science and Technology,* vol. 34, pp. 9-16. (1996)

Vinodgopal K. and Kamat P.V. "Enhanced rates of photocatalytic degradation of an azo dye using SnO_2/TiO_2 coupled semiconductor thin films". *Environmental Science and Technology,* vol. 29, pp. 841-845. (1995)

Vlyssides A.G., Loizidou M., Karlis P.K., Zorpas A.A. and Papaioannou D. "Electrochemical oxidation of a textile dye wastewater using Pt/Ti electrode". *Journal of Hazardous Materials*, vol. 70, pp. 41-52. (1999)

Vuilleumier L., Harley R.A. and Brown N.J. "First- and second-order sensitivity analysis of a photochemically reactive system (a Green's function approach)". *Environmental Science and Technology,* vol. 31, pp. 1206-1217. (1997)

Walker G.M. and Weatherley L.R. "Adsorption of acid dyes on to granular activated carbon in fixed beds". *Water Research*, vol. 31, pp. 2093-2101. (1997)

Wang Y. "Solar Photocatalytic Degradation of Eight Commercial Dyes in TiO_2 Suspension". *Water Research*, vol. 34, pp. 990-994. (2000)

Wang C.Y., Liu C.Y., Wang W.Q. and Shen T. "Photochemical events during the photosensitization of colloidal TiO_2 particles by a squaraine dye". *Journal of Photochemistry and Photobiology A: Chemistry*, vol. 109, pp. 159-164. (1997)

Waring R. and Hallas G. *The Chemistry and Application of Dyes*, Plenum Press, New York. (1990)

Wayne R.P. *Principles and applications of photochemistry.* Oxford Secience publications, pp. 117-119. (1988)

Wolfgang W., Ralf K., Oliver S. and Andreas D. "Combined zero-and first-order kinetic model of the degradation of TCE and cis-DCE with commerical iron". *Environmental Science and Technology,* vol. 33, pp. 4304-4309. (1999)

Wu K., Xie. Y., Zhao J. and Hidaka H., "Photo-fenton degradation of a dye under visible light irradiation". *Journal of Molecular Catalysis A: Chemical*, vol. 144, pp. 77-84. (1999)

Wu T., Lin.T, Zhao J., Hidaka H. and Serpone N. "TiO_2-assisted photodegradation of dyes. 9. Photooxidation of a squarylium cyanine dye in aqueous dispersions under visible light irradiation". *Environmental Science and Technology,* vol. 33, pp. 1379-1387. (1999)

Yang Y., Wyatt D.T. and Bahorsky M., "Decolorization of dyes using UV/H_2O_2 photochemical oxidation". *Textile Chemists and Colorists*, vol. 30, pp. 27-35. (1998)

Yang Y.J., Wilkinson J.G. and Russell A.G., "Fast, direct sensitivity analysis of multdimensional photochemical models". *Environmental Science and Technology,* vol. 31, pp. 2859-2868. (1997)

Yasui S., Munekazu T., Kenji I. And Atsuyoshi O., "Quenching of a photosensitized dye through single-electron transfer from trivalent phosphorus compounds". *Journal of Organic Chemistry,* vol. 65, pp. 4715-4720. (2000)

Yoshida H. and Takemori T., "Adsorption of direct dye on cross-linked chitosan fiber: breakthroug curve". *Environmental Science and Technology,* vol. 35, pp. 29-37. (1997)

Young L. and Yu J., "Ligninase-catalysed decolorization of synthetic dyes". *Water Research,* vol. 31., pp.1187-1193. (1997)

Zepp R.G. and Cline D.M., "Rates of Direct Photolysis in Aquatic Environment". *Environmental Science and Technology,* vol. 11, pp. 359–366. (1977)

Zhao J., Wu T., Wu K., Hidaka H. and Serpone N., "Photoassisted degradation of dye pollutants. 3. Degradation of the cationic dye Rhodamine B in aqueous anionic surfactant/TiO_2 dispersions under visible light irradiation: Evidence for the need of substrate adsorption on TiO_2 particles". *Environmental Science and Technology,* vol. 32, pp. 2394-2400. (1998)

Zhao J., Zhang F., Shen T., Hidaka H., Pelizzetti E. and Serpone N., "Photoassisted degradation of dye pollutants in aqueous TiO_2 dispersions under irrradiation by visible light". *Environmental Science and Technology,* vol. 120, pp. 173-178. (1997)

Zollinger H., *Color chemistry: syntheses, properties, and applications of organic dyes and pigments.* Weinheim, New York. (1991)

APPENDICES

APPENDIX I: PHOTOS

Photodecolorization of DY7 in 1:2 ACE/H_2O (v/v) aqueous solution at 253.7 nm and initial pH 11.
The irradiation time is 0, 300, 900,1800 and 2700 sec. (From left to right).
Exp. No: DYpH04

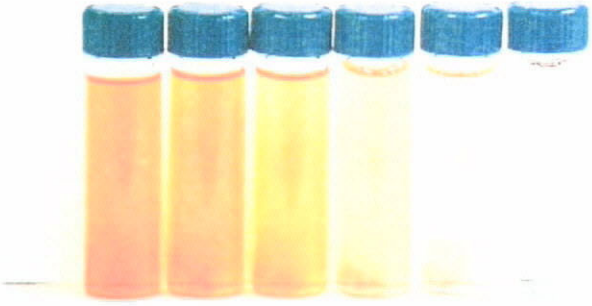

Photodecolorization of DO11 in 1:4 ACE/H_2O (v/v) aqueous solution at 253.7 nm and initial pH 9.
The irradiation time is 0, 300, 900,1800, 2700 and 3600 sec. (From left to right).
Exp. No.: DOA/W03

Photodegradation of DO11 in Cocktail solution (TEA/ACE = 1:192 (M/M) at 253.7 nm and initial pH 9.
The irradiation time is 0, 300, 600, 900, 1200 and 1800 sec. (From left to right).
Exp. No: DOT/A06

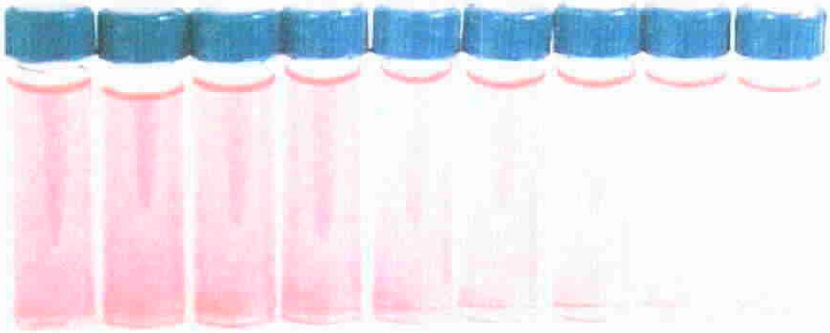

Control experiment: Photodegradation of RR2 in water at 253.7 nm and initial pH 11.
The irradiation time is 0, 60, 120, 180, 240, 300, 360, 480 and 600 sec. (From left to right). Exp. No.: RRACE01

Photodegradation of RR2 in 0.108 mol L^{-1} ACE aqueous solution at 253.7 nm. The initial pH was 11 and the light intensity was 1.5×10^{-5} Einstein L^{-1} s^{-1}. The irradiation time is 0, 30, 60, 90, 120, 150, 180 and 240 sec. (From left to right). Exp. No.: RRACE08

Photodegradation of RR2 in 0.04 mol L^{-1} TEA solution at 253.7 nm. The initial pH was 11 and the light intensity was 1.5×10^{-5} Einstein L^{-1} s^{-1}. The irradiation time is 0, 60, 120, 180, 240, 300, 360, 480 and 600 sec. (From left to right). Exp. No.: RRTEA05

Photodegradation of RR2 in Cocktail solution at 253.7 nm. The initial concentration of [TEA] and [ACE] are 0.02 and 0.108 mol L^{-1} respectively. The irradiation time is 0, 15, 30, 45, 60, 75 and 90 sec. (From left to right). Exp. No.: RRCT03.

APPENDIX II: The Photodegradation of C.I. Disperse Yellow 7 (DY7)

Effect of ACE/H_2O ratio

Exp. No.: DYA/W01 – DYA/W08

DYA/W01 (ACE/H_2O = 0:1 v/v)

Time (sec)	Conc. (ppm)	D_t/D_0	Ln D_t/D_0	pH
0	22.3100	1.0000	0.0000	7.1
300	22.3095	1.0000	0.0000	7.03
900	22.3057	0.9998	-0.0002	6.71
1800	21.1700	0.9489	-0.0524	6.57
2700	18.6330	0.8352	-0.1801	6.22
3600	16.0990	0.7216	-0.3263	6.06

DYA/W02 (ACE/H_2O = 1:2.33 v/v)

Time (sec)	Conc. (ppm)	D_t/D_0	Ln D_t/D_0	pH
0	25.3671	1.0000	0.0000	7.03
300	21.2505	0.8377	-0.1771	5.85
900	15.6110	0.6154	-0.4855	5.01
1800	9.7248	0.3834	-0.9588	4.55
2700	6.1020	0.2405	-1.4248	4.53
3600	3.5245	0.1389	-1.9737	4.27
4500	2.5114	0.0990	-2.3126	4.15
5400	1.2516	0.0493	-3.0090	3.96

DYA/W03 (ACE/H_2O = 1:2.13 v/v)

Time (sec)	Conc. (ppm)	D_t/D_0	Ln D_t/D_0	pH
0	21.9470	1.0000	0.0000	7.04
300	16.2021	0.7382	-0.3035	5.59
900	10.6068	0.4833	-0.7271	4.56
1800	6.6053	0.3010	-1.2008	4.17
2700	4.6900	0.2137	-1.5432	4.15
3600	2.1952	0.1000	-2.3024	3.99
5400	0.4469	0.0204	-3.8941	3.74

DYA/W04 (ACE/H_2O = 1:2 v/v)

Time (sec)	Conc. (ppm)	D_t/D_0	Ln D_t/D_0	pH
0	22.0000	1.0000	0.0000	6.92
300	16.2581	0.7390	-0.3025	5.31
900	10.2947	0.4679	-0.7594	4.56
1800	3.5903	0.1632	-1.8128	4.45
2700	0.8332	0.0379	-3.2735	4.25
3600	0.3871	0.0176	-4.0401	4.08

DYA/W05 (ACE/H_2O = 1:1.78 v/v)

Time (sec)	Conc. (ppm)	D_t/D_0	Ln D_t/D_0	pH
0	23.0141	1.0000	0.0000	6.94
300	18.5070	0.8042	-0.2180	5.58
900	11.2178	0.4874	-0.7186	4.80
1800	6.9654	0.3027	-1.1952	4.28
2700	4.8028	0.2087	-1.5669	4.14
3600	1.3280	0.0577	-2.8524	4.13

DYA/W06 (ACE/H_2O = 1:1 v/v)

Time (sec)	Conc. (ppm)	D_t/D_0	Ln D_t/D_0	pH
0	22.9788	1.0000	0.0000	7.06
300	18.8993	0.8225	-0.1954	5.81
900	14.1521	0.6159	-0.4847	4.75
1800	7.3802	0.3212	-1.1358	4.12
2700	2.7890	0.1214	-2.1089	3.90
3600	1.8048	0.0785	-2.5441	3.77

DYA/W07 (ACE/H_2O = 2:1 v/v)

Time (sec)	Conc. (ppm)	D_t/D_0	Ln D_t/D_0	pH
0	25.0163	1.0000	0.0000	7.08
300	22.6692	0.9062	-0.0985	5.67
900	16.1050	0.6438	-0.4404	5.06
1800	9.2177	0.3685	-0.9984	4.89
2700	4.5030	0.1800	-1.7148	4.39
3600	2.0881	0.0835	-2.4833	4.29
5400	0.7911	0.0316	-3.4539	4.20

DYA/W08 (ACE/H_2O = 3:1 v/v)

Time (sec)	Conc. (ppm)	D_t/D_0	Ln D_t/D_0	pH
0	23.6180	1.0000	0.0000	7.10
300	21.5254	0.9114	-0.0928	6.44
900	16.2179	0.6867	-0.3759	5.85
1800	8.8400	0.3743	-0.9827	5.17
2700	4.6321	0.1961	-1.6290	4.83
3600	1.8933	0.0802	-2.5237	4.57

Reaction Rates and Quantum Yields

Exp. No.	ACE/H_2O (v/v)	k x 10^{-4} (s^{-1})	r^2	Φ x 10^{-5}
DYA/W01	0:1.00	7.17	0.8291	9.03
DYA/W02	1:2.33	5.40	0.9971	6.81
DYA/W03	1:2.13	6.80	0.9832	8.57
DYA/W04	1:2.00	11.25	0.9879	14.18
DYA/W05	1:1.78	7.12	0.9888	8.97
DYA/W06	1:1.00	6.78	0.9931	8.55
DYA/W07	2:1.00	6.43	0.9919	8.11
DYA/W08	3:1.00	6.40	0.9868	8.07

Effect of pH
Exp. No.: DYpH01 – DYpH04

DYpH01 (Initial pH 4, ACE/H_2O = 1:2 v/v)

Time (sec)	Conc. (ppm)	D_t/D_0	Ln D_t/D_0	pH
0	24.0141	1.0000	0.0000	4.18
300	17.2507	0.7184	-0.3308	4.14
900	9.8822	0.4115	-0.8879	4.07
1800	4.7553	0.1980	-1.6194	3.76
2700	2.4470	0.1019	-2.2838	3.72

DYpH02 (Initial pH 5.5, ACE/H_2O = 1:2 v/v)

Time (sec)	Conc. (ppm)	D_t/D_0	Ln D_t/D_0	pH
0	22.7582	1.0000	0.0000	5.60
300	16.8021	0.7383	-0.3034	4.90
900	11.3427	0.4984	-0.6964	4.46
1800	3.3668	0.1479	-1.9110	4.30
2700	1.3841	0.0608	-2.7999	4.15

DYpH03 (Initial pH 9.0, ACE/H_2O = 1:2 v/v)

Time (sec)	Conc. (ppm)	D_t/D_0	Ln D_t/D_0	pH
0	21.9103	1.0000	0.0000	8.96
300	15.8053	0.7214	-0.3266	6.64
900	8.2038	0.3744	-0.9824	5.49
1800	2.3931	0.1092	-2.2144	4.52
2700	0.7272	0.0332	-3.4055	4.51

DYpH04 (Initial pH 11.0, ACE/H_2O = 1:2 v/v)

Time (sec)	Conc. (ppm)	D_t/D_0	Ln D_t/D_0	pH
0	22.6758	1.0000	0.0000	10.91
300	14.6050	0.6441	-0.4399	8.24
900	7.4979	0.3307	-1.1067	6.78
1800	2.3422	0.1033	-2.2702	5.58
2700	0.6578	0.0290	-3.5402	5.20

Reaction Rates and Quantum Yields

Exp. No.	Initial pH	k x 10^{-3} (s^{-1})	r^2	Φ x 10^{-3}
DYpH01	4	0.09	0.9934	1.10
DYpH02	5.5	1.03	0.9898	1.28
DYpH03	9	1.24	0.9970	1.56
DYpH04	11	1.29	0.9986	1.63

BOD_5/COD tests

Exp. No.: DYBOD01 & DYCOD01

Time (sec)	BOD_5 (mg/L)	COD (mg/L)	BOD_5 / COD
0	23.7	114.5	0.207
900	51.0	220.8	0.231
1800	125.6	460.0	0.273
2700	235.5	674.7	0.349
3600	316.9	834.1	0.380
4500	459.0	1048.8	0.438

ACE Recovery

Exp. No. : ReACE01

Total vol. = vol. of H_2O (140ml) + vol. of ACE (70ml)

Time (min)	Q_{air} (L)	Vol. (ml)	ACE recovery ratio V/V_0	DO (mg/L)
0	0	210	0.0000	7.70
1	0.5	209	0.0143	7.80
5	2.5	207	0.0429	7.90
10	5	205	0.0714	7.98
15	7.5	203.5	0.0929	8.06
30	15	199	0.1571	8.26
45	22.5	196	0.2000	8.35
75	37.5	190	0.2857	8.45
105	52.5	185	0.3571	8.52
150	75	178	0.4571	8.58
195	97.5	172	0.5429	8.59
300	150	160	0.7143	8.59
360	180	156	0.7714	8.60
420	210	153	0.8143	8.60
540	270	147	0.9000	8.60

APPENDIX III: The Photodegradation of C.I. Disperse Orange 11 (DO11)

Effect of ACE/H_2O ratio

Exp. No.: DOA/W01 – DYA/W06

DOA/W01 (ACE/H_2O = 0:1 v/v)

Time (sec)	Conc. (ppm)	D_t/D_0	Ln D_t/D_0	pH
0	19.989	1.0000	0.0000	9.03
300	19.989	1.0000	0.0000	8.97
900	19.989	1.0000	0.0000	8.90
1800	19.988	1.0000	0.0000	8.89
2700	19.987	0.9999	-0.0001	8.84
3600	19.987	0.9999	-0.0001	8.83

DOA/W02 (ACE/H_2O = 1:5 v/v)

Time (sec)	Conc. (ppm)	D_t/D_0	Ln D_t/D_0	pH
0	17.461	1.0000	0.0000	8.90
300	12.795	0.7328	-0.3109	4.74
900	7.002	0.4010	-0.9138	3.92
1800	2.127	0.1218	-2.1053	3.73

DOA/W03 (ACE/H_2O = 1:4 v/v)

Time (sec)	Conc. (ppm)	D_t/D_0	Ln D_t/D_0	pH
0	19.871	1.0000	0.0000	8.87
300	11.472	0.5773	-0.5494	5.10
900	7.188	0.3617	-1.0168	4.05
1800	1.397	0.0703	-2.6549	3.89
2700	0.393	0.0198	-3.9232	3.88

DOA/W04 (ACE/H_2O = 1:3 v/v)

Time (sec)	Conc. (ppm)	D_t/D_0	Ln D_t/D_0	pH
0	20.113	1.0000	0.0000	9.10
300	14.140	0.7030	-0.3524	5.17
900	7.640	0.3799	-0.9680	4.04
1800	1.555	0.0773	-2.5599	3.69

DOA/W05 (ACE/H_2O = 1:2 v/v)

Time (sec)	Conc. (ppm)	D_t/D_0	Ln D_t/D_0	pH
0	20.298	1.0000	0.0000	8.90
300	15.174	0.7476	-0.2909	4.79
900	8.937	0.4403	-0.8203	4.05
1800	2.731	0.1345	-2.0059	4.06
2700	0.811	0.0400	-3.2200	3.92

DOA/W06 (ACE/H_2O = 1:1.5 v/v)

Time (sec)	Conc. (ppm)	D_t/D_0	Ln D_t/D_0	pH
0	19.990	1.0000	0.0000	9.04
300	15.250	0.7629	-0.2707	4.83
900	10.055	0.5030	-0.6872	4.27
1800	3.690	0.1846	-1.6896	4.13
2700	1.346	0.0673	-2.6981	3.96

Reaction Rates and Quantum Yields

Exp. No.	ACE/H_2O (v/v)	k x 10^{-3} (s^{-1})	r^2	Φ x 10^{-2}
DOA/W01	0:1	Nil	-	-
DOA/W02	1:5	1.14	0.9937	5.65
DOA/W03	1:4	1.44	0.9907	7.13
DOA/W04	1:3	1.35	0.9790	6.69
DOA/W05	1:2	1.15	0.9907	5.70
DOA/W06	1:1.5	0.97	0.9911	4.80

Effect of pH

Exp. No.: DOpH01 – DOpH04

DOpH01 (Initial pH 3, ACE/H_2O = 1:4 v/v)

Time (sec)	Conc. (ppm)	D_t/D_0	Ln D_t/D_0	pH
0	19.652	1.0000	0.0000	2.97
300	13.384	0.6811	-0.3841	2.75
900	6.653	0.3385	-1.0831	2.76
1800	1.766	0.0899	-2.4095	2.73
2700	0.687	0.0350	-3.3536	2.73

DOpH02 (Initial pH 5, ACE/H_2O = 1:4 v/v)

Time (sec)	Conc. (ppm)	D_t/D_0	Ln D_t/D_0	pH
0	20.158	1.0000	0.0000	5.10
300	14.231	0.7060	-0.3482	3.43
900	7.692	0.3816	-0.9634	3.30
1800	1.718	0.0852	-2.4624	3.25
2700	-			3.20

DOpH03 (Initial pH 7, ACE/H_2O = 1:4 v/v)

Time (sec)	Conc. (ppm)	D_t/D_0	Ln D_t/D_0	pH
0	19.871	1.0000	0.0000	6.87
300	13.127	0.6606	-0.4146	5.95
900	5.507	0.2771	-1.2832	4.06
1800	1.300	0.0654	-2.7269	4.06
2700	0.520	0.0262	-3.6432	3.82

DOpH04 (Initial pH 11, ACE/H_2O = 1:4 v/v)

Time (sec)	Conc. (ppm)	D_t/D_0	Ln D_t/D_0	pH
0	18.502	1.0000	0.0000	10.93
300	12.907	0.6976	-0.3601	10.67
900	8.432	0.4557	-0.7858	10.24
1800	2.941	0.1590	-1.8391	8.71
2700	1.168	0.0631	-2.7626	6.99

Reaction Rates and Quantum Yields

Exp. No.	Initial pH	k x 10^{-3} (s^{-1})	r^2	Φ x 10^{-2}
DOpH01	3	1.27	0.9969	6.29
DOpH02	5	1.31	0.9833	6.49
DOpH03	7	1.40	0.9935	6.93
DOpH04	11	1.01	0.9961	5.00

Effect of TEA in Cocktail Solution
Exp. No.: DOT/A01 – DOT/A12

DOT/A01 (Initial pH 9, TEA/ACE = 1:644 M/M)

Time (sec)	Conc. (ppm)	D_t/D_0	Ln D_t/D_0	pH
0	18.500	1.0000	0.0000	8.91
300	12.033	0.6504	-0.4301	7.00
600	6.777	0.3663	-1.0043	5.19
900	4.914	0.2656	-1.3256	4.87
1200	2.962	0.1601	-1.8320	4.44
1800	-	-	-	4.32

DOT/A02 (Initial pH 9, TEA/ACE = 1:385 M/M)

Time (sec)	Conc. (ppm)	D_t/D_0	Ln D_t/D_0	pH
0	19.443	1.0000	0.0000	9.10
300	13.109	0.6742	-0.3942	7.67
600	7.732	0.3977	-0.9221	7.02
900	5.543	0.2851	-1.2549	6.23
1200	2.303	0.1184	-2.1333	4.60
1800	0.865	0.0445	-3.1125	4.30

DOT/A03 (Initial pH 9, TEA/ACE = 1:297 M/M)

Time (sec)	Conc. (ppm)	D_t/D_0	Ln D_t/D_0	pH
0	18.501	1.0000	0.0000	9.07
300	12.400	0.6702	-0.4001	8.64
600	6.954	0.3759	-0.9785	7.23
900	3.844	0.2078	-1.5713	5.92
1200	1.968	0.1064	-2.2408	5.54
1800	-	-	-	4.45

DOT/A04 (Initial pH 9, TEA/ACE = 1:256 M/M)

Time (sec)	Conc. (ppm)	D_t/D_0	Ln D_t/D_0	pH
0	19.181	1.0000	0.0000	8.99
300	12.858	0.6704	-0.4000	7.23
600	7.822	0.4078	-0.8970	6.55
900	5.505	0.2870	-1.2483	4.99
1200	2.032	0.1059	-2.2449	4.70
1800	0.611	0.0319	-3.4466	4.56

DOT/A05 (Initial pH 9, TEA/ACE = 1:227 M/M)

Time (sec)	Conc. (ppm)	D_t/D_0	Ln D_t/D_0	pH
0	21.031	1.0000	0.0000	9.03
300	14.051	0.6681	-0.4033	7.33
600	8.404	0.3996	-0.9173	6.45
900	5.132	0.2440	-1.4106	5.00
1200	2.152	0.1023	-2.2798	4.68
1800	0.688	0.0327	-3.4204	4.60

DOT/A06 (Initial pH 9, TEA/ACE = 1:192 M/M)

Time (sec)	Conc. (ppm)	D_t/D_0	Ln D_t/D_0	pH
0	19.181	1.0000	0.0000	8.93
300	12.773	0.6659	-0.4066	7.42
600	7.826	0.4080	-0.8965	6.05
900	4.974	0.2593	-1.3497	4.78
1200	1.827	0.0953	-2.3512	4.70
1800	0.627	0.0327	-3.4207	4.64

DOT/A07 (Initial pH 9, TEA/ACE = 1:154 M/M)

Time (sec)	Conc. (ppm)	D_t/D_0	Ln D_t/D_0	pH
0	18.994	1.0000	0.0000	9.00
300	12.965	0.6826	-0.3819	8.52
600	7.635	0.4020	-0.9114	7.42
900	5.074	0.2671	-1.3200	6.25
1200	1.953	0.1028	-2.2748	5.01
1800	0.597	0.0314	-3.4600	4.80

DOT/A08 (Initial pH 9, TEA/ACE = 1:148 M/M)

Time (sec)	Conc. (ppm)	D_t/D_0	Ln D_t/D_0	pH
0	19.995	1.0000	0.0000	8.98
300	14.072	0.7038	-0.3513	8.44
600	7.656	0.3829	-0.9600	7.58
900	5.081	0.2541	-1.3700	6.31
1200	2.679	0.1340	-2.0099	5.18
1800	0.710	0.0355	-3.3383	4.87

DOT/A09 (Initial pH 9, TEA/ACE = 1:142 M/M)

Time (sec)	Conc. (ppm)	D_t/D_0	Ln D_t/D_0	pH
0	18.335	1.0000	0.0000	9.06
300	11.677	0.6369	-0.4512	8.75
600	7.925	0.4322	-0.8388	7.18
900	4.733	0.2581	-1.3543	6.97
1200	2.319	0.1265	-2.0678	6.25
1800	-			5.01

DOT/A10 (Initial pH 9, TEA/ACE = 1:138 M/M)

Time (sec)	Conc. (ppm)	D_t/D_0	Ln D_t/D_0	pH
0	20.211	1.0000	0.0000	8.95
300	11.520	0.5700	-0.5621	8.76
600	8.677	0.4293	-0.8456	6.81
900	4.837	0.2393	-1.4300	6.32
1200	2.735	0.1353	-2.0001	5.99
1800	1.246	0.0616	-2.7866	5.32

DOT/A11 (Initial pH 9, TEA/ACE = 1:135 M/M)

Time (sec)	Conc. (ppm)	D_t/D_0	Ln D_t/D_0	pH
0	19.855	1.0000	0.0000	9.02
300	11.895	0.5991	-0.5123	8.28
600	8.546	0.4304	-0.8430	6.59
900	4.783	0.2409	-1.4234	6.49
1200	2.976	0.1499	-1.8978	6.01
1800	1.219	0.0614	-2.7903	5.54

DOT/A12 (Initial pH 9, TEA/ACE = 1:128 M/M)

Time (sec)	Conc. (ppm)	D_t/D_0	Ln D_t/D_0	pH
0	19.225	1.0000	0.0000	9.14
300	13.274	0.6905	-0.3704	8.93
600	8.220	0.4276	-0.8496	8.56
900	5.492	0.2857	-1.2529	8.49
1200	3.525	0.1834	-1.6963	7.43
1800	1.014	0.0527	-2.9423	6.96

Reaction Rates and Quantum Yields

Exp. No.	TEA/ACE (M/M)	k x 10^{-3} (s^{-1})	r^2	Φ x 10^{-2}
DOT/A01	1:644	1.53	0.9896	7.56
DOT/A02	1:385	1.68	0.9839	8.30
DOT/A03	1:297	1.78	0.9882	8.82
DOT/A04	1:256	1.80	0.9704	8.91
DOT/A05	1:227	1.82	0.9835	9.03
DOT/A06	1:192	1.83	0.9769	9.06
DOT/A07	1:154	1.82	0.9754	9.01
DOT/A08	1:148	1.74	0.9833	8.62
DOT/A09	1:142	1.61	0.9827	7.96
DOT/A10	1:138	1.58	0.9937	7.82
DOT/A11	1:135	1.55	0.9940	7.70
DOT/A12	1:128	1.53	0.9852	7.58

[TEA], mol L^{-1}	k_r x 10^9 L mol^{-1} s^{-1}	k_d x 10^6 s^{-1}
0.0175	5.83	8.40
0.0182	5.60	8.08
0.0189	5.40	7.78
0.0196	5.20	7.50
0.0200	5.10	7.35
0.0210	4.86	7.00
0.0240	4.25	6.13

APPENDIX IV: The Photodegradation of C.I. Reactive Red 2 (RR2)

Effect of ACE

Exp. No.: RRACE01 - RRACE11

RRACE01 ([ACE] = 0 mol L^{-1})

Time (sec)	Conc. (x 10^{-5} mol L^{-1})	D_t/D_0	Ln D_t/D_0	pH
0	1.690	1.0000	0.0000	10.95
60	1.650	0.9763	-0.0240	10.86
120	1.590	0.9408	-0.0610	10.84
180	1.590	0.9408	-0.0610	10.51
240	1.560	0.9231	-0.0800	10.46
300	1.560	0.9231	-0.0800	10.44
360	1.540	0.9112	-0.0929	10.43
480	1.490	0.8817	-0.1260	10.40
600	1.410	0.8343	-0.1811	10.39

RRACE02 ([ACE] = 0.003 mol L^{-1})

Time (sec)	Conc. (x 10^{-5} mol L^{-1})	D_t/D_0	Ln D_t/D_0	pH
0	1.652	1	0.0000	10.99
30	1.570	0.9503	-0.0510	10.67
60	1.491	0.9026	-0.1025	10.02
90	1.426	0.8633	-0.1470	9.53
120	1.394	0.844	-0.1696	9.22
150	1.341	0.8118	-0.2085	8.60
180	1.173	0.7103	-0.3421	7.99
270	1.042	0.631	-0.4604	7.61
300	0.888	0.5378	-0.6203	7.04

RRACE03 ([ACE] = 0.008 mol L^{-1})

Time (sec)	Conc. (x 10^{-5} mol L^{-1})	D_t/D_0	Ln D_t/D_0	pH
0	1.679	1	0.0000	11.05
30	1.485	0.8846	-0.1226	10.53
60	1.218	0.7257	-0.3206	9.65
90	0.956	0.5693	-0.5633	8.40
120	0.792	0.4717	-0.7514	7.21
180	0.633	0.3771	-0.9752	6.53
240	0.428	0.2548	-1.3673	6.17

RRACE04 ([ACE] = 0.014 mol L^{-1})

Time (sec)	Conc. (x 10^{-5} mol L^{-1})	D_t/D_0	Ln D_t/D_0	pH
0	1.754	1	0.0000	10.98
30	1.576	0.8988	-0.1067	9.63
60	1.274	0.7265	-0.3195	9.29
90	1.144	0.6522	-0.4274	8.63
120	0.845	0.4817	-0.7304	8.09
150	0.591	0.3372	-1.0871	6.64
180	0.529	0.3015	-1.1990	6.51
240	0.307	0.175	-1.7430	5.91
300	0.180	0.1026	-2.2769	5.40

RRACE05 ([ACE] = 0.027 mol L^{-1})

Time (sec)	Conc. (x 10^{-5} mol L^{-1})	D_t/D_0	Ln D_t/D_0	pH
0	1.800	1	0.0000	11.03
30	1.405	0.7805	-0.2478	8.95
60	0.994	0.5524	-0.5935	8.77
90	0.654	0.3636	-1.0117	8.21
120	0.396	0.22	-1.5141	6.77
150	0.254	0.1411	-1.9583	6.48
180	0.201	0.1115		5.82
240	0.115	0.0641		5.43
300	0.077	0.0428		5.30

RRACE06 ([ACE] = 0.054 mol L^{-1})

Time (sec)	Conc. (x 10^{-5} mol L^{-1})	D_t/D_0	Ln D_t/D_0	pH
0	1.739	1	0.0000	11.02
30	1.234	0.7095	-0.3432	9.90
60	0.687	0.3949	-0.9291	9.28
90	0.359	0.2067	-1.5765	8.47
120	0.247	0.1418	-1.9533	7.47
150	0.157	0.0905	-2.4024	6.39
180	0.110	0.0634		6.01
240	0.073	0.042		5.86
300	0.064	0.0367		5.43

RRACE07 ([ACE] = 0.081 mol L^{-1})

Time (sec)	Conc. (x 10^{-5} mol L^{-1})	D_t/D_0	Ln D_t/D_0	pH
0	1.731	1	0.0000	10.97
30	0.924	0.5338	-0.6277	9.46
60	0.492	0.2845	-1.2570	8.13
90	0.247	0.1428	-1.9463	6.93
120	0.180	0.1041	-2.2624	5.85
150	0.113	0.0651	-2.7318	5.65
180	0.095	0.0548		5.19
240	0.072	0.0417		4.57
300	0.069	0.0397		4.09

RRACE08 ([ACE] = 0.108 mol L^{-1})

Time (sec)	Conc. (x 10^{-5} mol L^{-1})	D_t/D_0	Ln D_t/D_0	pH
0	1.800	1	0.0000	10.95
30	0.929	0.5158	-0.6620	9.67
60	0.457	0.2541	-1.3700	8.54
90	0.230	0.128	-2.0557	7.09
120	0.122	0.0677	-2.6927	6.32
150	0.087	0.0486		5.91
180	0.074	0.0409		5.72
240	0.055	0.0306		5.33
300	0.051	0.0283		4.88

RRACE09 ([ACE] = 0.135 mol L^{-1})

Time (sec)	Conc. (x 10^{-5} mol L^{-1})	D_t/D_0	Ln D_t/D_0	pH
0	1.632	1	0.0000	11.09
30	0.871	0.5337	-0.6279	9.35
60	0.450	0.2759	-1.2877	6.65
90	0.302	0.1851	-1.6869	5.88
120	0.158	0.0968	-2.3351	5.49
150	0.090	0.0552	-2.8968	5.01
180	0.083	0.051		4.42
240	0.080	0.0492		4.16

RRACE10 ([ACE] = 0.162 mol L^{-1})

Time (sec)	Conc. (x 10^{-5} mol L^{-1})	D_t/D_0	Ln D_t/D_0	pH
0	1.681	1	0.0000	11.03
30	0.946	0.5626	-0.5752	8.72
60	0.525	0.3121	-1.1644	7.38
90	0.319	0.1898	-1.6618	6.76
120	0.178	0.1058	-2.2462	5.19
150	0.111	0.066	-2.7181	4.61
180	0.084	0.0502		4.34
240	0.057	0.0338		4.32

RRACE11 ([ACE] = 0.216 mol L^{-1})

Time (sec)	Conc. (x 10^{-5} mol L^{-1})	D_t/D_0	Ln D_t/D_0	pH
0	1.670	1	0.0000	11.02
30	0.881	0.5273	-0.6400	8.78
60	0.679	0.4066	-0.8999	7.13
90	0.470	0.2812	-1.2687	6.72
120	0.269	0.1613	-1.8245	5.30
150	0.205	0.1225	-2.0996	5.04
180	0.157	0.0939		4.61
240	0.118	0.0707		4.27
300	0.095	0.0568		4.11

Reaction Rates and Quantum Yields

Exp. No.	[ACE], mol L^{-1}	k x 10^{-2} (s^{-1})	r^2	Φ x 10^{-3}
RRACE01	0	0.03	0.9520	0.30
RRACE02	0.003	0.17	0.9856	1.72
RRACE03	0.008	0.57	0.9912	5.78
RRACE04	0.014	0.71	0.9758	7.20
RRACE05	0.027	1.23	0.9792	12.47
RRACE06	0.054	1.62	0.9916	16.42
RRACE07	0.081	1.92	0.9841	19.46
RRACE08	0.108	2.26	0.9997	22.91
RRACE09	0.135	1.94	0.9963	19.66
RRACE10	0.162	1.85	0.9986	18.75
RRACE11	0.216	1.46	0.9812	14.80

Effect of pH
Exp. No.: RRApH01 – RRApH04

RRApH01 (Initial pH 3.0, [ACE] = 0.108 mol L^{-1})

Time (sec)	Conc. (x 10^{-5} mol L^{-1})	D_t/D_0	Ln D_t/D_0	pH
0	1.640	1	0.0000	3.05
30	1.314	0.801	-0.2219	2.89
60	0.907	0.5529	-0.5926	2.84
90	0.608	0.3707	-0.9924	2.81
120	0.444	0.2706	-1.3071	2.77
150	0.250	0.1527	-1.8793	2.76
180	0.189	0.115	-2.1628	2.76
240	0.114	0.0695	-2.6664	2.75

RRApH02 (Initial pH 5.0, [ACE] = 0.108 mol L^{-1})

Time (sec)	Conc. (x 10^{-5} mol L^{-1})	D_t/D_0	Ln D_t/D_0	pH
0	1.624	1	0.0000	5.08
30	1.203	0.7407	-0.3002	5.02
60	0.839	0.5167	-0.6603	4.46
90	0.559	0.3439	-1.0674	4.14
120	0.354	0.218	-1.5233	3.90
150	0.253	0.1555	-1.8611	3.59
180	0.166	0.1019	-2.2838	3.57
240	0.093	0.0572	-2.8612	3.55

RRApH03 (Initial pH 7.0, [ACE] = 0.108 mol L^{-1})

Time (sec)	Conc. (x 10^{-5} mol L^{-1})	D_t/D_0	Ln D_t/D_0	pH
0	1.828	1	0.0000	6.95
30	1.260	0.6897	-0.3715	5.83
60	0.795	0.4351	-0.8322	5.47
90	0.481	0.2633	-1.3345	5.33
120	0.335	0.1835	-1.6955	5.23
150	0.246	0.1346	-2.0054	4.53
180	0.167	0.0914	-2.3925	4.38
240	0.105	0.0575	-2.8560	4.09
300	0.092	0.0503	-2.9898	3.86

RRApH04 (Initial pH 8.5, [ACE] = 0.108 mol L^{-1})

Time (sec)	Conc. (x 10^{-5} mol L^{-1})	D_t/D_0	Ln D_t/D_0	pH
0	1.781	1.0000	0.0000	8.49
30	1.229	0.6900	-0.3711	7.02
60	0.770	0.4324	-0.8384	6.28
90	0.495	0.2780	-1.2801	5.99
120	0.304	0.1709	-1.7667	5.56
150	0.173	0.0971	-2.3320	5.10
180	0.140	0.0788	-2.5408	4.76
240	0.110	0.0619	-2.7822	4.42
300	0.081	0.0454	-3.0922	4.12

Reaction Rates and Quantum Yields

Exp. No.	Initial pH	k x 10^{-2} (s^{-1})	r^2	Φ x 10^{-3}
RRApH01	3.0	1.15	0.9886	11.66
RRApH02	5.0	1.22	0.9961	12.37
RRApH03	7.0	1.38	0.9947	13.99
RRApH04	8.5	1.49	0.9940	15.10

Anion determination
Exp. No.: RRAN01

			$[Anion]_{released}$ (x 10^{-5} mol L^{-1})	
Time (s)	[RR2] (x 10^{-5} mol L^{-1})	Chromophore (x 10^{-5} mol L^{-1})	Cl^-	SO_3^-
0	2.04	2.05	0.00	0.00
60	1.65	1.70	0.52	0.00
120	1.39	1.38	1.22	0.00
180	1.18	1.18	1.43	0.00
300	0.72	0.70	2.11	0.00
420	0.48	0.42	2.39	0.65
600	0.22	0.14	2.77	0.99
900	0.12	0.04	2.81	1.54

Effect of TEA
Exp. No.: RRTEA01 - RRTEA07

RRTEA01 ([TEA] = 0.005 mol L^{-1})

Time (sec)	Conc. (x 10^{-5} mol L^{-1})	D_t/D_0	pH
0	1.854	1.0000	10.95
60	1.699	0.9164	10.48
120	1.574	0.8490	10.48
180	1.447	0.7805	10.46
240	1.386	0.7476	10.46
300	1.249	0.6737	10.45
360	1.144	0.6170	10.44
480	0.938	0.5059	10.43
600	0.763	0.4115	10.42

RRTEA02 ([TEA] = 0.01 mol L^{-1})

Time (sec)	Conc. (x 10^{-5} mol L^{-1})	D_t/D_0	pH
0	1.787	1.0000	10.90
60	1.592	0.8909	10.79
120	1.492	0.8348	10.76
180	1.306	0.7307	10.76
240	1.183	0.6620	10.73
300	1.009	0.5646	10.72
360	0.875	0.4896	10.71
480	0.639	0.3576	10.68
600	0.430	0.2406	10.68

RRTEA03 ([TEA] = 0.02 mol L^{-1})

Time (sec)	Conc. (x 10^{-5} mol L^{-1})	D_t/D_0	pH
0	1.839	1.0000	10.96
60	1.660	0.9027	10.96
120	1.511	0.8216	10.96
180	1.348	0.7330	10.96
240	1.187	0.6455	10.96
300	0.961	0.5226	10.95
360	0.837	0.4551	10.95
480	0.579	0.3148	10.95
600	0.137	0.0745	10.95

RRTEA04 ([TEA] = 0.03 mol L^{-1})

Time (sec)	Conc. (x 10^{-5} mol/L)	D_t/D_0	pH
0	1.821	1.0000	11.09
60	1.618	0.8885	11.09
120	1.368	0.7512	11.09
180	1.211	0.6650	11.08
240	1.043	0.5728	11.08
300	0.859	0.4717	11.08
360	0.660	0.3624	11.08
480	0.148	0.0813	11.07
600	0.121	0.0664	11.07

RRTEA05 ([TEA] = 0.04 mol L^{-1})

Time (sec)	Conc. (x 10^{-5} mol L^{-1})	D_t/D_0	pH
0	1.821	1.0000	11.02
60	1.629	0.8946	10.97
120	1.415	0.7770	10.96
180	1.212	0.6656	10.96
240	1.041	0.5717	10.96
300	0.826	0.4536	10.96
360	0.609	0.3344	10.96
480	0.173	0.0950	10.96
600	0.122	0.0670	10.96

RRTEA06 ([TEA] = 0.05 mol L^{-1})

Time (sec)	Conc. (x 10^{-5} mol L^{-1})	D_t/D_0	pH
0	1.739	1.0000	11.04
60	1.581	0.9091	11.04
120	1.345	0.7734	11.03
180	1.106	0.6360	11.03
240	0.901	0.5181	11.03
300	0.737	0.4238	11.03
360	0.541	0.3111	11.03
480	0.138	0.0794	11.03
600	0.114	0.0656	11.02

RRTEA07 ([TEA] = 0.06 mol L^{-1})

Time (sec)	Conc. (x 10^{-5} mol L^{-1})	D_t/D_0	pH
0	1.820	1.0000	11.03
60	1.675	0.9203	11.00
120	1.392	0.7648	11.00
180	1.127	0.6192	11.00
240	0.917	0.5038	10.98
300	0.773	0.4247	10.98
360	0.642	0.3527	10.98
480	0.147	0.0808	10.98
600	0.114	0.0626	10.98

RRTEA08 ([TEA] = 0.07 mol L^{-1})

Time (sec)	Conc. (x 10^{-5} mol L^{-1})	D_t/D_0	pH
0	1.875	1.0000	11.07
60	1.648	0.8789	11.07
120	1.349	0.7195	11.06
180	1.158	0.6176	11.06
240	0.902	0.4811	11.06
300	0.717	0.3824	11.06
360	0.417	0.2224	11.06
480	0.143	0.0763	11.06
600	0.121	0.0645	11.06

Reaction Rates and Quantum Yields

Exp. No.	[TEA] (mol L^{-1})	k x 10^{-8} (mol L^{-1} s^{-1})	r^2
RRTEA01	0.005	1.90	0.9920
RRTEA02	0.01	2.50	0.9968
RRTEA03	0.02	2.80	0.9972
RRTEA04	0.03	3.2	0.9965
RRTEA05	0.04	3.3	0.9994
RRTEA06	0.05	3.4	0.9973
RRTEA07	0.06	3.5	0.9848
RRTEA08	0.07	4	0.9972

Effect of pH

Exp. No.: RRTpH01 – RRTpH04

RRTpH01 (Initial pH 3.0, [TEA] = 0.04 mol L^{-1})

Time (sec)	Conc. (x 10^{-5} mol L^{-1})	D_t/D_0	pH
0	1.773	1	3.09
60	1.747	0.9853	3.06
120	1.737	0.9797	3.05
180	1.719	0.9695	3.04
240	1.699	0.9583	3.01
300	1.684	0.9498	2.99
360	1.652	0.9318	2.99
480	1.644	0.9272	2.99
600	1.630	0.9193	2.99

RRTpH02 (Initial pH 5.0, [TEA] = 0.04 mol L^{-1})

Time (sec)	Conc. (x 10^{-5} mol L^{-1})	D_t/D_0	pH
0	1.923	1	5.02
120	1.842	0.9577	4.98
180	1.807	0.9396	4.98
240	1.762	0.9163	4.96
300	1.702	0.8851	4.96
360	1.673	0.8702	4.96
480	1.573	0.8182	4.95
600	1.568	0.8156	4.94

RRTpH03 (Initial pH 7.0, [TEA] = 0.04 mol L^{-1})

Time (sec)	Conc. (x 10^{-5} mol L^{-1})	D_t/D_0	pH
0	1.753	1	7.05
60	1.665	0.949800342	7.04
120	1.639	0.934968625	7.03
180	1.628	0.928693668	7.02
240	1.583	0.903023388	7.02
300	1.542	0.879634912	7.02
360	1.500	0.855675984	7.01
480	1.483	0.845978323	7.01
600	1.406	0.802053622	6.98

RRTpH04 (Initial pH 8.5, [TEA] = 0.04 mol L^{-1})

Time (sec)	Conc. (x 10^{-5} mol L^{-1})	D_t/D_0	pH
0	1.899	1	8.48
60	1.848	0.9734	8.44
120	1.802	0.9488	8.42
240	1.630	0.8585	8.40
300	1.629	0.8577	8.40
420	1.614	0.8501	8.39
600	1.390	0.732	8.37
720	1.245	0.6557	8.37

Reaction Rates and Quantum Yields

Exp. No.	Initial pH	k x 10^{-8} (mol L^{-1} s^{-1})	r^2
RRTpH01	3	0.30	0.9726
RRTpH02	5	0.30	0.9595
RRTpH03	7	0.40	0.9390
RRTpH04	8.5	0.50	0.9687

Effect of TEA in Cocktail Photosensitization Process
Exp. No.: RRCT01 – RRCT06

RRCT01 (Initial pH 11, [ACE] = 0.108 mol L^{-1}, [TEA] = 0.005 mol L^{-1})

Time (sec)	Conc. (x 10^{-5} mol L^{-1})	D_t/D_0	pH
0	1.893	1.0000	11.10
15	1.813	0.9577	11.08
30	1.396	0.7375	11.06
45	0.717	0.3788	11.05
60	0.323	0.1706	10.92
75	0.138	0.0729	10.81
90	0.086	0.0454	10.75
120	0.068	0.0359	10.67

RRCT02 (Initial pH 11, [ACE] = 0.108 mol L^{-1}, [TEA] = 0.01 mol L^{-1})

Time (sec)	Conc. (x 10^{-5} mol L^{-1})	D_t/D_0	pH
0	1.898	1.0000	11.06
15	1.776	0.9357	11.04
30	0.959	0.5053	10.99
45	0.482	0.2540	10.96
60	0.182	0.0959	10.92
75	0.115	0.0606	10.87
90	0.102	0.0537	10.86
120	0.092	0.0485	10.86

RRCT03 (Initial pH 11, [ACE] = 0.108 mol L^{-1}, [TEA] = 0.02 mol L^{-1})

Time (sec)	Conc. (x 10^{-5} mol L^{-1})	D_t/D_0	pH
0	1.891	1.0000	11.11
15	1.770	0.9360	11.03
30	0.743	0.3929	10.98
45	0.332	0.1756	10.84
60	0.137	0.0724	10.80
75	0.126	0.0666	10.79
90	0.111	0.0587	10.79

RRCT04 (Initial pH 11, [ACE] = 0.108 mol L^{-1}, [TEA] = 0.03 mol L^{-1})

Time (sec)	Conc. (x 10^{-5} mol L^{-1})	D_t/D_0	pH
0	1.961	1.0000	11.04
30	1.721	0.9585	11.01
45	0.773	0.3942	11.00
60	0.289	0.1474	10.99
75	0.147	0.0750	10.99
90	0.128	0.0653	10.99
120	0.122	0.0622	10.99

RRCT05 (Initial pH 11, [ACE] = 0.108 mol L^{-1}, [TEA] = 0.04 mol L^{-1})

Time (sec)	Conc. (x 10^{-5} mol L^{-1})	D_t/D_0	pH
0	1.870	1.0000	11.06
15	1.764	0.9433	11.04
30	0.805	0.4305	11.03
45	0.269	0.1439	11.00
60	0.150	0.0802	10.98
75	0.140	0.0749	10.97
90	0.133	0.0711	10.97
120	0.103	0.0551	10.97

RRCT06 (Initial pH 11, [ACE] = 0.108 mol L^{-1}, [TEA] = 0.05 mol L^{-1})

Time (sec)	Conc. (x 10^{-5} mol L^{-1})	D_t/D_0	pH
0	1.860	1.0000	10.97
15	1.666	0.8957	10.82
30	0.912	0.4903	10.70
45	0.510	0.2742	10.40
60	0.215	0.1156	10.40
75	0.152	0.0817	10.38
90	0.141	0.0758	10.38
120	0.121	0.0651	10.37

Reaction Rates and Quantum Yields

Exp. No.	[TEA], (mol L^{-1})	k_s x 10^{-2} (s^{-1})
RRCT01	0.005	4.39
RRCT02	0.010	5.28
RRCT03	0.020	5.91
RRCT04	0.030	6.03
RRCT05	0.040	5.84
RRCT06	0.050	4.40

Effect of Light Intensity in Cocktail Photosensitization Process

Exp. No.: RRCTLI01 – RRCT05

[ACE] = 0.108 mol/L; [TEA] = 0.04 mol/L

RRCTLI01 (Light intensity = 3.0 x 10^{-6} Einstein L^{-1} s^{-1})

Time (sec)	Conc. (x 10^{-5} mol L^{-1})	D_t/D_0	pH
0	2.109	1	11.05
30	2.088	0.9899	11.03
60	2.014	0.955	11.00
120	1.739	0.8245	11.00
180	0.549	0.2604	11.00
240	0.099	0.0469	10.96
300	0.028	0.0134	10.91

RRCTLI02 (Light intensity = 6.0 x 10^{-6} Einstein L^{-1} s^{-1})

Time (sec)	Conc. (x 10^{-5} mol L^{-1})	D_t/D_0	pH
0	2.006	1	11.02
30	1.923	0.9585	11.00
60	1.773	0.8837	10.99
90	0.668	0.3329	10.99
120	0.343	0.1712	10.98
180	0.042	0.0207	10.94

RRCTLI03 (Light intensity = 9.0 x 10^{-6} Einstein L^{-1} s^{-1})

Time (sec)	Conc. (x 10^{-5} mol L^{-1})	D_t/D_0	pH
0	2.036	1.0000	11.02
30	1.655	0.8128	11.02
60	0.981	0.4819	11.02
90	0.190	0.0935	10.98
120	0.042	0.0207	10.98

RRCTLI04 (Light intensity = 12 x 10^{-6} Einstein L^{-1} s^{-1})

Time (sec)	Conc. (x 10^{-5} mol L^{-1})	D_t/D_0	pH
0	2.008	1.0000	10.99
30	1.603	0.7985	10.99
60	0.563	0.2802	10.97
90	0.083	0.0411	10.96
120	0.029	0.0142	10.94

RRCTLI05 (Light intensity = 18 x 10^{-6} Einstein L^{-1} s^{-1})

Time (sec)	Conc. (x 10^{-5} mol L^{-1})	D_t/D_0	pH
0	2.183	1.0000	11.07
15	2.015	0.9231	11.07
30	1.420	0.6505	11.03
45	0.492	0.2254	11.01
60	0.111	0.0508	11.00
75	0.044	0.0202	11.00

Reaction Rates and Quantum Yields

Exp. No.	Light Intensity (x 10^{-6} Einstein L^{-1} s^{-1})	k_s x 10^{-2} (s^{-1})	Φ x 10^{-2}
RRCTLI01	3.0	2.35	11.91
RRCTLI02	6.0	3.42	8.67
RRCTLI03	9.0	4.26	7.21
RRCTLI04	12.0	4.69	5.94
RRCTLI05	18.0	6.79	5.74

Cocktail model

Lag phase of the Cocktail system

[TEA] (mol L^{-1})	D_L x 10^{-5} (mol L^{-1})	t_L (sec)
0.005	1.706	24
0.01	1.7369	20
0.02	1.7684	16
0.03	1.7763	15
0.04	1.7763	15
0.05	1.7763	15

Coefficients α and β in the Cocktail system

[TEA] (mol L^{-1})	α	β
0.005	1.7256	2.6343
0.01	2.0579	2.1116
0.02	2.3076	1.6896
0.03	2.4197	1.1273
0.04	2.3963	0.8601
0.05	1.8206	0.7159

Sensitivity analysis

RR2 + 0.108 mol L^{-1} [ACE] + 0.02 mol L^{-1} [TEA]

D_L = 1.7072E-5 mol L^{-1}

t=50 sec

α	D_t (mol L^{-1})	$1-D_t/D_L$	$d(1-Dt/D_L)$	dα	$d(1-Dt/D_L)/d\alpha$
1	6.41E-06	0.625	0	0.00	-
1.2	5.36E-06	0.686	0.06150	0.20	0.30752
1.5	4.08E-06	0.761	0.07498	0.30	0.24992
2.03	2.47E-06	0.855	0.09431	0.53	0.17794
2.5	1.52E-06	0.911	0.05565	0.47	0.11840
3	8.55E-07	0.950	0.03895	0.50	0.07791
4	1.39E-07	0.992	0.04194	1.00	0.04194

β	D_t (mol L^{-1})	$1-D_t/D_L$	$d(1-Dt/D_L)$	dβ	$d(1-Dt/D_L)/d\beta$
1	2.94E-06	0.828	0	0.00	-
1.2	2.85E-06	0.833	0.00527	0.20	0.02636
1.5	2.70E-06	0.842	0.00879	0.30	0.02929
1.96	2.47E-06	0.855	0.01347	0.46	0.02929
2.5	2.21E-06	0.871	0.01523	0.54	0.02820
3	1.97E-06	0.885	0.01406	0.50	0.02812
4	1.48E-06	0.913	0.02870	1.00	0.02870
6	5.04E-07	0.970	0.05717	2.00	0.02858